Time-Series with Multiple Seasonal Periods: Modeling and Forecasting

Thesis for the Degree of Doctor of Philosophy (PhD)

Chudo Solomon Buke
Supervisor: Prof. Dr. Gyorgy Terdik

University of Debrecen
Doctoral Council for Natural Sciences and Engineering
Doctoral School of Informatics
Debrecen, 2025

Hereby I declare that I prepared this thesis within the Doctoral Council for Natural Sciences and Engineering, Doctoral School of Informatics, University of Debrecen in order to obtain a PhD Degree in Informatics at Debrecen University.

The results published in the thesis are not reported in any other PhD theses.

Debrecen, 202.....

.....
signature of the candidate

Hereby I confirm that Solomon Buke candidate conducted his studies with my supervision within the Applied Information Technology and its Theoretical Background, Program of the Doctoral School of Informatics between 2020 and 2025. The independent studies and research work of the candidate significantly contributed to the results published in the thesis.

I also declare that the results published in the thesis are not reported in any other theses.

I support the acceptance of the thesis.

Debrecen, 202.....

.....
signature of the supervisor

TIME-SERIES WITH MULTIPLE SEASONAL PERIODS: MODELING AND FORECASTING

Dissertation submitted in partial fulfillment of the requirements for the doctoral (PhD) degree in Informatics

Written by Chudo Solomon Buke, Master of Science in Applied Statistics

Prepared in the framework of the doctoral school of the University of Debrecen (Applied Information Technology and its Theoretical Background doctoral programme)

Dissertation advisor: Dr. Gyorgy Terdik

The official opponents of the dissertation:

Dr. .....
Dr. .....

The evaluation board:

Chairperson:	Dr. .....
Members:	Dr. .....
	Dr. .....
	Dr. .....
	Dr. .....

The date and venue of the dissertation defence: ..... 20...

Abstract

This dissertation addresses trends in the death of COVID-19 in Hungary and energy consumption patterns in Brazil, with the objective of modeling and forecasting time-series data using sophisticated statistical methodologies. Initially, a unified theoretical framework was established by deriving the state space representations for core time series models (AR, MA, ARMA, ARIMA, HW). Secondly, we utilized World Health Organization data from 2020 to 2021 and employed a Seasonal ARIMA model to forecast daily death from COVID-19 in Hungary. The fitted SARIMA model $(1,1,2)(1,0,1)_{[7]}$ indicates that the residuals were normally distributed and exhibited significant metrics. The daily fatalities were anticipated to decrease. The subsequent phase of study findings involved assessing the potential enhancement of the Double Seasonal Holt-Winters model through the incorporation of ARMA(3,1) errors. For energy consumption data with different seasonalities, in particular, the combined (modified) model improved prediction reliability and successfully addressed residual autocorrelation, outperforming standard DSHW across various performance metrics (ME, RMSE, MAPE). Lastly, a modified method based on periodograms was implemented to identify various seasonalities (daily, half-daily and sub-daily) in data on energy consumption collected hourly. In the analysis of multi-seasonal trends, STL + ETS(A,N,N) exhibited the most accurate forecasts compared to the BATS and TBATS models. The dissertation emphasizes the need of choosing appropriate time series models for various seasonal structures, giving practitioners significant insights for decision-making in dynamic situations. Key contributions include formulating the state space representations for core time series models, enhanced SARIMA forecasting for epidemiological data, better DSHW-ARMA combined modeling, and a strong framework for selecting dominant frequency and modeling multi-seasonal time series.

Contents

List of Abbreviations

- SIN - Sistema Interligado Nacional (Brazil), which translates to the National Interconnected System.
- EPE - Forecasting errors in Empresa de Pesquisa Energética (Brazil).
- AR - Auto-Regressive
- MA - Moving Average
- IMA - Integrated Moving Average
- ARMA - Auto-Regressive Moving Average
- ARIMA - Auto-Regressive Integrated Moving Average
- ARI - Auto-Regressive Integrated
- SARIMA - Seasonal Auto-Regressive Integrated Moving Average
- SARI - Seasonal Auto Regression Integrated
- BATS - Box-Cox transformation, ARMA errors, Trend, and Seasonal components
- TBATS - Trigonometric seasonality, Box-Cox transformation, ARMA errors, Trend, and Seasonal components
- DSHW - Double-Seasonal Holt-Winters
- STL - Seasonal and Trend decomposition using Loess
- COVID-19 - Coronavirus Disease of 2019
- ARIMAX - Autoregressive Integrated Moving Average with Exogenous Variable
- SARIMAX - Seasonal Autoregressive Integrated Moving Average with Exogenous Variables
- HW - Holt-Winters
- ETS - Exponential Smoothing Methods Combine Error, Trend, and Seasonal components
- SAR - Seasonal Autoregressive
- SMA - Seasonal Moving Average
- MSARIMA - Multiple Seasonal Auto-Regressive Integrated Moving Average
- GARCH - Generalized AutoRegressive Conditional Heteroskedasticity
- VARIMA - Vector Autoregressive Integrating Moving Average
- RNNs - Recurrent Neural Networks
- LSTM - Long Short-Term Memory
- SSMs - State Space Models
- GAMs - Generalized Additive Models
- AIC - Akaike Information Criterion

- BIC - Bayesian Information Criterion
- WHO - World Health Organization
- SARS-CoV-2 - Severe Acute Respiratory Syndrome Coronavirus 2
- ACF - Autocorrelation Function
- PACF - Partial Autocorrelation Function
- ADF - Augmented Dickey-Fuller test
- QQ-Plot - Quantile-Quantile plot
- H_0 - Null hypothesis
- H_1 - Alternative hypothesis
- CI - Confidence Interval
- ME - Mean Error
- RMSE - Root Mean Squared Error
- MAE - Mean Absolute Error
- MPE - Mean Percentage Error
- MAPE - Mean Absolute Percentage Error
- Theil's U - Theil's Statistic
- PJM - Pennsylvania-New Jersey-Maryland Interconnection
- ISSM - Innovations State Space Model
- MSTL - Multiple Seasonal and Trend decomposition using Loess
- KPSS - Kwiatkowski, Phillips, Schmidt, and Shin test
- HEGY - Hylleberg-Engle-Granger-Yoo test
- dB - decibels
- LOESS - LOcal regrESSion
- AICc - Akaike's Information Corrected Criterion

List of Tables

List of Figures

1 Introduction

1.1 Background of the study

Observations presented in a sequential manner are known as time series. Although time is the most common metric for ordering, especially when considering a series of equally spaced time periods, other dimensions, such as space, can also be used. Time series are common in many different sectors, and in agriculture, for example, they are used to track crop production and pricing on an annual basis. Various economic and business metrics are tracked on a daily basis, including stock prices, interest rates, monthly price indices, quarterly sales, and annual earnings. As engineers, we listen for and analyze electrical signals, voltage, and sound. Earthquakes and other forms of turbulence are recorded in geophysics. Electroencephalogram and electrocardiogram traced in medical research. The hourly wind speeds, the daily temperatures, and the annual rainfall are the main variables studied by meteorologists. During quality control, we keep an eye on a process in relation to an established goal. Birth, death, accident, and crime rates are some of the key variables studied in the social sciences every year. Just a few of the many sources that note and study time series are [89], and [26].

A natural sequential arrangement exists in time-series data, which is well-known [77]. This distinguishes time-series analysis from cross-sectional investigations, which are observational studies examining data from a population at a given moment, lacking a natural sequence of observations. Time series analysis is fundamentally different from spatial data analysis, in which observations are generally associated with geographical locations [84].

Particular time series statistical models such as the MA, AR, ARMA, and ARIMA models in the time domain can help in this direction, using only recorded data from the past to model and forecast future cases [12]. Reference [92] said that many time series contain seasonal periodic components. Box and Jenkins have generalized the ARIMA model to mul-

tiplicative seasonal ARIMA (abbreviated SARIMA model). Many time series exhibit multiple seasonality [28]. They have introduced an innovative state space modeling framework based on a trigonometric formulation and the existing exponential smoothing models capable of tackling all of these seasonal complexities. As a result, practitioners can better understand and anticipate data fluctuations that are influenced by seasonal effects.

Periodic patterns overlap and interact with each other, which makes data with many seasonal periods, such as electricity use, more difficult to understand. Human actions impact daily cycles, while weekly and annual cycles reflect more systemic patterns of behavior and the natural world. SARIMA and other classic approaches have limitations in accommodating diverse seasonalities, so it is important to apply more modern methods.

Traditional forecasting methods fail to capture the intricacies of time series data with numerous seasonalities, necessitating the creation of specialized approaches. Periodograms, which study the frequency domain of time series data, are an effective technique for recognizing and modeling periodic components. Periodograms can identify underlying seasonal patterns that typical time-domain approaches may miss.

BATS, STL, and the TBATS model are important improvements when it comes to handling various seasonalities. These methods are adaptable, but they do not do a good job of exploiting frequency-domain insights to locate periodic patterns more accurately. That is why we use the periodogram that was discussed by [77] to examine the density of the spectrum and to detect important seasonalities. we established a systematic approach to identify and integrate the predominant seasonal periods into the models. Subsequently, we train and evaluate BATS, TBATS, and STL models with the chosen seasonalities utilizing conventional accuracy metrics. The suggested spectral density-based technique efficiently identifies the predominant seasonalities and improves the configuration of the models [21].

Within the realms of energy management and grid stability, there has

been a substantial amount of attention in the desire for accurate projections of power use. Both neural networks and ensemble methods are excellent examples of approaches that fall into the category of machine learning. In spite of the fact that these research show promise, they frequently call very large datasets and major feature engineering work. Power consumption data naturally exhibit periodicity, which frequency-domain approaches take into account when providing a supplementary perspective.

Previous research has shown that there are discernible trends in electric power use on a daily, monthly, and annual basis. During the week, when most people are at work, demand is at its peak, and on the weekends it is at its lowest. Local factors, such as holidays and weather, compound the impact of seasonal changes. Periodograms are well-suited for assessing data on power use due to these qualities.

Reference [85] asserts, and [21] indicates that power forecasting aids in evaluating energy demands for system growth, assessing power plant availability relative to installed capacity, and ensuring system operability. In order to forecast power usage from 2021–2025, the author uses historical data from Brazil and its underlying systems to analyze three time series approaches and their combinations. Simultaneously, the researcher computes the fraction of inaccurate EPE estimates. The second method employed historical data from SIN and its subsystems to calculate the proportion of erroneous power demand from 2014 to 2019 [85]. The findings of this study indicate that the optimal strategy is Regression with Seasonality, and approximation errors can be minimized by integrating time series methodologies [21]. These data and results serve as a reference point for our dissertation objectives.

The proliferation of high-frequency data in fields such as energy management and epidemiology has created a pressing need for robust forecasting methods capable of capturing complex, multiple seasonal patterns [80]. Traditional time series models, often designed for single seasonality, frequently fall short in these environments, leading to suboptimal decisions

in critical areas like public health policy and resource allocation. This work addresses this gap by advancing the theoretical and methodological toolkit for multi-seasonal forecasting.

Building on foundational research into time series decomposition [23], this dissertation establishes a unified state-space framework for core models and introduces significant enhancements to existing methods. We demonstrate the application of these advanced hybrid models, guided by spectral analysis (Periodogram) for seasonality detection, to achieve superior forecasting performance. The following sections detail these contributions, validating the approaches on real-world datasets from energy consumption and the COVID-19 pandemic [20], and [21], and ultimately providing practitioners with more accurate and interpretable tools for a data-driven world.

1.2 Research Questions

Chapters 2 and 3 address the following research concerns about time-series modeling and COVID-19 forecasting:

1. Which time-series model is best for forecasting the number of death rates of the COVID-19 pandemic?

2. By modifying the standard ARIMA model with new state and observation equations, how can one formulate a State Space ARIMA model?

Chapter 4 address the following research questions about DSHW model and Error Correction:

1. How can ARMA (p, q) error corrections be incorporated into a state-of-the-art DSHW modeling framework?

2. Do time series forecasts become more accurate if ARMA error adjustments are incorporated into the DSHW model?

Chapter 5 addresses the following research concerns about Seasonality Detection and Model Comparison:

1. Are major seasonal phases in time series data efficiently identified by periodograms produced from spectral density analysis?

2. How accurate are seasonal models for predicting time series that ex-

hibit different levels of seasonality?
3. How do seasonal models perform compared to other state-of-the-art methods for predicting time series?

1.3 Scientific Goals

1.3.1 Main Goal

To advance time series forecasting methodologies by modifying approaches capable of handling seasonal patterns in time series data.

1.3.2 Specific Objectives

The specific objectives of this dissertation:

1. Identifying and constructing the most suitable time series model for predicting future mortality rates of the COVID-19 outbreak.
2. Employing a new approach to state and observation equations for formulating the State Space ARIMA model derived from the conventional ARIMA model.
3. Creating an advanced modeling framework for the DSHW model, integrating ARMA (p,q) error corrections to improve forecasting precision.
4. Enhancing Time Series Forecasting using the DSHW and ARMA Error Corrections.
5. Presenting a new methodology utilizing periodograms derived from spectral density analysis to ascertain significant seasonal periods.
6. Forecasting and modeling time series with varying degrees of seasonality.
7. Comparing the forecasting performance of seasonal models with other advanced time series forecasting techniques.

1.4 Significance of the Dissertation

The dissertation, "Time-Series with Multiple Seasonal Periods: Modeling and Forecasting," holds profound significance for both the theory and practice of statistical forecasting. Its contributions are articulated across three interconnected domains: theoretical unification, methodological innovation, and tangible real-world impact.

1. Theoretical Significance: A Unified Framework The work provides a crucial theoretical consolidation of time series analysis by deriving state-space representations for fundamental models, including AR, MA, ARMA, ARIMA, and Holt-Winters. This unification is significant because it places disparate models under a single, coherent framework, simplifying their comparative analysis and enhancing their pedagogical clarity. By creating this common language, the dissertation bridges historically separate modeling traditions and provides a more robust foundation for future theoretical developments in stochastic processes.

2. Methodological Significance: Advancing Forecasting Precision The dissertation makes pivotal methodological contributions that directly enhance forecasting accuracy for complex, multi-seasonal data.

Enhanced Hybrid Modeling: It modifies the Double Seasonal Holt-Winters (DSHW) framework by integrating ARMA error correction. This innovation systematically addresses residual autocorrelation—a key limitation in the original model—leading to demonstrably improved forecast precision for data with multiple seasonal cycles.

Empirically Validated Model Selection: It establishes a rigorous, data-driven paradigm for model selection. By demonstrating that spectral analysis-guided STL+ETS models outperform sophisticated alternatives like TBATS on real-world energy data, the research provides a compelling, evidence-based framework for practitioners, moving beyond subjective model choice.

3. Practical and Societal Significance: Solving Real-World Problems The ultimate significance of this research lies in its successful application to urgent, real-world challenges, proving its utility beyond theoretical

constructs.

Public Health Crisis Response: During the acute phases of the COVID-19 pandemic, the dissertation's Seasonal ARIMA model was deployed to forecast daily deaths in Hungary. This application provided critical, timely insights for healthcare planning and policy-making, showcasing the direct life-saving potential of advanced time series analysis.

Cross-Sectoral Applicability: The developed frameworks are universally applicable to domains plagued by multi-seasonal data, such as energy load forecasting for grid management, epidemiology, and supply chain logistics. The research empowers organizations in these fields with more accurate and reliable tools for strategic planning and operational efficiency.

In conclusion, this dissertation's significance stems from its unique integration of theoretical rigor, methodological innovation, and practical validation. It not only advances the academic discipline of time series forecasting but also delivers robust, scalable tools that enable better decision-making in critical sectors, thereby bridging the long-standing gap between abstract statistical theory and the complex demands of a data-driven world.

1.5 Outline of the dissertation

The structure of this dissertation comprises 7 chapters. Chapter one provides the background , research questions, scientific goals, significance, and outline of the dissertation. Chapter two introduces the theoretical framework for state space ARIMA models such as state space AR(p), ARMA(p,q), MA(q), IMA(d,q), and ARIMA(p,d,q) models. Univariate general structural time series models and formulations of multiple seasonal time series models as state space models for innovations are the main discussion parts of this chapter, especially for the HW model. Seasonal ARIMA models, spectral analysis and periodograms, and multiple seasonal models, like BATS, TBATS, and STL models, are also discussed under this section. The original scientific results are provided in Chapters

3, 4, and 5 of this dissertation. The third chapter focuses on the main goals of the dissertation. Chapter 3 deals with Box-Jenkins methodology for seasonal ARIMA time series models. It includes the practical application of the model, results, discussions, and conclusion of the chapter. Improving the DSHW model by adding ARMA (3,1) errors is the focus of Chapter 4 of the dissertation. Based on the performance measurement values of the models, it shows the best forecasting model in the energy consumption data. In Chapter 5, We examine how to use periodograms to model and predict time series that exhibit several seasonal patterns. The chapter includes a state space model that highlights new developments in the MS processes for BATS, TBATS, and STL models of time series with multiple seasonal patterns. The rest of the chapters include the conclusion and future directions of the dissertation, a collection of articles that are pertinent to the dissertation , acknowledgments, and references to which the dissertation basically refers.

2 Theoretical Background

2.1 State Space Models

A State Space model offers a mathematical framework by representing dynamic systems and time series data through unobserved (latent) states that evolve over time. This is a mathematical depiction of a state-space model. In this equation, y_t signifies the observed time series at time t, $\mathbf{F}_t$ represents the observation equation matrix, and G indicates the state transition equation matrix. Furthermore, $\mathbf{x}_t$ denotes the state vector at time t. The observation and state disturbances are denoted by the vectors x_t and w_t, respectively. The equation for the observation is as follows [30], and [19]:

$$y_t = \mathbf{F}\mathbf{x}_t + v_t \tag{1}$$

In this equation, $\mathbf{F}$ is a matrix that delineates the contribution of state variables to the observed variable, whereas v_t represents the observation disturbance. The matrices $\mathbf{G}$ and $\mathbf{R}$ are presumed to be initially known. The equation for state transition is provided as follows [19], and [30]:

$$\mathbf{x}_{t+1} = \mathbf{G}\mathbf{x}_t + \mathbf{R}w_t \tag{2}$$

2.1.1 Kalman Filter for State Space Models

In environmental sciences, economics, finance, engineering, and when precise predictions are vital for decision-making, time-series forecasting is absolutely important. For linear time-dependent structures, conventional models include ARIMA [14], and its seasonal variation SARIMA offers a strong framework. Their typical formulation, however, is not flexible enough to address high-dimensional state representations, missing data, and intricate patterns.

Where the underlying dynamics are expressed by a latent state vector that develops over time, the state-space technique presents a consistent and computationally efficient means to characterize time series models. Expressing ARIMA, SARIMA [39], and other advanced models (like DSHW,

BATS, TBATS, and STL decomposition) in state space form allows us to use the Kalman filter [54] for best estimate, smoothing, and forecasting. The Kalman filter is highly effective for real-time updating in adaptive forecasting. It is capable of incorporating structural components, accurately computing likelihood [30], and managing missing data without ad-hoc imputation. This is accomplished by modifying the state estimates in response to new observations, thereby reducing the mean-squared error. Beyond classical ARIMA models, more sophisticated approaches such as: DSHW [80] for multiple seasonal patterns, BATS and TBATS [28] for complex, high-frequency seasonality, and STL [22] for non-parametric trend and seasonal decomposition, can all be formulated in state space form and estimated via the Kalman filter. This dissertation explores the theoretical underpinnings, computational advantages, and practical uses of ARIMA and other models using the state space framework, therefore demonstrating how the Kalman filter increases their adaptability, scalability, and predictive capacity.

2.1.2 Controllability Canonical Form

In this chapter, we employed the controllable canonical form to ascertain the aforementioned metrics such as F, G, and R. A robust framework for analysis and control is established for time series models when represented in state-space forms [6] through the application of the Controllability Canonical Form (CCF) concept. Time series models can be analyzed and managed for various control objectives through the conversion into state-space representations.

By utilizing the Controllability Canonical Form to represent time series models in state-space forms, researchers can leverage a wide range of control methodologies to adjust and improve the performance of the system. These approaches may make use of optimal control, state feedback control, observer design, and other similar techniques. We may better understand and manage complex dynamic systems and develop more effective control strategies for many applications when we define time series

models in state-space forms utilizing the Controllability Canonical Form. See [17] for further information.

2.1.3 Overview of ARIMA Models

A class of statistical models known as ARIMA models accomplishes time series forecasting. ARIMA models, according to Box-Jenkins [14], are very helpful for capturing temporal relationships in the data set and, therefore, interpreting and projecting future values in a time series. Key components of ARIMA models are AR, MA, and I (integrated). It signified ARIMA(p,d,q). Fitting an ARIMA model in practical uses requires several steps [19]. These steps include data preparation, stationarity checking, model identification, parameter estimate, model validation, and future point forecasting. Among the several benefits the models offer are flexibility to manage a large spectrum of time series data, interpretability of components, and extensive applicability in many fields for analysis of time series data. Many time series models have limits, such as the assumption of linearity, parameter selection challenges, and computational difficulty for vast datasets. ARIMA models extend themselves to SARIMA, ARIMAX, and SARIMAX. In summary Regarding time series analysis and prediction, ARIMA models are rather successful. By mastering and appropriately applying the AR, I, and MA components, one may build trustworthy models that totally reflect time-series data. Despite their shortcomings, ARIMA models' adaptability and interpretability make them a pillar in the field of time-series forecasting.
AR, MA, ARMA and ARIMA models are transformed into a state space representation in the [30] procedure for deriving the state space form from a time series equation. Applying contemporary estimate methods for forecasting, model diagnostics, and parameter estimation—such as the Kalman filter and smoother—needs this transition.
Using [30]'s technique, models are transformed into state-space form by expressing the model in terms of unobserved states and observation equations. Then, in order to account for unobserved states and disruptions,

they use state space models.

Advantages of State Space ARIMA Models

There are a number of benefits to using state-space ARIMA models. These include being able to incorporate additional components like seasonality and exogenous variables, being efficient with computationally effective estimation using the Kalman filter, naturally handling missing data, and providing confidence intervals for forecasts to quantify uncertainty.

In time series, ARIMA(p,d,q) model formula is given by:

$$y_t^* = \phi_1 y_{t-1}^* + \phi_2 y_{t-2}^* + ... + \phi_p y_{t-p}^* + w_t + \theta_1 w_{t-1} + ... + \theta_q w_{t-q} \qquad (3)$$

Where: $y^* = \Delta^d y_t$

The matrices are given below:

$$\mathbf{G} = \begin{bmatrix} 1 & . & . & . & 1 & 1 & 0 & 0 & . & . & . & 0 \\ 0 & . & & & . & . & . & & & & & . \\ . & & . & & . & . & . & & & & & . \\ . & & & . & . & . & . & & & & & . \\ . & . & . & 0 & 1 & 1 & 0 & . & . & . & 0 & 0 \\ 0 & . & . & . & 0 & \phi_1 & 1 & 0 & . & . & . & 0 \\ . & & & & . & \phi_2 & 0 & 1 & 0 & . & . & . \\ . & & & & . & . & . & & . & & & . \\ . & & & & . & . & . & & & . & & . \\ 0 & & & & 0 & . & . & & & & . & 0 \\ 0 & . & . & . & 0 & \phi_{m-1} & 0 & . & . & . & 0 & 1 \\ 0 & . & . & . & 0 & \phi_m & 0 & . & . & . & 0 & 0 \end{bmatrix},$$

$$\mathbf{R} = \begin{bmatrix} \mathbf{0} \\ 1 \\ \theta_1 \\ \theta_2 \\ . \\ . \\ . \\ \theta_{m+d-1} \end{bmatrix}, \mathbf{F} = \begin{bmatrix} \mathbf{1} & 1 & 0 & \mathbf{0} \end{bmatrix}, \text{and State vector: } \mathbf{x}_t = \begin{bmatrix} x_{1,t} \\ x_{2,t} \\ . \\ . \\ . \\ x_{m+d,t} \end{bmatrix}$$

State equation, Equation 2, is given by [19]:

$$\begin{bmatrix} x_{1,t+1} \\ x_{2,t+1} \\ . \\ . \\ . \\ x_{m+d,t+1} \end{bmatrix} = \begin{bmatrix} 1 & . & . & . & 1 & 1 & 0 & 0 & . & . & . & 0 \\ 0 & . & & & . & . & . & & & & & . \\ . & & . & & . & . & . & & & & & . \\ . & & & . & . & . & . & & & & & . \\ . & . & . & 0 & 1 & 1 & 0 & . & . & . & 0 & 0 \\ 0 & . & . & . & 0 & \phi_1 & 1 & 0 & . & . & . & 0 \\ . & & & & . & \phi_2 & 0 & 1 & 0 & . & . & . \\ . & & & & . & . & . & & . & & & . \\ . & & & & . & . & . & & & . & & . \\ 0 & & & & 0 & . & . & & & & . & 0 \\ 0 & . & . & . & 0 & \phi_{m-1} & 0 & . & . & . & 0 & 1 \\ 0 & . & . & . & 0 & \phi_m & 0 & . & . & . & 0 & 0 \end{bmatrix} \begin{bmatrix} x_{1,t} \\ x_{2,t} \\ . \\ . \\ . \\ x_{m+d,t} \end{bmatrix} + \begin{bmatrix} \mathbf{0} \\ 1 \\ \theta_1 \\ \theta_2 \\ . \\ . \\ . \\ \theta_{m+d-1} \end{bmatrix} w_t \tag{4}$$

The aggregate form of Equation 4 is:

$$\mathbf{x}_{t+1} = \begin{bmatrix} \mathbf{t}_{d\times d} & \mathbf{1}_{d\times 1} & \mathbf{0}_{d\times p} \\ \mathbf{0}_{(m-1)\times d} & \boldsymbol{\phi}_{(m-1)\times 1} & \mathbf{I}_{(m-1)\times p} \\ \mathbf{0}_{1\times d} & \phi & \mathbf{0}_{1\times p} \end{bmatrix} \mathbf{x}_t + \begin{bmatrix} \mathbf{0}_{d\times 1} \\ 1 \\ \boldsymbol{\theta}_{(m-1)\times 1} \end{bmatrix} w_t \tag{5}$$

Where:
$p \rightarrow$ is the order of the AR part,
$d \rightarrow$ is the degree of differencing,
$q \rightarrow$ is the order of the MA part.
$m \rightarrow max(p + d, q + d + 1)$
$\mathbf{0}_{1\times d} \rightarrow 1 \times d$ zero matrix

$\mathbf{1}_{d\times 1}\rightarrow d\times 1$ unit vector
$\boldsymbol{\phi}_{(m-1)\times 1}\rightarrow (m-1)\times 1$ matrix for AR parameters
$\mathbf{I}_{(m-1)\times p}\rightarrow (m-1)\times p$ diagonal identity matrix
$\boldsymbol{\theta}_{(m-1)\times 1}\rightarrow (m-1)\times 1$ vector for MA parameters
$\mathbf{0}_{(m-1)\times d}\rightarrow (m-1)\times d$ zero matrix
$\mathbf{0}_{1\times p}\rightarrow 1\times p$ zero matrix
$\mathbf{0}_{d\times 1}\rightarrow d\times 1$ zero vector transpose
$\mathbf{0}_{d\times p}\rightarrow d\times p$ zero vector
$\mathbf{t}_{d\times d}\rightarrow \begin{cases} 1, & \text{if } d\in \triangle, \text{ where } \triangle \text{ is upper triangle of the block} \\ 0, & \text{if } d\notin \triangle \end{cases}$, it is $d\times d$ matrix.

2.1.4 Extensions

Combining state-space models with seasonality forms a state-space SARIMA model. Time-series data would be perfect for this strong framework. This model expands based on the classic state-space ARIMA as another representation of the classical ARIMA model. An expansion of the ARIMA paradigm used by the State Space SARIMA includes seasonal dynamics directly in the state vector [77]. To better show periodic patterns in time series data, SARIMA is a development of ARIMA that uses seasonal AR/MA components and seasonal differencing.
This combined method makes it much easier to estimate, predict, and understand changes in time series that occur over time, whether seasonal or not. It works exceptionally well for state space form. This all-encompassing method can handle complicated time series data showing both seasonal and short-term behavior patterns, leading to better forecasting models. The next Section discuss SARIMA in detail [20].

2.2 Seasonal ARIMA Model

2.2.1 Overview of SARIMA Model

Designed to handle time series data displaying seasonal trends, one version of the ARIMA model—the SARIMA model—combines the conventional ARIMA components and adds seasonal terms to explain data reliant on seasonal and nonseasonal variables. The components of SARIMA are given by SARIMA (p, d, q) (P, D, Q) s, where p, d, and q are nonseasonal components. P, D, and Q are seasonal components [14]. The essential things in SARIMA model applications are differencing, AR and MA non-seasonal terms, SAR and SMA terms, model fitting, and forecasting. Handling nonseasonal and seasonal patterns, flexibility, and interpretability are advantages of this model. According to [49], it is an effective instrument for modeling and predicting time series data that exhibit seasonal trends.

When observations show persistent patterns or cycles throughout time, it is called seasonality. This is a common feature in time-series data. Most of the time, when dealing with time series data that just has one seasonal component, traditional time series models like ARIMA and SARIMA are used [11] and [5]. Nonetheless, numerous real-world datasets display multiple seasonal cycles. Retail sales may exhibit annual trends (attributed to holidays or annual events) and weekly cycles (resulting from workweek behaviors) [49].

Models such as SARIMA can accommodate a single seasonal component, but struggle with numerous or interacting seasonalities, resulting in excessive complexity [16]. Recent research has investigated techniques like the MSARIMA model [15], which seeks to enhance the SARIMA framework to incorporate multiple seasonal cycles. Nonetheless, these models may encounter constraints in fully representing the intricate nature of multi-seasonal time series.

2.2.2 Example (Contributions): SARIMA(1, 1, 2)(1, 0, 1)$_7$

My model, SARIMA(1, 1, 2)(1, 0, 1)$_7$, was fitted using daily COVID-19 death data collected in Hungary from October 4, 2020, to May 12, 2021. Each week marks a new season. The equation for the model is then:

$$(1 - \phi_1 B)(1 - \Phi_1 B^7)(1 - B))y_t = (1 + \theta_1 B + \theta_1 B^2)(1 + \Theta_1 B^7)\epsilon_t$$

Refer to Chapter 3 for more details.

2.2.3 Extensions

SARIMA can be expanded to include: SARIMAX, which includes exogenous variables [49, 14]; MSARIMA, which handles multiple seasonal patterns [80, 49]; ARIMAX with Fourier, which uses Fourier terms for smooth seasonality [42, 49]; Nonlinear SARIMA, which captures nonlinear relationships [82]; Hybrid SARIMA, which combines SARIMA with other techniques (e.g, neural networks, GARCH) [95]; Bayesian SARIMA, which uses Bayesian inference to estimate parameters [32]; and VARIMA, which models multiple time series [59]. In the next subtopics, the SARIMA model is extended to multiple seasonal models.

Summary

There have been changes made to the SARIMA model so that it can be used for a wider range of real-world time series situations. These add-ons make forecasts more accurate and reliable for large, complex datasets by taking into account different seasonality, outside factors, modeling nonlinear relationships, or mixing different methods. What kind of extension to use depends on the situation and the properties of the time series.

2.3 Univariate General Structural Time Series Models

Univariate structural time-series models are statistical tools for analyzing time series data; these models isolate the effects of a single variable's

evolution across the data. With these models, it is much easier to see patterns, trends, and underlying structures in the data. Parts such as trend, erratic fluctuations, and seasonal parts are separated from the time-series by these methods [30].

Model Equations

Observation Equation:

$$y_t = \mu_t + \beta_t + \gamma_t + \varepsilon_t \tag{6}$$

Where:

y_t : Observed value of the time-series at time t.

μ_t : Level element at time t.

β_t : Trend element at time t.

γ_t : Seasonal element at time t.

ε_t : Irregular element at time t.

Interpretation

- The time series' baseline level is represented by the level element μ_t
- The long-term movement or orientation of the time series is captured by the trend element β_t.
- Seasonal patterns that reoccur at predetermined intervals are represented by the seasonal element γ_t.
- ε_t, the irregular element, takes measurement error and random fluctuations into consideration.

Level Equation: In the context of a state space model, the level equation can be represented as [18]:

$$\mu_{t+1} = \mu_t + \xi_t$$

The evolution of the level component over time is represented by the level equation in a unified structural time series model [37]. The level component, which represents the normal or average value around which the series varies, reflects the baseline or underlying level of the time series data. Reference [28] applied this concept when developing their BATS and TBATS models. [30] are called this term slope.

Trend Equation: It can be defined as follows:

$$y_t = \beta_t + \varepsilon_t$$

$$\beta_{t+1} = \beta_t + \mu_t + \delta_t$$

$$\mu_{t+1} = \mu_t + \xi_t$$

ξ_t : Level irregular part at time t.

δ_t : Trend irregular part at time t.

The state space representation is find as:

$$\mathbf{y}_t = \begin{bmatrix} 1 & 0 \end{bmatrix} \begin{bmatrix} \beta_t \\ \mu_t \end{bmatrix} + \boldsymbol{\varepsilon}_t, \tag{7}$$

$$\begin{bmatrix} \beta_{t+1} \\ \mu_{t+1} \end{bmatrix} = \begin{bmatrix} 1 & 1 \\ 0 & 1 \end{bmatrix} \begin{bmatrix} \beta_t \\ \mu_t \end{bmatrix} + \begin{bmatrix} \delta_t \\ \xi_t \end{bmatrix} \tag{8}$$

Seasonal Equation:

It often contains seasonal components that repeat itself over specific time intervals, such months, quarters, or years. These parts record the cyclical changes caused by things like seasons, holidays, or other repeating events.

$$\gamma_{t+1} = -\sum_{j=1}^{s-1} \gamma_{t+1-j} + \varepsilon_t, \tag{9}$$

$$\varepsilon_t \sim N(0, \sigma_\varepsilon^2)$$

$$t = s-1, s, s+1, ...$$

Adding an error term to this relation allows the seasonal pattern to change over time. The authors [41] suggested the effect of season j at time t by γ_{jt} as an alternative. Then

$\gamma_{j,t+1} = \gamma_{jt} + w_{jt}$

where: t is given by (i-1)s + j, for i=1,2,3,...,(years) j=1,2,3,...,s (months). We can express the seasonal component term in a trigonometric form (for a constant seasonal) [68]:

$$\gamma_t = \sum_{j=1}^{s/2} (a_j cos \frac{2(\pi)j}{s} t + b_j sin \frac{2(\pi)j}{s} t) \tag{10}$$

$$where : j = 1, 2, 3, ..., [s/2]$$

Also, indicated by [30], [56], and [70], an alternative form of trigonometric is given by:

$$\gamma_t = \sum_{j=1}^{s/2} (\gamma_{jt})$$

where

$$\gamma_{j,t+1} = \gamma_{j,t} \cos \frac{2(\pi)j}{s} + \gamma^*_{j,t} \sin \frac{2(\pi)j}{s} + \omega_{j,t},$$

$$\gamma^*_{j,t+1} = -\gamma_{j,t} \sin \frac{2(\pi)j}{s} + \gamma^*_{j,t} \cos \frac{2(\pi)j}{s} + \omega^*_{j,t},$$

for $j = 1, \ldots, \left(\frac{s}{2}\right)$.

Parameter Estimation

Estimating the parameters of the model [83] entails figuring out the variances or covariances of the irregular components $(\sigma^2_\xi, \sigma^2_\delta, \sigma^2_\varepsilon)$, as well as the initial values of the components $(\mu_0, \beta_0, \gamma_0)$.

State variables:

$$\mathbf{x}_t = \begin{bmatrix} \mu_t \\ \beta_t \\ \gamma_t \end{bmatrix}$$

State vector at time t, consisting of the level (μ_t), trend (β_t) and seasonal (γ_t) components.

State Transition Matrix $\mathbf{F}_t$:

$$\mathbf{F}_t = \begin{bmatrix} 1 & 1 & 0 \\ 0 & 1 & 0 \\ 0 & 0 & -1 \end{bmatrix}$$

The state's evolution over time is controlled by this matrix. It displays variations in the seasonal, trend, and level components.

State Equation:

$$\mathbf{x}_{t+1} = \mathbf{F}_t \mathbf{x}_t + \mathbf{R}\omega_t$$

where w_t is the process noise, which captures the irregular fluctuations in the state variables.

Observation Equation:

$$y_t = \mathbf{Z}_t \mathbf{x}_t + f v_t$$

where $\mathbf{Z}_t = [1, 1, 1]$ is the observation matrix that maps the state variables to the observed value at time t and v_t is the observation noise.
Error Terms: The irregular oscillations in the state variables are represented by the process w_t. Given $\mathbf{0}$ as the mean and $\mathbf{Q}_t$ as the covariance matrix, it is distributed according to a multivariate normal distribution.
Observation noise v_t: The predicted value of the time series given the state variables is different from the actual value of the time series [25]. A normal distribution is indicated by its mean of 0 and variance of σ_ε^2.

2.4 Formulations of Multiple Seasonal Time-Series Models as Innovations State Space Models

According to [50], the innovation formulation of the state-space model can be written as:

$y_t = \mathbf{F}\mathbf{x}_t + \omega_t$

$\mathbf{x}_{t+1} = \mathbf{G}\mathbf{x}_t + \mathbf{R}\omega_t$

where:

$y_t \rightarrow$ denotes the observation at time t

$\mathbf{x}_t \rightarrow$ represents state vector the containing Level, Trand, and Seasonality

$\omega_t \rightarrow$ be a series of white noise.

Based on his references, Hyndman's innovation state-space formula relates the error of the state equation to the error of the observation equation as follows: $\omega_t \approxeq \mathbf{R}\omega_t$,where $\mathbf{R}$ is a fixed vector of persistence parameters [9]. It is a "innovations" state space model since these two equations use the same errors, or innovations [9]. Since the models explicitly indicate the level, trend, and seasonal components, the state-space model philosophy aligns nicely with the exponential smoothing technique. ARIMA models, on the other hand, make it less straightforward to figure out these components [11].

2.4.1 A Holt-Winters (HW) Method Innovations State Space Model

A well-liked method for time-series forecasting, especially for data containing seasonality and trends, is the HW method [35]. In order to evaluate the level, trend, and seasonal components of the data and use them to construct forecasts, the procedure entails smoothing the data. To provide a formal mathematical context for the description of the HW technique, one might create an innovative state-space model [9].

The value of the series y_t is broken down into an error w_t, a level l_t, a trend b_t and a seasonal component s_t by a model for the additive seasonal

HW technique. The $ETS(A, A, A)$ model is the underlying innovations state space model [93]:

$$y_t = l_{t-1} + b_{t-1} + s_{t-m} + w_t \tag{11}$$

$l_t = l_{t-1} + b_{t-1} + \alpha w_t$
$b_t = b_{t-1} + \beta w_t$
$s_t = s_{t-m} + \gamma w_t$
where:
$w_t \sim NID(0, \sigma^2)$

The smoothing parameters for the level, trend, and seasonal factors are denoted by α, β, and γ, respectively. The number of seasons in a single seasonal cycle is denoted by m.

This HW model corresponds to the state space model with the following vectors and metrics [35].

$$\mathbf{x}_t = \begin{bmatrix} l_t & b_t & s_t & s_{t-1} & . & . & . & s_{t-m+1} \end{bmatrix}^T$$

$$\mathbf{R} = \begin{bmatrix} \alpha & \beta & \gamma & 0 & . & . & . & 0 \end{bmatrix}^T$$

$$\mathbf{G} = \begin{bmatrix} 1 & 1 & 0 & 0 & . & . & . & 0 & 0 \\ 0 & 1 & 0 & 0 & . & . & . & 0 & 0 \\ 0 & 0 & 0 & 0 & . & . & . & 0 & 1 \\ 0 & 0 & 1 & 0 & . & . & . & 0 & 0 \\ 0 & 0 & 0 & 1 & . & . & . & 0 & 0 \\ . & . & . & . & . & & & . & . \\ . & . & . & . & & . & & . & . \\ . & . & . & . & & & . & . & . \\ 0 & 0 & 0 & 0 & . & . & . & 1 & 0 \end{bmatrix}$$

$$\mathbf{F} = \begin{bmatrix} 1 & 1 & 0 & . & . & . & 0 & 1 \end{bmatrix}$$

As in Equation (2), we can define the state-space model equation as follows [77], and [44]:

$\mathbf{x}_{t+1} = \mathbf{G}\mathbf{x}_t + \mathbf{R}w_t$

$$\begin{bmatrix} l_{t+1} \\ b_{t+1} \\ s_{t+1} \\ s_t \\ . \\ . \\ . \\ s_{t-m+2} \end{bmatrix} = \begin{bmatrix} 1 & 1 & 0 & 0 & . & . & . & 0 & 0 \\ 0 & 1 & 0 & 0 & . & . & . & 0 & 0 \\ 0 & 0 & 0 & 0 & . & . & . & 0 & 1 \\ 0 & 0 & 1 & 0 & . & . & . & 0 & 0 \\ 0 & 0 & 0 & 1 & . & . & . & 0 & 0 \\ . & . & . & . & . & & & . & . \\ . & . & . & . & & . & & . & . \\ . & . & . & . & & & . & . & . \\ 0 & 0 & 0 & 0 & . & . & . & 1 & 0 \end{bmatrix} \begin{bmatrix} l_t \\ b_t \\ s_t \\ s_{t-1} \\ . \\ . \\ . \\ s_{t-m+1} \end{bmatrix} + \begin{bmatrix} \alpha \\ \beta \\ \gamma \\ 0 \\ 0 \\ . \\ . \\ . \\ 0 \end{bmatrix} w_t$$

The aggregate form of the above equation is given as follows [38]:

$$\begin{bmatrix} l_{t+1} \\ b_{t+1} \\ \mathbf{c}_{t+1} \end{bmatrix} = \begin{bmatrix} \mathbf{G}_1 & \mathbf{0} \\ \mathbf{0} & \mathbf{G}_2 \end{bmatrix} \begin{bmatrix} l_t \\ b_t \\ \mathbf{c}_t \end{bmatrix} + \begin{bmatrix} \alpha \\ \beta \\ \gamma \\ \mathbf{0} \end{bmatrix} w_t$$

Where:

Seasonal cycle $\mathbf{c}_t = \begin{bmatrix} s_t & s_{t-1} & . & . & . & s_{t-m+1} \end{bmatrix}^T$,

$$\mathbf{G}_1 = \begin{bmatrix} 1 & 1 \\ 0 & 1 \end{bmatrix},$$

$$\mathbf{G}_2 = \begin{bmatrix} 0 & 0 & . & . & . & 0 & 0 \\ 1 & 0 & . & . & . & 0 & 0 \\ 0 & 1 & . & . & . & 0 & 0 \\ . & . & . & & & . & . \\ . & . & & . & & . & . \\ . & . & & & . & . & . \\ 0 & 0 & . & . & . & 1 & 0 \end{bmatrix}$$

Example: To further clarify the preceding generalization, let us look at the straightforward example for HW(m).

The general equation for a single seasonal cycle is given by Equation (30).

Let:

$\mathbf{x}_t = \begin{bmatrix} l_t & b_t & s_{t-m+1} \end{bmatrix}^T$

$\mathbf{R} = \begin{bmatrix} \alpha & \beta & \gamma \end{bmatrix}^T$

$$\mathbf{G} = \begin{bmatrix} 1 & 1 & 0 \\ 0 & 1 & 0 \\ 0 & 0 & 1 \end{bmatrix}$$
$$\mathbf{F} = \begin{bmatrix} 1 & 1 & 1 \end{bmatrix}$$

The state space model equation is given by:

$$\begin{aligned} \mathbf{x}_{t+1} &= \mathbf{G}\mathbf{x}_t + \mathbf{R}w_t \\ \begin{bmatrix} l_{t+1} \\ b_{t+1} \\ s_{t-m+2} \end{bmatrix} &= \begin{bmatrix} 1 & 1 & 0 \\ 0 & 1 & 0 \\ 0 & 0 & 1 \end{bmatrix} \begin{bmatrix} l_t \\ b_t \\ s_{t-m+1} \end{bmatrix} + \begin{bmatrix} \alpha \\ \beta \\ \gamma \end{bmatrix} w_t \\ &= \begin{bmatrix} l_t + b_t \\ b_t \\ s_{t-m+1} \end{bmatrix} + \begin{bmatrix} \alpha w_t \\ \beta w_t \\ \gamma w_t \end{bmatrix} \end{aligned}$$

When we add the right-hand matrices, we get the following equation:

$$\begin{bmatrix} l_{t+1} \\ b_{t+1} \\ s_{t-m+2} \end{bmatrix} = \begin{bmatrix} l_t + b_t + \alpha w_t \\ b_t + \beta w_t \\ s_{t-m+1} + \gamma w_t \end{bmatrix} \tag{12}$$

According to Equation (1), the observation equation is given by:

$$\begin{aligned} y_t &= \mathbf{F}\mathbf{x}_t + v_t \equiv \mathbf{F}\mathbf{x}_t + w_t, \quad \text{since } w_t \text{ is an innovation} \\ &= \mathbf{F}\mathbf{x}_t + w_t \\ &= \begin{bmatrix} 1 & 1 & 1 \end{bmatrix} \begin{bmatrix} l_t \\ b_t \\ s_{t-m+1} \end{bmatrix} + w_t \\ &= l_t + b_t + s_{t-m+1} + w_t \end{aligned}$$

According to the relationship between the observation equation and the state equation, we have the following [35].

$$
\begin{aligned}
y_t &= l_t + b_t + s_{t-m+1} + w_t \\
&= l_{t-1} + b_{t-1} + \alpha w_t + b_{t-1} + \beta w_t + s_{t-m} + \gamma w_t + w_t
\end{aligned}
\tag{13}
$$

Equation 13 is equal to Equation 11, where:

$l_t = l_{t-1} + b_{t-1} + \alpha w_t$

$b_t = b_{t-1} + \beta w_t$

$s_t = s_{t-m} + \gamma w_t$

Therefore, we have an additive seasonal HW(m) that is specified under Equation 11 above when we explicitly describe the level, trend, and seasonality.

2.5 Multiple Seasonal Models

Time series containing several seasonal patterns, such as retail sales or power consumption, can be forecasted using the DSHW model. Integrating ARMA error structures into the DSHW model is a well-discussed enhancement in the literature. Reference [77] stated that residual autocorrelation can include underlying stochastic dependencies to increase prediction accuracy. Combining these techniques will help us correct the established prejudices in the model and produce better forecasts.

There is a great deal of study on time-series predicating, including several seasonal patterns; state-space models and exponential smoothing techniques have made significant contributions to this discipline. The HW exponential smoothing method is a basic technique used frequently in seasonal data forecasting [93]. Although the approach is simple and effective, it suffers from complex seasonal patterns, since it depends on a great number of beginning values and inflexible structural updates of seasonal components.

Reference [80] suggested the DS exponential smoothing method as a way to get around some of these problems. It does this by combining two levels of seasonal cycles, such as daily and weekly patterns. However, the DS method, which assumes the same intra-day cycles every day, ignores real-world variances.

One flexible way to describe time series data is with SSMs, which depict the data using time-varying, unobservable state variables. Engineering, econometrics, and environmental research are among the many areas that utilize SSMs, according to [76]. This is due to their ability to account for measurement noise with system dynamics.
In SSMs, the Kalman filter is an essential tool for estimating states from noisy data and finding optimal solutions with Gaussian assumptions [54], [97], and [97].
State-space models potentially offer exponential smoothing, improved flexibility, and Kalman filter-free parameter prediction, according to [65] and [52]. These models manage missing values and produce additive and multiplicative seasonal trends.
Reference [42] proposed unobserved component models with numerous error sources, while [65] proposed a single-source error model that enhances computational efficiency and interpretability. State-space models are more interpretable and flexible than sophisticated and tuning-intensive ARIMA models [11]. Reference [28] introduced the BATS and TBATS models to analyze complicated seasonal cycles. To stabilize variance and resolve non-linearity, the BATS model is used. But dual-calendar effects and non-integer seasonalities create challenges. With trigonometric representation, Box-Cox transformation, ARMA error structure, and a trend component, the TBATS model increases performance. The TBATS model effectively controls non-integer seasonality and dual-calendar effects, therefore enhancing forecasting accuracy and processing efficiency.
An instrument for spectral analysis, the periodogram approximates the power distribution of a time series over several frequencies. One of its most important features for selecting and refining models is its capacity to detect salient frequencies, as Shumway and Stoffer emphasize. To better predict and understand cyclical behavior, the periodogram can be used to identify periodic components in the data. These components can then be incorporated into SSMs. Advantages include being applicable to both stationary and nonstationary series, being computationally efficient,

and being simple.
Finding dominant frequencies requires periodograms; the DSHW model's ARMA error inclusion greatly increases forecasting accuracy. According to the literature, time series analysis benefits from SSMs. These strategies taken collectively help to improve the clarity and longevity of time series models.

2.5.1 DSHW Model

Reference [80] developed a novel approach to estimating short-term power demand using the DSHW exponential smoothing model. Particularly well-suited to this paradigm are time series data sets that exhibit numerous seasonal patterns, such as the daily and weekly fluctuations in power demand.
[80]'s research revealed that the DSHW model is a helpful tool for utility companies and lawmakers, since it is good at capturing both short-term and long-term seasonality. Autocorrelation in the error terms was looked at using AR(1) residuals in Taylor's method. As we refer above, he used an AR(1) structure to handle short-term dependencies in error prediction, improving model accuracy. Despite its success, the AR(1) technique may not be flexible enough to capture more complex error structures in real-world electrical demand data.
Chapter 5 adds to what is known by filling in the gaps left by the AR(1) technique limitations by adding ARMA (p, q) residuals to the DSHW model. The improved performance for the recommended improvement should give practitioners a more efficient tool for power consumption estimates. The state space formulation also promises more adaptability to different forecasting conditions because it gives a logical framework for model estimates and inferences.

2.5.2 STL Model

Separating time series data into its component pieces—seasonal, trend, and remainder—has been a major challenge in statistical analysis and

forecasting [75]. Over the years, several attempts have been made to address this issue; nonetheless, most conventional decomposition techniques depend on parametric models or moving averages. Still, using these traditional approaches, complex seasonal patterns, missing data, and non-linear trends can sometimes be challenging.

Introduced by [23], the STL showed a clear development in this field of research. Local weighted regression (Loess) for trend and seasonal component estimation offers the STL approach a flexible and dependable way of dissecting time-series data. This decomposition technique is unique in that it allows adaptive smoothing, therefore capturing temporal variations and non-linear patterns.

A large number of studies conducted since the introduction of STL have highlighted the advantages of using it in comparison to more conventional approaches, particularly in areas such as climatology, economics, and the social sciences. According to the findings of studies, STL is widely used in situations with real-world data quality difficulties, as it is able to deal with missing values and outliers [74]. The iterative process of STL is able to capture trend-seasonal interactions, resulting in more reliable insights than static decomposition methods.

Later research has investigated ways to improve and extend STL, such as tactics to improve processing efficiency and scalability for massive data. This is something that has been done despite the fact that STL has its virtues. Hybrid models that mix STL with periodogram techniques have also been presented as a means of improving the accuracy of predictions through the utilization of deconstructed components in predictive models.

Finally, an important development in time series analysis was the introduction of STL decomposition by [23]. This tool is crucial for those who examine complex temporal data characterized by various seasonal and trend patterns due to its versatility, resilience, and adaptability.

2.5.3 BATS Model

Reference [27] addresses the need for consistent automated forecasting systems capable of managing complex time series data, particularly including data with many seasonal trends. Even in cases where conventional exponential smoothing techniques perform effectively for time series neither non-seasonal nor single-seasonal, they often fail when handling data showing various seasonalities or non-linear features.
[27] enhances the exponential smoothing state-space framework by integrating an ARMA model to account for residual autocorrelation and a Box-Cox transformation to manage non-linearity. This enhanced framework broadens the scope of traditional methods to accommodate more complex time series designs; it is known as BATS.
The BATS model distinguishes itself from other autonomous forecasting systems mostly by its capacity to manage several seasonal patterns. Stabilizing non-linear data variance with the Box-Cox transformation and obtaining residual autocorrelation with the ARMA component help to attain enhanced forecast accuracy [21]. [27]'s work marks a major progress in the field of historical data event prediction. It offers an automated approach that is more flexible and applicable in many situations, including those with complicated seasonal trends.

2.5.4 TBATS Model

Time series forecasting literature emphasizes the difficulties of reproducing intricate seasonal patterns including many seasonalities and non-integer periodicity. These kinds of seasonal pattern are not compatible for conventional techniques such as ARIMA and exponential smoothing. Examined have been several techniques including SARIMA, Fourier series approximations, GAMs, and wavelet modifications. Each of these techniques does, however, have restrictions in terms of interpretability, scalability, and adaptability.
The TBATS model, created by [28] and [1], uses trigonometric seasonal components (Fourier terms), Box-Cox transformations, ARMA errors,

trend components, and seasonal adjustments to address these concerns. In various applications, such as energy consumption and transportation data, this model accurately forecasts complex seasonal patterns.
In environments with unpredictable and long seasonal cycles, TBATS performs better than conventional methods, according to comparative research. The benefits aren't stopping researchers from working to make it even better by making it more scalable and making it work with all the latest machine learning methods. With its robust basis for handling complex seasonal fluctuations, the TBATS model is a major advancement in time series forecasting.

2.6 Spectral Analysis and Periodograms

Spectral analysis in general and periodograms specifically can assist find seasonal trends in time series data. Based on [67], periodograms graphically show the frequency spectrum of time series, hence illuminating the data periodicity. Periodograms clearly show seasonal cycles as prominent frequencies by moving the data to the frequency domain.
A bunch of studies have used periodograms to examine time series data that have complex seasonal trends. For instance, periodograms have been helpful in the stock market and economic data to identify trends [33]. Data from the weather and climate can be studied using periodograms because of the many seasonalities that occur in this type of data [13].
Periodograms have their uses, but they are not always immune to noise that could mask important trends. The Lomb-Scargle periodogram [72] and other advanced statistical methods have been suggested to overcome this issue by improving the frequency spectrum's resolution and reliability.
A possible approach for data displaying multiple seasonalities has been to combine traditional time series models with spectral analysis based on periodograms. The frequency domain properties identified in the periodograms can be used to inform predicting models, including state-space models and machine learning approaches [88].

Hybrids combining ideas from the time domain (such as ARIMA) and frequency domain (such as periodograms) are the most successful multi-seasonal forecasting models. These models try to reflect the cyclical character of the frequency spectrum and its temporal dependence. Reference [50] tried to improve forecasts when several seasonalities are present by including Fourier terms as explanatory variables in forecasting models.
Additionally, RNNs and LSTM networks, two types of deep learning models, have been used to model complex seasonal behaviors. From employing LSTMs as stand-alone black-box models to incorporating them into hybrid frameworks that capitalize on both the advantages of deep learning (non-linear pattern identification) and traditional time series principles (explicit decomposition), the literature has a clear trajectory. According to the state-of-the-art, architectures that either intelligently pre-process the data or directly model the interactions between various seasonal cycles using more sophisticated mechanisms like attention appear to be the most promising route for handling multiple seasonality, rather than pure LSTM models [7], and [73]. Reference [94] states that when dealing with scenarios including many overlapping seasonal cycles, these deep learning models outperform classical statistical models. Using periodograms is one approach to feed these models the data in the frequency domain.

3 State Space ARIMA Model Formulation and Its Application

3.1 Introduction

Time series forecasting is a cornerstone of econometric and statistical modeling, with applications spanning economics, engineering, and environmental science. The Autoregressive Integrated Moving Average (ARIMA) model, introduced by Box and Jenkins [12], stands as a foundational methodology due to its flexibility in modeling a wide range of stochastic processes. By integrating autoregressive (AR), differencing (I), and moving average (MA) components, ARIMA provides a robust framework for analyzing and forecasting stationary time series data.

However, a primary limitation of the classical ARIMA model is its assumption of fixed parameters over time, which restricts its ability to capture complex, evolving dynamics in systems where the underlying state variables are non-stationary or subject to structural shifts. This shortcoming is particularly evident in applications such as energy demand forecasting, where consumption patterns are influenced by a confluence of seasonal, economic, and behavioral factors that change over time.

To address these limitations, state-space models offer a powerful and flexible alternative. Originating from control theory [54] and later formalized in statistical time series analysis [42], and [30], the state-space framework explicitly models a system's latent (unobserved) states as they evolve dynamically. This formulation provides a unified approach for smoothing, filtering, and forecasting, and has been successfully integrated with traditional methods, such as exponential smoothing [50].

Building upon this synergy, the State-Space ARIMA (SSARIMA) model emerges as a significant advancement, merging the descriptive strengths of ARIMA with the dynamic adaptability of state-space representations. By recasting the ARIMA structure within a state-space formulation, the SSARIMA model can incorporate time-varying parameters and latent components, potentially yielding more accurate and statistically efficient

forecasts [24], and [76].
This dissertation makes two primary contributions to the field of time series forecasting. First, it provides a rigorous and detailed derivation of the SSARIMA model from its conventional ARIMA counterpart, explicitly formulating its state and observation equations. Second, it demonstrates the practical utility and enhanced predictive performance of the SSARIMA framework through an empirical application to forecasting electricity consumption in Hungary. By conducting a comparative analysis with standard ARIMA models, this research illustrates how the state-space approach improves forecast accuracy by more effectively capturing the underlying dynamics of complex temporal data.
The following sections elaborate on the theoretical foundation of the SSARIMA model, detail the methodological framework for its estimation and forecasting, and present empirical results that validate its superior performance in a real-world forecasting scenario.

3.1.1 State Space Model Formulation

State Space AR(p) Model

The autoregressive AR(p) model is formally equivalent to the ARIMA(p,0,0) specification. To elucidate this relationship within the state-space paradigm, this section employs the AR(2) model as a canonical example.
A state-space representation of the AR(2) process is first derived. Subsequently, it is demonstrated that the canonical AR(2)—and, by generalization, the AR(p)—difference equation is recovered from this state-space formulation. The representation employs the Controllability Canonical Form for its structural clarity and analytical utility [17].
The general form of the discrete-time AR(2) or ARIMA(2,0,0) model is given by:

$$y_t = \phi_1 y_{t-1} + \phi_2 y_{t-2} + w_t \tag{14}$$

where:
y_t, y_{t-1}, y_{t-2} are the values at time t, t-1, and t-2.

ϕ_1, ϕ_2 are the autoregressive coefficients.
w_t is white noise with mean zero and constant variance.
Let: $\mathbf{G}$, $\mathbf{R}$, $\mathbf{F}$, and $\mathbf{x}_t$ represents a state transition matrix, Observation disturbance matrix, Observation equation matrix, and State vector, respectively. Let us represent them as [17].

$$\mathbf{G} = \begin{bmatrix} \phi_1 & 1 \\ \phi_2 & 0 \end{bmatrix}_{2\times 2}, \quad \mathbf{R} = \begin{bmatrix} 1 \\ 0 \end{bmatrix}_{2\times 1}, \quad \mathbf{F} = \begin{bmatrix} 1 & 0 \end{bmatrix}_{1\times 2}$$

$\mathbf{x}_t = [x_{1,t}, x_{2,t}]^T$, is the state vector, where T represents "Transpose"
From Equation 2, we have the following:

$$\mathbf{x}_{t+1} = \begin{bmatrix} \phi_1 & 1 \\ \phi_2 & 0 \end{bmatrix} \mathbf{x}_t + \begin{bmatrix} 1 \\ 0 \end{bmatrix} w_t, \text{just substituting by } \mathbf{G} \text{ and } \mathbf{R}$$

The state space equation that results from updating the components of the state vector in the previous expression is as follows.

$$\begin{bmatrix} x_{1,t+1} \\ x_{2,t+1} \end{bmatrix} = \begin{bmatrix} \phi_1 & 1 \\ \phi_2 & 0 \end{bmatrix} \begin{bmatrix} x_{1,t} \\ x_{2,t} \end{bmatrix} + \begin{bmatrix} 1 \end{bmatrix} w_t \tag{15}$$

Equation 15 is a state space form of AR(2). Now, let us drive the general formula of AR(2) time series model from equation 15 as follows:

$$\begin{aligned} \begin{bmatrix} x_{1,t+1} \\ x_{2,t+1} \end{bmatrix} &= \begin{bmatrix} \phi_1 & 1 \\ \phi_2 & 0 \end{bmatrix} \begin{bmatrix} x_{1,t} \\ x_{2,t} \end{bmatrix} + \begin{bmatrix} 1 \\ 0 \end{bmatrix} w_t \\ &= \begin{bmatrix} \phi_1 x_{1,t} + x_{2,t} \\ \phi_2 x_{1,t} \end{bmatrix} + \begin{bmatrix} w_t \\ 0 \end{bmatrix} \\ &= \begin{bmatrix} \phi_1 x_{1,t} + \phi_2 x_{1,t-1} + w_t \\ \phi_2 x_{1,t} \end{bmatrix} \end{aligned}$$

$\rightarrow$ this is the simplification form of state transition equation.

An observation equation is defined by Equation 1. So, observation

equation is general given by:

$$\begin{aligned} y_t &= [1,0]\,\mathbf{x}_t \\ &= [1,0]\begin{bmatrix} x_{1,t} \\ x_{2,t} \end{bmatrix} \\ &= x_{1,t} \\ &= \phi_1 x_{1,t-1} + \phi_2 x_{1,t-2} + w_t \\ &= \phi_1 y_{t-1} + \phi_2 y_{t-2} + w_t \end{aligned}$$

$\Rightarrow y_t = \phi_1 y_{t-1} + \phi_2 y_{t-2} + w_t$.
Where $(y_t = x_{1,t})$ shows the r/ship b/n state transition and observation equation.
This equation is the general formula for the AR(2) time series model. So, Equation 15 above is a good representation of the state space model for the AR(2) time series model.
Based on the above subtopic, the generalized state-space representation form for the AR(p) time series model is presented as follows.
The form of an autoregressive model of order p, or AR(p), is stated as:

$$y_t = \phi_1 y_{t-1} + \phi_2 y_{t-2} + \ldots + \phi_p y_{t-p} + w_t; \quad w_t \sim NID(0, \sigma_w^2) \qquad (16)$$

Let us define the following: $\mathbf{x}_t = \begin{bmatrix} x_{1,t} \\ x_{2,t} \\ . \\ . \\ . \\ x_{p,t} \end{bmatrix}_{p\times 1}$, $\mathbf{R} = \begin{bmatrix} 1 \\ 0 \\ . \\ . \\ . \\ 0_{p-1} \end{bmatrix}_{p\times 1}$,

$$\mathbf{G} = \begin{bmatrix} \phi_1 & 1 & 0 & \cdots & 0 \\ \phi_2 & 0 & 1 & \cdots & 0 \\ \vdots & \vdots & \vdots & \ddots & \vdots \\ \phi_{p-1} & 0 & \cdots & 0 & 1 \\ \phi_p & 0 & 0 & \cdots & 0 \end{bmatrix}_{p\times p} \quad \text{,and} \quad \mathbf{F} = \begin{bmatrix} 1 & 0 & 0 & ... & 0 \end{bmatrix}_{1\times p}$$

Then, the observation equation $y_t = \begin{bmatrix} 1 & 0 & 0 & \cdots & 0 \end{bmatrix} \mathbf{x}_t$ and the state transition equation are given as follows:

$$\mathbf{x}_{t+1} = \begin{bmatrix} \phi_1 & 1 & 0 & \cdots & 0 \\ \phi_2 & 0 & 1 & \cdots & 0 \\ \vdots & \vdots & \vdots & \ddots & \vdots \\ \phi_{p-1} & 0 & \cdots & 0 & 1 \\ \phi_p & 0 & 0 & \cdots & 0 \end{bmatrix} \mathbf{x}_t + \mathbf{R} w_t$$

When we substitute the values of $\mathbf{x}_{t+1}$, $\mathbf{x}_t$, and $\mathbf{R}$, the equation would be:

$$\begin{bmatrix} x_{1,t+1} \\ x_{2,t+1} \\ \vdots \\ x_{p,t+1} \end{bmatrix} = \begin{bmatrix} \phi_1 & 1 & 0 & \cdots & 0 \\ \phi_2 & 0 & 1 & \cdots & 0 \\ \vdots & \vdots & \vdots & \ddots & \vdots \\ \phi_{p-1} & 0 & \cdots & 0 & 1 \\ \phi_p & 0 & 0 & \cdots & 0 \end{bmatrix} \begin{bmatrix} x_{1,t} \\ x_{2,t} \\ \vdots \\ x_{p,t} \end{bmatrix} + \begin{bmatrix} 1 \\ 0 \\ \vdots \\ 0 \end{bmatrix} w_t \tag{17}$$

The aggregate form of Equation 17 is:

$$\mathbf{x}_{t+1} = \begin{bmatrix} \boldsymbol{\phi}_{(p-1)\times 1} & \mathbf{I}_{(p-1)\times p-1} \\ \phi & \mathbf{0}_{1\times p-1} \end{bmatrix} \mathbf{x_t} + \begin{bmatrix} 1 \\ \mathbf{0}_{p\times 1} \end{bmatrix} w_t \tag{18}$$

Where:

$p \rightarrow$ is the order of the AR

$\boldsymbol{\phi}_{(p-1)\times 1} \rightarrow (p-1) \times 1$ vector of AR parameters

$\mathbf{I}_{(p-1)\times p-1} \rightarrow (p-1) \times p-1$ identity matrix

$\mathbf{0}_{1\times p-1} \rightarrow 1 \times p-1$ transpose zero vector

$\mathbf{0}_{p\times 1} \rightarrow p \times 1$ zero vector

$\mathbf{x} \rightarrow p \times 1$ state vector

Thus, the state space form of the AR(p) time series model is defined by Equations 17, and 18, as previously explained.

Formulation for State Space ARMA(p,q) Model

Example(2):Let us formulate an ARMA(2,2) time series model in state-

space form as an example. ARMA model of order p and q (ARMA(p,q)), has the following form:

$$y_t = \phi_1 y_{t-1} + \phi_2 y_{t-2} + w_t + \theta_1 w_{t-1} + \theta_2 w_{t-2}, w_t \sim NID(0, \sigma_w^2) \quad (19)$$

where: y_t is stationary
$w_t \sim NID(0, \sigma_w^2)$
$\theta_1, \theta_2, ..., \theta_p$ are constant parameters, and the mean of y_t is assumed to be zero.
We defined **G**, **R**, **F**, and $\mathbf{x}_t$ matrices to express the ARMA(2,2) model in state-space form as follows:

$$\mathbf{G} = \begin{bmatrix} \phi_1 & 1 & 0 \\ \phi_2 & 0 & 1 \\ 0 & 0 & 0 \end{bmatrix}_{3\times 3}, \mathbf{R} = \begin{bmatrix} 1 \\ \theta_1 \\ \theta_2 \end{bmatrix}_{3\times 1}, and \qquad \mathbf{F} = \begin{bmatrix} 1 & 0 & 0 \end{bmatrix}_{1\times 3}$$

The state vector is given by: $\mathbf{x}_t = [x_{1,t}, x_{2,t}, x_{3,t}]^T$

So, the state equation 2 is formulated as follows:

$$\begin{aligned} \mathbf{x}_{t+1} &= \mathbf{G}\mathbf{x}_t + \mathbf{R}w_t \\ &= \begin{bmatrix} \phi_1 & 1 & 0 \\ \phi_2 & 0 & 1 \\ 0 & 0 & 0 \end{bmatrix} \mathbf{x}_t + \begin{bmatrix} 1 \\ \theta_1 \\ \theta_2 \end{bmatrix} w_t \\ \begin{bmatrix} x_{1,t+1} \\ x_{2,t+1} \\ x_{3,t+1} \end{bmatrix} &= \begin{bmatrix} \phi_1 & 1 & 0 \\ \phi_2 & 0 & 1 \\ 0 & 0 & 0 \end{bmatrix} \begin{bmatrix} x_{1,t} \\ x_{2,t} \\ x_{3,t} \end{bmatrix} + \begin{bmatrix} 1 \\ \theta_1 \\ \theta_2 \end{bmatrix} w_t \end{aligned} \quad (20)$$

Hence, Equation 20 represents ARMA(2,2) time series model in state space form.
Here is the proof. Let us start from Equation 20

$$
\begin{aligned}
\begin{bmatrix} x_{1,t+1} \\ x_{2,t+1} \\ x_{3,t+1} \end{bmatrix} &= \begin{bmatrix} \phi_1 & 1 & 0 \\ \phi_2 & 0 & 1 \\ 0 & 0 & 0 \end{bmatrix} \begin{bmatrix} x_{1,t} \\ x_{2,t} \\ x_{3,t} \end{bmatrix} + \begin{bmatrix} 1 \\ \theta_1 \\ \theta_2 \end{bmatrix} w_t \\
&= \begin{bmatrix} \phi_1 x_{1,t} + x_{2,t} \\ \phi_2 x_{1,t} + x_{3,t} \\ 0 \end{bmatrix} + \begin{bmatrix} w_t \\ \theta_1 w_t \\ \theta_2 w_t \end{bmatrix} \\
&= \begin{bmatrix} \phi_1 x_{1,t} + x_{2,t} + w_t \\ \phi_2 x_{1,t} + x_{3,t} + \theta_1 w_t \\ \theta_2 w_t \end{bmatrix} \\
&= \begin{bmatrix} \phi_1 x_{1,t} + x_{2,t} + w_t \\ \phi_2 x_{1,t} + \theta_2 w_{t-1} + \theta_1 w_t \\ \theta_2 w_t \end{bmatrix} \\
&= \begin{bmatrix} \phi_1 x_{1,t} + \phi_2 x_{1,t-1} + \theta_2 w_{t-2} + \theta_1 w_{t-1} + w_t \\ \phi_2 x_{1,t} + \theta_2 w_{t-1} + \theta_1 w_t \\ \theta_2 w_t \end{bmatrix}
\end{aligned}
$$

On the other hand, the error for observation Equation 1 is assumed to be zero. So, we have the following relationship:

$$
\begin{aligned}
y_t &= [1, 0, 0]\, \mathbf{x}_t \\
&= [1, 0, 0] \begin{bmatrix} x_{1,t} \\ x_{2,t} \\ x_{3,t} \end{bmatrix} \\
&= x_{1,t} \\
&= \phi_1 x_{1,t-1} + \phi_2 x_{1,t-2} + \theta_2 w_{t-2} + \theta_1 w_{t-1} + w_t \\
&= \phi_1 y_{t-1} + \phi_2 y_{t-2} + \theta_2 w_{t-2} + \theta_1 w_{t-1} + w_t
\end{aligned}
$$

$\Rightarrow y_t = \phi_1 y_{t-1} + \phi_2 y_{t-2} + \theta_2 w_{t-2} + \theta_1 w_{t-1} + w_t$
Ultimately, we demonstrated that the generic formula for the ARMA(2,2) time series model can be obtained from Equation 20.
The state space form for the ARMA(p,q) time series model will now be

generalized as follows: Let:

$$\mathbf{G} = \begin{bmatrix} \phi_1 & 1 & 0 & \cdots & 0 \\ \phi_2 & 0 & 1 & \cdots & 0 \\ \vdots & \vdots & \vdots & \ddots & \vdots \\ \phi_{m-1} & 0 & \cdots & 0 & 1 \\ \phi_m & 0 & 0 & \cdots & 0 \end{bmatrix}_{m \times m} , \mathbf{F} = \begin{bmatrix} 1 & 0 & 0 & ... & 0 \end{bmatrix}_{1 \times m}$$

$$\mathbf{R} = \begin{bmatrix} 1 \\ \theta_1 \\ \theta_2 \\ \vdots \\ \theta_{m-1} \end{bmatrix}_{m \times 1}$$

,and $\mathbf{x}_t = \begin{bmatrix} x_{1,t}, x_{2,t}, \cdots, x_m \end{bmatrix}^T$

Then, the state space equation 2 is given by:

$$\mathbf{x}_{t+1} = \begin{bmatrix} \phi_1 & 1 & 0 & \cdots & 0 \\ \phi_2 & 0 & 1 & \cdots & 0 \\ \vdots & \vdots & \vdots & \ddots & \vdots \\ \phi_{m-1} & 0 & \cdots & 0 & 1 \\ \phi_m & 0 & 0 & \cdots & 0 \end{bmatrix} \mathbf{x}_t + \begin{bmatrix} 1 \\ \theta_1 \\ \theta_2 \\ \vdots \\ \theta_{m-1} \end{bmatrix} w_t$$

$$\begin{bmatrix} x_{1,t+1} \\ x_{2,t+1} \\ \vdots \\ x_{m,t+1} \end{bmatrix} = \begin{bmatrix} \phi_1 & 1 & 0 & \cdots & 0 \\ \phi_2 & 0 & 1 & \cdots & 0 \\ \vdots & \vdots & \vdots & \ddots & \vdots \\ \phi_{m-1} & 0 & \cdots & 0 & 1 \\ \phi_m & 0 & 0 & \cdots & 0 \end{bmatrix} \begin{bmatrix} x_{1,t} \\ x_{2,t} \\ \vdots \\ x_{m,t} \end{bmatrix} + \begin{bmatrix} 1 \\ \theta_1 \\ \theta_2 \\ \vdots \\ \theta_{m-1} \end{bmatrix} w_t \tag{21}$$

Where, $m = max(p, q+1)$, $\theta_l = 0$, for $q < l \leq m$, and $\phi_k = 0$, for $p < k \leq m$.

The aggregate form of Equation 21 is:

$$\mathbf{x}_{t+1} = \begin{bmatrix} \boldsymbol{\phi}_{(m-1)\times 1} & \mathbf{I}_{(m-1)\times(m-1)} \\ \phi & \mathbf{0}_{1\times(m-1)} \end{bmatrix} \mathbf{x}_t + \begin{bmatrix} 1 \\ \boldsymbol{\theta}_{(m-1)\times 1} \end{bmatrix} w_t \tag{22}$$

Where:

$\boldsymbol{\phi}_{(m-1)\times 1} \rightarrow (m-1) \times 1$ vector of AR parameters

$\mathbf{I}_{(m-1)\times(m-1)} \rightarrow (m-1) \times (m-1)$ identity matrix

$\mathbf{0}_{1\times(m-1)} \rightarrow 1 \times m-1$ transpose zero vector

$\boldsymbol{\theta}_{(m-1)\times 1} \rightarrow (m-1) \times 1$ MA parameters

$\mathbf{x} \rightarrow m \times 1$ state vector

Formulation for State Space MA(q) Model

The MA with order q can be found by applying the Equation 21 that was shown earlier in the case where there are no parameters for AR. In order to show them, let's begin with the fundamental MA example, also known as MA(2), and work our way up to the generalization state space form associated with the time series model MA(q) or ARMA(0,q). MA(2) model is given by:

$$y_t = w_t + \theta_1 w_{t-1} + \theta_2 w_{t-2} \tag{23}$$

Where:

θ_1 and θ_2 are the coefficients of the first and second lagged error terms.

Matrices:

$$\mathbf{G} = \begin{bmatrix} 0 & 1 & 0 \\ 0 & 0 & 1 \\ 0 & 0 & 0 \end{bmatrix}_{3\times 3}, \mathbf{R} = \begin{bmatrix} 1 \\ \theta_1 \\ \theta_2 \end{bmatrix}_{3\times 1} \text{,and } \mathbf{F} = \begin{bmatrix} 1 & 0 & 0 \end{bmatrix}_{1\times 3}$$

The state vector is defined as: $\mathbf{x}_t = \begin{bmatrix} x_{1,t} & x_{2,t} & x_{3,t} \end{bmatrix}^T$, T represents the transpose.

To utilize the general state equation, which is represented by Equation 2, let us make use of it. The following is what we obtain when we substitute the matrices that were discussed earlier in the state equation:

$$\begin{bmatrix} x_{1,t+1} \\ x_{2,t+1} \\ x_{3,t+1} \end{bmatrix} = \begin{bmatrix} 0 & 1 & 0 \\ 0 & 0 & 1 \\ 0 & 0 & 0 \end{bmatrix} \begin{bmatrix} x_{1,t} \\ x_{2,t} \\ x_{3,t} \end{bmatrix} + \begin{bmatrix} 1 \\ \theta_1 \\ \theta_2 \end{bmatrix} w_t \tag{24}$$

Equation 24 is the companion form for MA(2) in the state space. Following that, we are going to demonstrate that Equation 24 provides the formula for the MA(2) model.

$$\begin{aligned}
\begin{bmatrix} x_{1,t+1} \\ x_{2,t+1} \\ x_{3,t+1} \end{bmatrix} &= \begin{bmatrix} 0 & 1 & 0 \\ 0 & 0 & 1 \\ 0 & 0 & 0 \end{bmatrix} \begin{bmatrix} x_{1,t} \\ x_{2,t} \\ x_{3,t} \end{bmatrix} + \begin{bmatrix} 1 \\ \theta_1 \\ \theta_2 \end{bmatrix} \omega_t \\
&= \begin{bmatrix} x_{2,t} \\ x_{3,t} \\ 0 \end{bmatrix} + \begin{bmatrix} w_t \\ \theta_1 w_t \\ \theta_2 w_t \end{bmatrix} \\
&= \begin{bmatrix} x_{2,t} + w_t \\ \theta_2 w_{t-1} + \theta_1 w_t \\ \theta_2 w_t \end{bmatrix} \\
&= \begin{bmatrix} \theta_2 w_{t-2} + \theta_1 w_{t-1} + w_t \\ \theta_2 w_{t-1} + \theta_1 w_t \\ \theta_2 w_t \end{bmatrix}
\end{aligned}$$

(we substitute $x_{2,t}$ and $x_{3,t}$ from above relationship).

From observation equation (Equation 1), we have that:

$y_t = \mathbf{F}\mathbf{x}_t = \begin{bmatrix} 1 & 0 & 0 \end{bmatrix} \begin{bmatrix} x_{1,t} \\ x_{2,t} \\ x_{3,t} \end{bmatrix} = x_{1,t} = \theta_2 w_{t-2} + \theta_1 w_{t-1} + w_t$, where $x_{1,t+1} = \theta_2 w_{t-2} + \theta_1 w_{t-1} + w_t$

$\implies y_t = w_t + \theta_1 w_{t-1} + \theta_2 w_{t-2}$. This time series model is a moving average of order two.

Here, we established that Equation 24 represents the formula for the MA(2) time series model in state space.

Based on the instances of MA(2) that were presented before, the following is a generalization of the model for MA(q) or ARMA(0,q):

$$\mathbf{G} = \begin{bmatrix} 0 & 1 & 0 & . & . & . & 0 \\ 0 & & . & & & & . \\ . & & & . & & & . \\ . & & & & . & & . \\ . & & & & & . & 0 \\ 0 & & & & & 0 & 1 \\ 0 & 0 & . & . & . & 0 & 0 \end{bmatrix}_{(q+1)\times(q+1)} ; \mathbf{R} = \begin{bmatrix} 1 \\ \theta_1 \\ \theta_2 \\ . \\ . \\ . \\ \theta_q \end{bmatrix}_{q+1\times 1}, and,$$

$\mathbf{F} = \begin{bmatrix} 1 & \mathbf{0} \end{bmatrix}$, $1 * q$ matrix

Let us define the state vector as:

$\mathbf{x}_t = \begin{bmatrix} x_{1,t} & x_{2,t} & . & . & . & x_{q+1,t} \end{bmatrix}^T$

The observation equation is given by :

$y_t = \mathbf{F}\mathbf{x}_t$

Following this, the state space representation companion form for the MA(q) model is provided as follows in Equation 25:

$$\begin{bmatrix} x_{1,t+1} \\ x_{2,t+1} \\ . \\ . \\ . \\ x_{q+1,t+1} \end{bmatrix} = \begin{bmatrix} 0 & 1 & 0 & . & . & . & 0 \\ 0 & & . & & & & . \\ . & & & . & & & . \\ . & & & & . & & . \\ . & & & & & . & 0 \\ 0 & & & & & 0 & 1 \\ 0 & 0 & . & . & . & 0 & 0 \end{bmatrix} \begin{bmatrix} x_{1,t} \\ x_{2,t} \\ . \\ . \\ . \\ x_{q+1,t} \end{bmatrix} + \begin{bmatrix} 1 \\ \theta_1 \\ \theta_2 \\ . \\ . \\ . \\ \theta_q \end{bmatrix} w_t \quad (25)$$

The aggregate form of Equation 25 is given below:

$$\mathbf{x}_{t+1} = \begin{bmatrix} \mathbf{0}_{q\times 1} & \mathbf{I}_{q\times q} \\ 0 & \mathbf{0}_{1\times q} \end{bmatrix} \mathbf{x}_t + \begin{bmatrix} 1 \\ \boldsymbol{\theta}_{q\times 1} \end{bmatrix} w_t \quad (26)$$

Where:

$q \rightarrow$ is the order of the MA

$\mathbf{0}_{q\times 1} \rightarrow q \times 1$ zero vector

$\mathbf{I}_{q\times q} \rightarrow q \times q$ identity matrix
$\mathbf{0}_{1\times q} \rightarrow 1 \times q$ transposed zero vector
$\boldsymbol{\theta}_{q\times 1} \rightarrow q \times 1$ vector of MA parameters
$\mathbf{x}_{(q+1)\times 1} \rightarrow (q+1) \times 1$ state vector

Formulation for State Space IMA(d,q) Model

The state-space formulation uses the IMA model with d-order differencing and q-order moving average components. This versatile and robust method models, estimates, and predicts time-series data using the Kalman filter for recursive calculations. The basic formula for IMA(1,2), which is provided as follows, is the same as ARIMA(0,1,2):

$$y_t = y_{t-1} + w_t + \theta_1 w_{t-1} + \theta_2 w_{t-2} \tag{27}$$

$y_t - y_{t-1} = w_t + \theta_1 w_{t-1} + \theta_2 w_{t-2}$
$(1-B)y_t = (1 + \theta_1 B + \theta_2 B^2) w_t$
Let us define $\mathbf{G}$,$\mathbf{R}$,$\mathbf{F}$, and $\mathbf{x}_t$ as follows:

$$\mathbf{G} = \begin{bmatrix} 1 & 1 & 0 & 0 \\ 0 & 0 & 1 & 0 \\ 0 & 0 & 0 & 1 \\ 0 & 0 & 0 & 0 \end{bmatrix}, \mathbf{R} = \begin{bmatrix} 0 \\ 1 \\ \theta_1 \\ \theta_2 \end{bmatrix}, \mathbf{F} = \begin{bmatrix} 1 & 1 & 0 & 0 \end{bmatrix}, \text{ and}$$

The state vector is defined as: $\mathbf{x}_t = \begin{bmatrix} x_{1,t} & x_{2,t} & x_{3,t} & x_{4,t} \end{bmatrix}$

As [30], the state equation is given by: $\mathbf{x}_{t+1} = \mathbf{G}\mathbf{x}_t + \mathbf{R}\omega_t$

$$
\begin{aligned}
\begin{bmatrix} x_{1,t+1} \\ x_{2,t+1} \\ x_{3,t+1} \\ x_{4,t+1} \end{bmatrix} &= \begin{bmatrix} 1 & 1 & 0 & 0 \\ 0 & 0 & 1 & 0 \\ 0 & 0 & 0 & 1 \\ 0 & 0 & 0 & 0 \end{bmatrix} \begin{bmatrix} x_{1,t} \\ x_{2,t} \\ x_{3,t} \\ x_{4,t} \end{bmatrix} + \begin{bmatrix} 0 \\ 1 \\ \theta_1 \\ \theta_2 \end{bmatrix} w_t \\
&= \begin{bmatrix} x_{1,t} + x_{2,t} \\ x_{3,t} + \omega_t \\ x_{4,t} + \theta_1\omega_t \\ \theta_2\omega_t \end{bmatrix} \\
&= \begin{bmatrix} x_{1,t} + x_{2,t} \\ x_{3,t} + w_t \\ \theta_2 w_{t-1} + \theta_1 w_t \\ \theta_2 w_t \end{bmatrix} \\
&= \begin{bmatrix} x_{1,t} + x_{2,t} \\ \theta_2 w_{t-2} + \theta_1 w_{t-1} + w_t \\ \theta_2 w_{t-1} + \theta_1 w_t \\ \theta_2 w_t \end{bmatrix} \\
&= \begin{bmatrix} x_{1,t} + x_{2,t} \\ \theta_2\omega_{t-2} + \theta_1\omega_{t-1} + \omega_t \\ \theta_2\omega_{t-1} + \theta_1\omega_t \\ \theta_2\omega_t \end{bmatrix}
\end{aligned}
\tag{28}
$$

Now, the observation equation is given by:

$$
\begin{aligned}
y_t &= \mathbf{F}\mathbf{x}_t \\
&= \begin{bmatrix} 1 & 1 & 0 & 0 \end{bmatrix} \begin{bmatrix} x_{1,t} \\ x_{2,t} \\ x_{3,t} \\ x_{4,t} \end{bmatrix} = x_{1,t} + x_{2,t} \\
&= x_{1,t} + x_{2,t}, \quad \text{r/ship b/n the observation and the state.} \\
&= x_{1,t-1} + x_{2,t-1} + \theta_2 w_{t-2} + \theta_1 w_{t-1} + w_t, \quad \text{from the above equation.} \\
&= y_{t-1} + \theta_2 w_{t-2} + \theta_1 w_{t-1} + w_t, \quad \text{from the relationship.} \\
\implies y_t - y_{t-1} &= w_t + \theta_1 w_{t-1} + \theta_2 w_{t-2} \\
\implies (1-B)y_t &= (1 + \theta_1 B + \theta_2 B^2) w_t, \quad \text{the general formula for ARIMA(0,1,2).}
\end{aligned}
$$

The generalized state-space formula for the ARIMA(0,d,q) or IMA(d,q) time series model is obtained by setting all autoregressive parameters in the aforementioned ARIMA(p,d,q) generalized formula to zero.

Formulation for State Space ARIMA(p, d, q) Model

Combining state space with ARIMA, the state space ARIMA model (p, d, q) is a sophisticated time series framework. I model and project trend, seasonality, and stochastic data. For stationarity the model employs p AR, d differencing, and q MA terms [36]. For parameter estimation, forecasting, and missing data handling, state-space ARIMA models apply the Kalman filter. Reference [19] refers mainly to the example and state-space formulations of this topic (2.1.6.5). Basically, it shows the real applications of the ARIMA model in state-space form.

Example (6): We can consider the state-space form of the ARIMA(2,1,2) model [19] as an example. The ARIMA(2,1,2) time series model given by:

$$
\left(1 - \phi_1 B - \phi_2 B^2\right)(1 - B)\, y_t = (1 + \theta_1 B + \theta_2 B^2) w_t, \tag{29}
$$

Let:

$$\mathbf{G} = \begin{bmatrix} 1 & 1 & 0 & 0 \\ 0 & \phi_1 & 1 & 0 \\ 0 & \phi_2 & 0 & 1 \\ 0 & 0 & 0 & 0 \end{bmatrix}, \mathbf{R} = \begin{bmatrix} 0 \\ 1 \\ \theta_1 \\ \theta_2 \end{bmatrix}, \mathbf{F} = \begin{bmatrix} 1 & 1 & 0 & 0 \end{bmatrix}$$

, and

$\mathbf{x}_t = [x_{1,t}, x_{2,t}, x_{3,t}, x_{4,t}]^T$

Then, the state equation is given by:

$$\mathbf{x}_{t+1} = \begin{bmatrix} 1 & 1 & 0 & 0 \\ 0 & \phi_1 & 1 & 0 \\ 0 & \phi_2 & 0 & 1 \\ 0 & 0 & 0 & 0 \end{bmatrix} \mathbf{x}_t + \begin{bmatrix} 0 \\ 1 \\ \theta_1 \\ \theta_2 \end{bmatrix} w_t$$

$$\begin{bmatrix} x_{1,t+1} \\ x_{2,t+1} \\ x_{3,t+1} \\ x_{4,t+1} \end{bmatrix} = \begin{bmatrix} 1 & 1 & 0 & 0 \\ 0 & \phi_1 & 1 & 0 \\ 0 & \phi_2 & 0 & 1 \\ 0 & 0 & 0 & 0 \end{bmatrix} \begin{bmatrix} x_{1,t} \\ x_{2,t} \\ x_{3,t} \\ x_{4,t} \end{bmatrix} + \begin{bmatrix} 0 \\ 1 \\ \theta_1 \\ \theta_2 \end{bmatrix} w_t \tag{30}$$

Equation 30 above [64] is the state-space representation of the time series model: $(1 - \phi_1 B - \phi_2 B^2)(1 - B) y_t = (1 + \theta_1 B + \theta_2 B^2) w_t$, Next, let us prove that the state-space model of Equation 3 gives the general

formula for the ARIMA(2,1,2) time series model, stated in Equation 30.

$$\begin{aligned}
\begin{bmatrix} x_{1,t+1} \\ x_{2,t+1} \\ x_{3,t+1} \\ x_{4,t+1} \end{bmatrix} &= \begin{bmatrix} 1 & 1 & 0 & 0 \\ 0 & \phi_1 & 1 & 0 \\ 0 & \phi_2 & 0 & 1 \\ 0 & 0 & 0 & 0 \end{bmatrix} \begin{bmatrix} x_{1,t} \\ x_{2,t} \\ x_{3,t} \\ x_{4,t} \end{bmatrix} + \begin{bmatrix} 0 \\ 1 \\ \theta_1 \\ \theta_2 \end{bmatrix} w_t \\
&= \begin{bmatrix} x_{1,t} + x_{2,t} \\ \phi_1 x_{2,t} + x_{3,t} \\ \phi_2 x_{2,t} + x_{4,t} \\ 0 \end{bmatrix} + \begin{bmatrix} 0 \\ w_t \\ \theta_1 w_t \\ \theta_2 w_t \end{bmatrix} \\
&= \begin{bmatrix} x_{1,t} + x_{2,t} \\ \phi_1 x_{2,t} + x_{3,t} + w_t \\ \phi_2 x_{2,t} + x_{4,t} + \theta_1 w_t \\ \theta_2 w_t \end{bmatrix}
\end{aligned}$$

Let us substitute, $x_{4,t}$, in the following equation:

$$\begin{bmatrix} x_{1,t+1} \\ x_{2,t+1} \\ x_{3,t+1} \\ x_{4,t+1} \end{bmatrix} = \begin{bmatrix} x_{1,t} + x_{2,t} \\ \phi_1 x_{2,t} + x_{3,t} + w_t \\ \phi_2 x_{2,t} + \theta_2 w_{t-1} + \theta_1 w_t \\ \theta_2 w_t \end{bmatrix}$$

Again substitute $x_{3,t}$

$$\begin{bmatrix} x_{1,t+1} \\ x_{2,t+1} \\ x_{3,t+1} \\ x_{4,t+1} \end{bmatrix} = \begin{bmatrix} x_{1,t} + x_{2,t} \\ \phi_1 x_{2,t} + \phi_2 x_{2,t-1} + \theta_2 w_{t-2} + \theta_1 w_{t-1} + w_t \\ \phi_2 x_{2,t} + \theta_2 w_{t-1} + \theta_1 w_t \\ \theta_2 w_t \end{bmatrix}$$

From the above, we have the following relationship:

$$\begin{aligned} x_{1,t+1} &= x_{1,t} + x_{2,t} \\ \Rightarrow x_{2,t} &= x_{1,t+1} - x_{1,t} \\ y_t - y_{t-1} &= x_{1,t} + x_{2,t} - x_{1,t-1} - x_{2,t-1} \\ &= x_{1,t-1} + x_{2,t-1} + x_{2,t} - x_{1,t-1} - x_{2,t-1} \\ &= x_{2,t} \end{aligned}$$

The observation equation is given by:

$$\begin{aligned} y_t &= [1,1,0,0]\,\mathbf{x}_t \\ &= [1,1,0,0] \begin{bmatrix} x_{1,t} \\ x_{2,t} \\ x_{3,t} \\ x_{4,t} \end{bmatrix} \\ &= x_{1,t} + x_{2,t} \\ &= x_{1,t-1} + x_{2,t-1} + \phi_1 x_{2,t-1} + \phi_2 x_{2,t-2} + \theta_2 w_{t-2} + \theta_1 w_{t-1} + w_t \\ &= y_{t-1} + \phi_1 (y_{t-1} - y_{t-2}) + \phi_2 (y_{t-2} - y_{t-3}) + w_t + \theta_1 w_{t-1} + \theta_2 w_{t-2} \end{aligned}$$

$\Rightarrow y_t - y_{t-1} - \phi_1 (y_{t-1} - y_{t-2}) - \phi_2 (y_{t-2} - y_{t-3}) = w_t + \theta_1 w_{t-1} + \theta_2 w_{t-2}$
$\Rightarrow y_t^* - \phi_1 \left(y_{t-1}^*\right) - \phi_2 \left(y_{t-2}^*\right) = w_t + \theta_1 w_{t-1} + \theta_2 w_{t-2}$
Here, (*) represents the back-shift operators.

$$\Rightarrow \left(1 - \phi_1 B - \phi_2 B^2\right)(1 - B)\, y_t = (1 + \theta_1 B + \theta_2 B^2) w_t,$$

This is the ARIMA(2,1,2) model equation (where B represents the back-shift operator as (*) above)
Therefore, as we showed above, Equation (21) is the state-space representation for the ARIMA(2,1,2) time series model [19].
$ARIMA(p, d, q)$ Model general representation as state space form [19].

Initial State Distribution

$x_0 \sim N(m_0, C_0)$

Specify the initial-state distribution. This is the distribution of the state vector at time $t = 0$.

m_0 is the mean vector and C_0 is the covariance matrix.

In summary, the state-space form expression of the ARIMA(p,d,q) model offers a thorough depiction of the underlying dynamics in a time series. The state space formulation is a potent tool for time series analysis and forecasting since it includes MA, AR, and differencing components. The observation equation connects the observed values to the state vector and accounts for both random and systematic components. In addition to this, the state equation represents how the latent state vector changes over time. Effective estimate, filtering, and prediction are made easier by this state-space representation, which improves our capacity to recognize and describe intricate temporal patterns in the data.

3.2 Results and Discussion

The state space formulation offers a powerful framework for time series analysis and forecasting by systematically integrating autoregressive, differencing, and moving average components. Representing an ARIMA(p, d, q) model in this form clearly captures the underlying dynamics of the series. This approach facilitates efficient estimation, filtering, and prediction through two core equations: the observation equation, which relates the observed data to a latent state vector, and the state equation, which governs the evolution of that state over time. Together, these equations distinguish between the systematic structure of the series and its random disturbances.

This thesis introduces a robust and new state-space formulation approach of the Autoregressive Integrated Moving Average (ARIMA) model, termed the State Space ARIMA (SSARIMA). The proposed framework leverages the structural versatility of state-space representations to enhance the standard ARIMA methodology. By explicitly modeling the data-

generating process through state and observation equations, the SSARIMA provides a more refined and interpretable characterization of time series dynamics, capturing both observed data and latent state variables. The model's forecasting performance is empirically evaluated against the conventional ARIMA model using monthly Hungarian energy consumption data. Results indicate that the SSARIMA achieves superior predictive accuracy, even when benchmarked against a well-specified ARIMA model. These findings suggest that the SSARIMA is a powerful tool for time series analysis, particularly in domains where understanding underlying structural dynamics is critical. The framework effectively bridges classical time series modeling with more complex approaches, offering a synergistic blend of interpretability and enhanced forecasting performance, thereby presenting a valuable new avenue for both researchers and practitioners.
The dissertation has developed and presented an original state-space formulation of the ARIMA model. The SSARIMA framework advances time series analysis by integrating a state-space perspective, which facilitates a deeper structural understanding of series dynamics. A comparative performance analysis, conducted using monthly Hungarian power consumption data, demonstrates that the SSARIMA model yields superior forecasting accuracy relative to its conventional ARIMA counterpart. The enhanced efficacy of the SSARIMA, particularly in capturing the intrinsic dynamics of complex systems, underscores the significant advantage of incorporating state-space representations into traditional time series models.
The results establish the SSARIMA as an effective and versatile forecasting tool with broad applicability across disciplines such as economics, statistics, engineering, and computer science, where state-space modeling can provide a more profound comprehension of underlying processes. Future research may focus on extending the application of SSARIMA models to diverse data types and further refining the model architecture to augment its predictive capability and robustness.
A comprehensive presentation of the results, their analysis, and inter-

pretation for this model has been published as Chudo (2025) [19]. This dissertation therefore provides an overview, while the cited paper contains the full methodological and analytical detail.

3.3 Key Question and Contribution

Key Question
By modifying the standard ARIMA model with new state and observation equations, how can one formulate a State Space ARIMA models?

Finding/Contribution
Derived and proved the state space formulations for major time series models (AR, MA, ARMA, ARIMA, HW), providing a unified theoretical framework. (See subsection 2.1.4 in the dissertation). Derivation and formal proof of state space representations for the foundational models of time series analysis is a significant theoretical advancement because it provides a unified framework for understanding and working with these models. This unification not only offers deeper theoretical insight but also creates a consistent foundation for developing more efficient estimation and forecasting algorithms across the entire spectrum of classical time series models [19].

4 Multiplicative Seasonal ARIMA Modeling and Forecasting

4.1 Introduction

The chapter addresses the worldwide effect of COVID-19. Research has concentrated on detection, prevention, therapy, and forecasting, as COVID-19 generates significant financial and medical problems. Time-series modeling, which examines past data to forecast future patterns, is one of the areas of research. To coordinate reasonable responses, governments and healthcare facilities have to project the path of infection. This work intends to use a multiplicative SARIMA model to anticipate daily COVID-19 death rates in Hungary, 2020. By use of an accurate time series model, healthcare facilities improve patient care and help to better divide resources. Epidemic forecasting has made great advantage of time series modeling, since it allows one to search for trends and patterns in historical data.

Previous studies have used several statistical models, including ARIMA, AR, MA, and SARIMA. Examining the transmission of infectious diseases using these models can help with decisions on lock downs, medical resource allocation, and public health campaigns [53]. One advantage of time-series models over structural models is that they simplify modeling and forecasting [61]. Structural models require sophisticated epidemiological data and assumptions, while time series models can conveniently utilize historical case data. The ability of the ARIMA and SARIMA models to capture data swings and trends over the seasons has led to their widespread use in various fields.

Recently, the ARIMA and SSARIMA models have become somewhat well-known and found application in several fields. From reference [20], these include the analysis of natural rubber production for modeling and forecasting output in Malaysia [60], agricultural production analysis for forecasting yields in China [87], the examination of goods and services to predict inflation in Ghana [4], economic analyses aimed at forecasting

gold prices [31], and the investigation of air disasters globally through the application of a univariate time series model [62]. Using their study of airplane catastrophes worldwide from 1960 to 2013, [62] determined that the Box-Jenkins ARIMA model performs the best for future projections. As calculated [20], the fitted ARIMA (0, 1, 1) model has an AIC of 323.14, a BIC of 327.04, and a stationary R^2 of 0.348 rather than ARIMA (1, 1, 1), ARIMA (1, 1, 2), and ARIMA model withother different orders [20]. Precipitation in the Mount Kenya region was predicted using a univariate time series model by the authors [55]. The best seasonal ARIMA model was fitted to the data, and the model with the lowest AIC and BIC values was chosen. Using the three Box-Jenkins methods, model identification, parameter estimation, and diagnostic checking—they also projected the substantial precipitation component of data from water resource applications. This model is the best and most important, according to the results of the normality test and the forecasting assessment, which indicate an RMSE of 0.98384. Therefore, the ARIMA model with a multiplicative seasonal component (1, 0, 1) (1, 0, 0) [12] worked well to predict Kenyan precipitation drops [20].

Using the SARIMA model for novel coronavirus daily fatalities in Hungary, Chapter 3 seeks to predict and forecast it. After finding, fitting and estimating the multiplicative seasonal ARIMA model for COVID-19 daily deaths, I used the best-fitting model for SARIMA to anticipate the values of daily deaths [20]. As everyone knows, the world was in the midst of a brand-new outbreak in 2020 caused by the novel coronavirus. It was commonplace in Hungary and other countries. Every day, new cases and fatalities emerged. It sparked movements for transformation on all continents. Consequently, in order to help the relevant bodies, make the necessary decisions, and take the necessary steps to restrict the pandemic, it is crucial to fit and model the best appropriate time series model for projecting future confirmed and fatality cases of the COVID-19 outbreak [20].

4.2 The Box-Jenkins Methodology

To determine the optimal time-series model fit to the historical values of a time series, developed by statisticians Gwilym Jenkins and George Box, the Box-Jenkins technique, which is named after them [14]. This method uses ARMA or ARIMA models. Since many real-world time-series are obviously non-stationary, this approach does not lend itself well to using stationary models. To make an observed time series look like it came from a stationary process, the standard procedure in Box-Jenkins modeling is to differentiate it. We have created Box-Jenkins endowed modeling, which not only provides a foundation for forecasting, but also explains the mechanism that generates the series [12].
The Box-Jenkins method involves finding a suitable ARIMA model, fitting it to the data, and then using that model to make forecasts. This approach is one of the most common ways to analyze time-series data [63]. The fact that it is versatile enough to deal with stationary or non-stationary series, with or without seasonal components, and that it comes with well-documented software makes it a popular choice [86]. Only stationary series or those made stationary by differencing can be described or represented by a Box-Jenkins model. Each model is either an AR, MA, or mixed process model (ARMA). To determine if the time series includes a seasonal periodic component, we utilized the SARIMA model [20].

4.2.1 ARIMA Model

Box-Jenkins introduced the ARIMA model, which combines the parameters of the ARMA models. One kind of model parameter is the autoregressive parameter, and the other is the moving average parameter. The Box-Jenkins introduced the notation known as $ARIMA(p, d, q)$ for these models [77] and [71], where:

$p \rightarrow$ AR component order.

$d \rightarrow$ Order of integration.

$q \rightarrow$ MA component order.

The mathematical expression of the ARIMA model can be expressed as follows [71].

$\phi_p(B)(1-B)^d y_t = \theta_q(B)\varepsilon_t$

Where:

$y_t \rightarrow$ Time series data at time t.

$\varepsilon_t \rightarrow$ White noise at time t.

$B \rightarrow$ Backshift operator ($By_t = y_t - 1$).

$\phi_p(B) \rightarrow$ AR order p:

$\phi_p(B) = 1 - \phi_1 B - \phi_2 B^2 - \cdots - \phi_p B^p$

$\theta_q(B) \rightarrow$ MA order q:

$\theta_q(B) = 1 + \theta_1 B + \theta_2 B^2 + \cdots + \theta_q B^q$

$(1-B)^d \rightarrow$ Differencing order d.

The ARIMA model incorporates differencing into the previously established class of ARMA models. ARIMA models have many parameters, as mentioned in [96]. Box and Jenkins suggest a three-step process to estimate these models effectively. These are model identification, parameter estimation, and model checking.

4.2.2 Seasonal ARIMA (SARIMA) Models

Seasonal periodic components are present in a large number of time series in practice. Seasonal time series with a period S are characterized by the similarity of observations spaced S intervals apart. A broad multiplicative seasonal ARIMA model, or SARIMA for short, has been defined by Box and Jenkins as a way to handle seasonality in the ARIMA model. With the inclusion of a seasonality constraint, the SARIMA model fitting technique is identical to the ARIMA model fitting procedure [75].

To account for seasonality, Box and Jenkins extended the ARIMA model and defined a general multiplicative seasonal ARIMA (or SARIMA) model is denoted as $SARIMA(p,d,q)(P,D,Q)_s$, where

p : Order of the part AR

$d \rightarrow$ Differencing

$q \rightarrow$ Order of the part MA

$P \rightarrow$ Order of the part AR

$Q \rightarrow$ Order of the MA component (for seasonal)

$D \rightarrow$ Differencing (for seasonal)

$s \rightarrow$ Seasonal period

The mathematical formula for the SARIMA model can be expressed as follows [11]:

$\phi_p(B)\Phi_P(B^s)(1-B)^d(1-B^s)^D y_t = \theta_q(B)\Theta_Q(B^s)\varepsilon_t$

$(1-\phi_1 B-\phi_2 B^2-\cdots-\phi_p B^p)(1-\Phi_1 B^s-\Phi_2 B^{2s}-\cdots-\Phi_P B^{Ps})(B^s)(1-B)^d(1-B^s)=(1+\theta_1 B+\theta_2 B^2+\cdots+\theta_q B^q)(1+\Theta_1 B^s+\Theta_2 B^{2s}+\cdots+\Theta_Q B^{Qs})\varepsilon_t$

Where:

$y_t \rightarrow$ Time series data at time t.

$\varepsilon_t \rightarrow$ White noise at time t.

B : Backshift operator ($By_t = y_t - 1$).

$\phi_p(B) \rightarrow$ AR order p (Non-seasonal):

$\phi_p(B) = 1 - \phi_1 B - \phi_2 B^2 - \cdots - \phi_p B^p$

$\Phi_P(B^s) \rightarrow$ AR order P (Seasonal):

$\Phi_P(B^s) = 1 - \Phi_1 B^s - \Phi_2 B^{2s} - \cdots - \Phi_P B^{Ps}$

$\theta_q(B) \rightarrow$ MA order q (Non-seasonal):

$\theta_q(B) = 1 + \theta_1 B + \theta_2 B^2 + \cdots + \theta_q B^q$

$\Theta_Q(B^s) \rightarrow$ MA order Q (Seasonal):

$\Theta_Q(B^s) = 1 + \Theta_1 B^s + \Theta_2 B^{2s} + \cdots + \Theta_Q B^{Qs}$

$(1-B)^d \rightarrow$ Differencing operator of order d (Non-seasonal).

$(1-Bs)^D \rightarrow$ Differencing operator of order D (Seasonal).

4.3 Results and Discussion

4.3.1 Data set and Primarily Analysis

The Hungarian government and the WHO collaborated to compile coronavirus statistics in Hungary for the COVID-19 pandemic country-wise profile. From January 3, 2020, to September 1, 2021, there were 812,531 confirmed cases of COVID-19, with 30,059 deaths, according to the WHO study. This data is available on the website;

https://ourworldindata.org/coronavirus/country/hungary [66]. The modeling in this work was based on the daily death data of COVID-19 from October 4, 2020, to May 12, 2021, which comprises approximately 221 observations [20].

According to the statistical overview of the data, an average of 127 people died each day in Hungary due to COVID-19. The maximum daily mortality rate was 311, while the minimum daily mortality rate was 10. As we can see in Figure 1, the highest number of deaths occurred on 7 April 2021. We collected the data set when the Delta version of SARS-CoV-2 was the most prevalent.

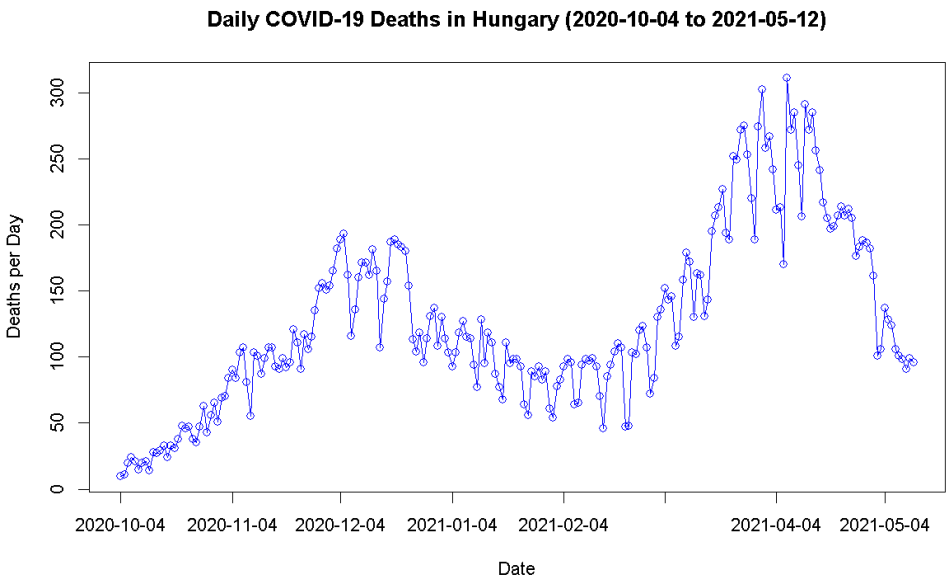

Figure 1: Deaths per day by COVID-19 in Hungary from October 4, 2020, to May 12, 2021

It is easy to infer from Figure 1 that it exhibits both an increasing and a declining tendency over time. This suggests that the time series may be trend stationary, which implies that the linear time trend can be removed to provide stationary results. The variances are also not stable, necessitating modification. The ADF test confirmed the non-stationarity of the data (Dickey-Fuller = -0.408, Lag order = 6, p-value = 0.99). Firstly, we

utilized the difference from the modified data method to make the trend stationary. Despite a non-constant variance, the mean is zero. Since the lambda for Box-Cox is 0.29 [20], which is close to zero, We tackled this problem by taking the original data set transformed logarithmically.

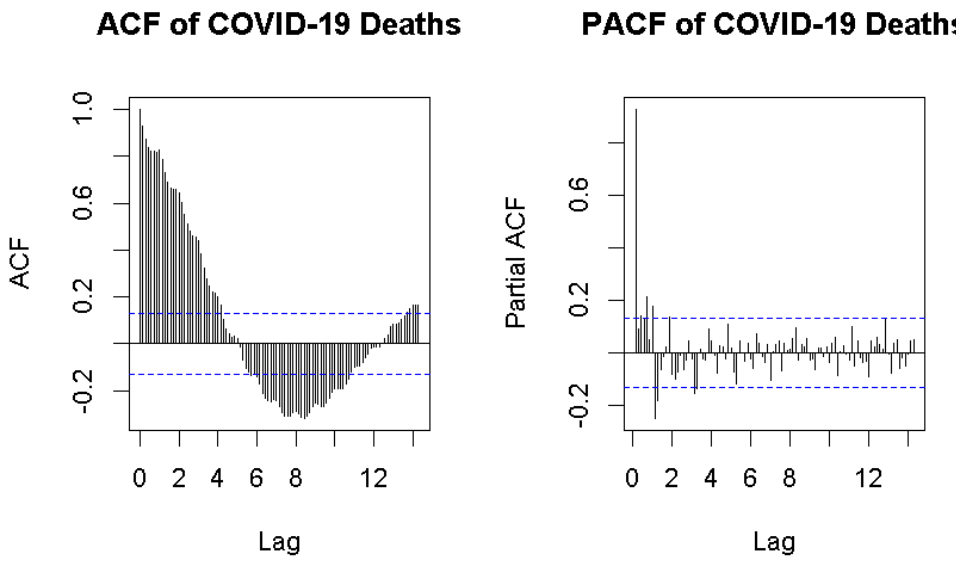

Figure 2: Data Stationarity Verification using ACF and PACF Plots

Figure 2 also shows that the time series plot clearly exhibits a seasonal pattern. The time series does not appear to be stationary based on these results [31]. This is due to the seasonal patterns in the ACF plot and the slow decay of the series across all lag levels. In a similar vein, the PACF figure displays a notable peak at lags 1, 7, 14, 21, etc., along with a few other lags that exhibit borderline spikes [20]. To ensure that the data are stationary in the series, I used the logarithmic transformation and the first seasonal difference. According to the ACF and PACF plots of the logarithmically transformed and the seasonal first-differenced data, COVID-19 deaths in Hungary are seasonal and fluctuate. The ACF plot shows a seasonal stationary time series, suggesting seasonal data modification. The ADF test with a p-value of 0.01 demonstrates it is seasonally

stationary (Dickey-Fuller = -7.199, lag order = 6, p-value $\leq$ 0.01); hence, we should evaluate the seasonality patterns in the ACF plot above. We modeled the time-series prior to data analysis by adjusting the seasonality factor to account for this seasonal pattern. Original trend and seasonal data are non-stationary. We recommend using approaches and models that account for series seasonality, like SARIMA models.

4.3.2 SARIMA Model Identification

After analyzing the data, we can model it. We analyze three models: SARI, SMA, and SARIMA. Based on autocorrelation, we should determine which time-series model fits the data best and which lag suits it before applying the model. We use ACF and PACF plots to characterize this reality as indicated in Figure 3.

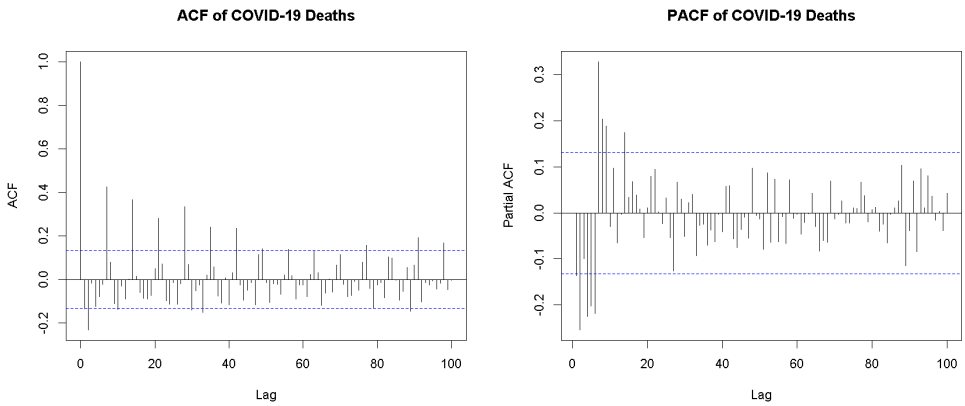

Figure 3: Propose candidate model ACF and PACF plot for first difference of the transformed data

Figure 3 shows that the repeating seasonal pattern has a duration of 7 days. Our S, then, is 7. The next step is to observe that the ARI and IMA approximated orders are 1 and 2, respectively, in the model's nonseasonal portion. Since the first data set was based on the first difference, d = 1. Figure 2 shows that the series does not have a consistent seasonal pattern over time. The first seasonal lag in the ACF is not

close to 1 and decreases slowly by 7. Consequently, seasonal differences in the ACF / PACF of the original data do not support the seasonal part of the model. The ACF plot reveals that the ARI (1) and IMA (1) seasonal parts of the model are the ones that are being considered. $SARIMA(1,1,2)(1,0,1)_{[7]}$ is the candidate model that can be identified based on estimates [20]. Within the confidence bounds, the analysis discovered that the $ARIMA(1,1,2)(1,0,1)_{[7]}$ model's estimated ACF and residuals' normal distribution are acceptable. Figure 4 shows that there is no noticeable pattern in the ACF and a normality of the residuals, indicating that the model is of excellent quality. With a significant p-value for each of the lags tested, the Ljung-Box test also gives its stamp of approval [20].

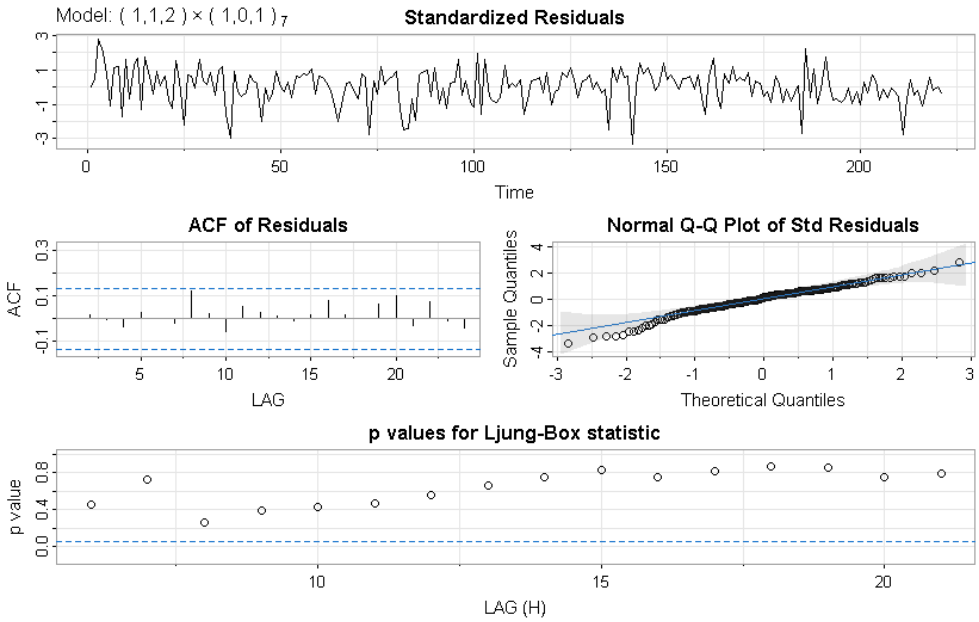

Figure 4: Plot of standardized residuals for the ARIMA model with parameters (1, 1, 2) × (1, 0, 1) [7]

The first plot in Figure 4 shows that the distribution is random [34], the variance is constant, and the mean is zero. The second residual plot (ACF) established that there is no correlation between the current resid-

ual value and the historical values. The third plot in the same image also shows the QQ-Plot fitting roughly around the line; thus we can assume that the standard residuals are nearly normal. In conclusion, the p-value for the Liung-Box statistics is significantly higher than 0.05. In this statistical analysis, "H0: There is no indication of lack of fit in the model." is the null hypothesis held. Now, we are inclined to reject the H0 (the model demonstrates an adequate level of fit) based on the p-value. Therefore, It would be a good idea to use the model for our forecasts. The estimated coefficients show the predicted values for the $ARIMA(1,1,2)(1,0,1)_{[7]}$ model. The model has an estimated sigma squared value of 0.028, a log likelihood of 80.4, and an Akaike Information Criterion (AIC) value of -148.8 [20]. This AIC value is the lowest compared to all other models for this dataset.

4.3.3 Forecasting using Multiplicative Seasonal ARIMA model

All parameter estimations show statistical significance, while there is no correlation between the residual series (i.e. white noise), and the model passes the diagnostic testing and estimation phases. The daily death series may now be predicted using a well-fitting multiplicative seasonal $ARIMA(1,1,2)(1,0,1)_{[7]}$ [20]. Making predictions about future daily death rates in Hungary based on known time series data for COVID-19 is known as forecasting.

This project's data only extends from 2020-10-04 to 2021-05-12; hence, Figure 5 displays the projected 14 daily fatalities in Hungary between May 13, 2021 to May 26, 2021. We used the $ARIMA(1,1,2)(1,0,1)_{[7]}$ fitted model to make the predictions. The Figure 5 shows the original data plot on the black line, the fitted line on the red line, the 14-day forecast of daily deaths using the fitted model on the green line, and the 95 percent CI for future daily deaths with COVID-19 on the blue line. The selected model is $ARIMA(1,1,2)(1,0,1)_{[7]}$ [20]. Over the specified date window, the forecast generally showed that the number of daily deaths

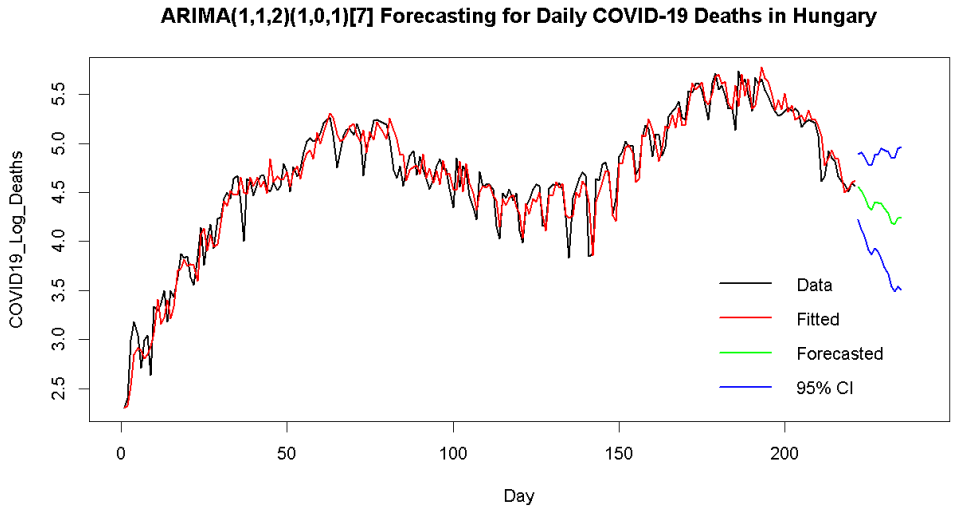

Figure 5: Predicting the number of fatalities in Hungary on a daily basis using $ARIMA(1,1,2)(1,0,1)_{[7]}$ model

[53] in Hungary caused by COVID-19 was decreasing.

4.4 Conclusions

This chapter's main goal is to model and forecast multiplicative SARIMA for the new coronavirus in Hungary using WHO COVID-19 data. We drew conclusions based on preliminary and subsequent data analysis, outcomes, and data output discussions. We used a well-fitted seasonal ARIMA model for forecasting. Generalizing the conclusions: From October 04, 2020, to May 12, 2021, COVID-19 killed 127 people daily in Hungary. The statistics show that the daily death rate ranges from 0 to 311. The box-Cox lambda value is 0.29, which approaches zero, and I logarithmically transformed the data set to make the variance constant. The ACF and PACF plots show seasonality in COVID-19 deaths in Hungary. We modeled the time series before data analysis, modifying the weekly seasonality term to account for this seasonal tendency. The estimated and recommended candidate model is Seasonal $ARIMA(1,1,2)(1,0,1)_{[7]}$. The normalized residuals plot reveals a normally distributed random residual

with a mean of 0 and a variance of 1. An ACF plot of residuals ensured that the present value is unconnected to prior values. Generally, QQ-plots fit around the line, and Ljung-Box statistics have p-values above 0.05. Thus, I recommend predicting using Seasonal $ARIMA(1,1,2)(1,0,1)_{[7]}$. The seasonal $ARIMA(1,1,2)(1,0,1)_{[7]}$ model has the lowest estimated value. Forecasting uses COVID-19 data to estimate future daily deaths. The prediction uses the fitted model $ARIMA(1,1,2)(1,0,1)_{[7]}$. The projection for the specified date period implies that daily deaths from COVID-19 are decreasing.

4.5 Key Question, and Contributions

Key Question
Which time-series model is best for forecasting the number of death rates of the COVID-19 pandemic?

Finding/Contributions
The optimal model for forecasting daily COVID-19 deaths in Hungary was determined to be the Seasonal $ARIMA(1,1,2)(1,0,1)_{[7]}$. This model was estimated, its accuracy was verified through diagnostic checks, and it was subsequently used for forecasting. Introduced during the height of the global COVID-19 crisis in 2020/21 and 2021/22, this contribution was designed specifically to address the urgent needs of that time.

5 Time Series Forecasting with DSHW Model and ARMA Error Corrections

5.1 Introduction

Techniques for time series forecasting have been developed to represent trends and seasonality in energy consumption data [90]. Accurate model-

ing and forecasting are hampered by time-series data errors and dynamic seasonality. This chapter adds ARMA anomalies to the DSHW model using a state space framework. Seasonal trend and auto-correlated error detection of this approach improve the accuracy of the DSHW model forecasting. Using state-space ideas, this new approach enhances the management of complex seasonal patterns and anomalies in time-series data. Based on extensive testing and analysis, forecasts are more accurate and reliable, therefore demonstrating the potential of the revised DSHW model with ARMA errors in a variety of real-world uses.

There has been a recent emergence of state-space models, which are designed to guarantee flexible models and reliable parameter forecasts. The performance of these techniques is superior to that of conventional forecasting in socio-economic and climatic contexts where the demand for energy is variable. Improving power grid stability, reducing operational costs, and reducing the possibility of energy shortages should be top priorities for politicians and energy planners [52].

Accurate time-series forecasting is crucial for efficient energy consumption management and planning [58]. Even though traditional methods like HW models have been around for a long time, they aren't always able to grasp the intricate seasonalities that can be found in datasets. In order to further develop the HW model, [80] presented the DSHW framework. Seasonal variations are no problem for this building. The accuracy of its prediction algorithms is frequently compromised, however, by residual autocorrelation.

The DSHW model is a great modeling technique for energy consumption data that shows several seasonal cycles, such as daily and weekly patterns. By including ARMA errors, which account for residual errors and stochastic components that the baseline seasonal components are unable to capture, the model's accuracy is increased. A comprehensive framework for improving the interpretability and adaptability of statistical models is offered by the state space method [80].

Already published studies validate the accuracy of DSHW models in en-

ergy consumption prediction. Research shows that by including ARMA errors in these models, complex energy consumption models benefit in terms of accuracy especially in scenarios influenced by outside factors like climatic variations or fast changes in human behavior. ARMA models are proven to be reliable in fixing auto-correlated errors based on [2] and [12]. ARMA corrections, employing state-space models, increase forecast accuracy and fit residuals. The research findings show that improving prediction accuracy depends on the process of refining model parameters being fundamental, as [50] has seen. This work improves the present method by using DSHW with ARMA (3,1) changes, thus generating a powerful system appropriate for demanding seasonal data.

5.2 Methodology

5.2.1 Double seasonal Holt-Winters Model

The standard Holt-Winters exponential smoothing technique does not include an algorithm that supports several seasonal patterns. This is because there is no such algorithm. Reference [80] made several modifications to the double season technique in 2003. Both additive trend and multiplicative seasonality are utilized in the Holt-Winters methodology. Multiplicative seasonality involves multiplying two seasonal factors together. Based on the information provided by [80], the Holt-Winters approach with a combination of our newly proposed approach for double multiplicative seasonality is as follows:

Combined Model

We used the following procedures to create our modified model, which we named a Combined Model. This model combines a Double Seasonal Holt-Winters (DSHW) framework with an ARMA process on the residuals:

Step 1: Equations of the model (State-Space Representation with Additive Error).

Model Type: ETS(A, A, M) - Error (Additive), Trend (Additive), Sea-

sonality (Multiplicative).
Observation equation: The observation equation with additive error [38]; $ETS(A, A, M)$ model form:

$$y_t = (l_t + b_t)s_t^1 s_t^2 + w_t \tag{31}$$

Where w_t is the additive error term, modeled as an ARMA(p,q) process.
Level Equation

$$\begin{aligned} l_t s^1_{t-m_1} s^2_{t-m_2} &= \alpha y_t + (1-\alpha)(l_{t-1} + b_{t-1})(s^1_{t-m_1} s^2_{t-m_2}) \\ &= \alpha y_t + (l_{t-1} + b_{t-1} - \alpha l_{t-1} - \alpha b_{t-1})(s^1_{t-m_1} s^2_{t-m_2}) \\ &= \alpha y_t + l_{t-1} s^1_{t-m_1} s^2_{t-m_2} + b_{t-1} s^1_{t-m_1} s^2_{t-m_2} \\ &\quad - \alpha l_{t-1} s^1_{t-m_1} s^2_{t-m_2} - \alpha b_{t-1} s^1_{t-m_1} s^2_{t-m_2} \end{aligned}$$

we divide both sides by $s^1_{t-m_1} s^2_{t-m_2}$

$$l_t = \left(\frac{\alpha y_t}{s^1_{t-m_1} s^2_{t-m_2}} \right) + l_{t-1} + b_{t-1} - \alpha l_{t-1} - \alpha b_{t-1} \tag{32}$$

Trend Equation

$$b_t = b_{t-1} - \beta b_{t-1} + \beta l_t - \beta l_{t-1} \tag{33}$$

First Seasonal Component

$$\begin{aligned} s_t^1 l_t s^2_{t-m_2} &= \gamma y_t + (s^1_{t-m_1} - \gamma s^1_{t-m_1})(l_t s^2_{t-m_2}) \\ &= \gamma y_t + s^1_{t-m_1} l_t s^2_{t-m_2} - \gamma s^1_{t-m_1} l_t s^2_{t-m_2} \\ \left(\frac{s_t^1 l_t s^2_{t-m_2}}{l_t s^2_{t-m_2}} \right) &= \left(\frac{\gamma y_t + s^1_{t-m_1} l_t s^2_{t-m_2} - \gamma s^1_{t-m_1} l_t s^2_{t-m_2}}{l_t s^2_{t-m_2}} \right) \end{aligned}$$

$$s_t^1 = \left(\frac{\gamma y_t}{l_t s^2_{t-m_2}} \right) + s^1_{t-m_1} - \gamma s^1_{t-m_1} \tag{34}$$

Second Seasonal Component

$$\begin{aligned} s_t^2 l_t s_{t-m_1}^1 &= \omega y_t + (s_{t-m_2}^2 - \omega s_{t-m_2}^2)(l_t s_{t-m_1}^1) \\ &= \omega y_t + s_{t-m_2}^2 l_t s_{t-m_1}^1 - \omega s_{t-m_2}^2 l_t s_{t-m_1}^1 \\ \left(\frac{s_t^2 l_t s_{t-m_1}^1}{l_t s_{t-m_1}^1}\right) &= \left(\frac{\omega y_t + s_{t-m_2}^2 l_t s_{t-m_1}^1 - \omega s_{t-m_2}^2 l_t s_{t-m_1}^1}{l_t s_{t-m_1}^1}\right) \end{aligned}$$

$$s_t^2 = \left(\frac{\omega y_t}{l_t s_{t-m_1}^1}\right) + s_{t-m_2}^2 - \omega s_{t-m_2}^2 \tag{35}$$

Where:

- y_t is the observed value.
- s_t^1 and s_t^2 represent the first and second seasonal components, respectively.
- m is the length
- α, β, γ, and ω are the smoothing parameters that control the influence of the components in the model.

Forecasting Equation

$$\widehat{y}_{t+h}(DSHW) = (l_t + hb_t)s_{t-m_{1+h}}^1 s_{t-m_{2+h}}^2 \tag{36}$$

Where: h represents the forecast horizon. Step 2: Calculating the error term

The forecast error w_t at time t is given as follows:

$$w_t = y_t - \widehat{y}_t \tag{37}$$

Where: y_t is the observed value

$\widehat{y}_t = (\widehat{l}_t + \widehat{b}_t)\widehat{s}_t^1 \widehat{s}_t^2$

Step 3: Model the error using ARMA(p,q)

As [12], the ARMA error of the above equation is given by:

$$w_t = \phi_1 w_{t-1} + \phi_2 w_{t-2} + ... + \phi_p w_{t-p} + \theta_1 \varepsilon_{t-1} + \theta_2 \varepsilon_{t-2} + ... + \theta_q \varepsilon_{t-q} + \varepsilon_t$$

$$w_t = \sum_{i=1}^{p} \phi_i w_{t-i} + \sum_{j=1}^{q} \theta_j \varepsilon_{t-j} \tag{38}$$

where: $\varepsilon_t \rightarrow$ a white noise

$\phi_i \rightarrow$ the AR(p) coefficients.

$\theta_j \rightarrow$ the MA (q) coefficients.

Step 4: Forecast the error using Step 3 at horizon h.

$\widehat{w}_{t+h} = \phi_1 \widehat{w}_{t+h-1} + \phi_2 \widehat{w}_{t+h-2} + ... + \phi_i \widehat{w}_{t+h-i} + \theta_1 \widehat{\varepsilon}_{t+h-1} + \theta_2 \widehat{\varepsilon}_{t+h-2} + ... + \theta_j \widehat{\varepsilon}_{t+h-j}$

$$\widehat{w}_{t+h} = \sum_{i=1}^{\min(p,t+h-1)} \phi_i \widehat{w}_{t+h-i} + \sum_{j=1}^{\min(q,t+h-1)} \theta_j \widehat{\varepsilon}_{t+h-j} \tag{39}$$

ARMA(p, q) on residuals (w_t) part models the unpredictable, random noise. After the DSHW model explains all it can, the leftovers (errors) are analyzed. If these errors show their own pattern (e.g., a high error today is likely followed by a high error tomorrow), the ARMA model captures this, making the final forecast even smarter.

Step 5: Combined Forecasting Formula

$$\widehat{y_t} = (\widehat{l_t} + \widehat{b_t})\widehat{s}_t^{(1)}\widehat{s}_t^{(2)} + \widehat{w}_t \tag{40}$$

Where:

$\widehat{l_t}, \widehat{b_t}, \widehat{s}_t^{(1)}$, and $\widehat{s}_t^{(2)}$ are the forecasts from the DSHW model.

$\widehat{w}_t$ is the forecast from the ARMA model.

OR

$\widehat{y}_{t+h}(Combined) = \widehat{y}_{t+h}(DSHW) + \widehat{w}_{t+h}$ .... forecast on horizon h

Combining the structural forecast from the DSHW model with the ARMA model's error adjustments produces a more accurate overall projection.

5.3 Results and Discussions

5.3.1 Preliminary Analysis

This chapter used the most recent three months of Brazilian hourly energy utilization data from 2021 to 2022 [79]. The Figure 6 clearly shows seasonality and a trend pattern. Before analyzing time series, consider models that change seasonality and trend patterns. Figure 6 shows that summer and winter power demand peaks because individuals consume more electricity for cooling and heating. We propose to adjust models and procedures to accommodate seasonality of the data. This Figure 6 shows seasonal relationships in the time series and provide more information. Seasonality must be considered or adjusted to model time series data. These must be taken into account before analyzing. Due to our data's numerous seasonal trends, we advocate advanced multiple seasonal time series models like DSHW, BATS, TBATS, SARIMA, and STL. This chapter uses the DSHW model with ARIMA errors to handle complicated seasonal dynamics and increase forecast accuracy.

As can be seen in Figure 7, I carried out the time series decomposition in order to identify a number of seasonal patterns that were present in the data set. On the basis of the findings of the decomposition: A daily seasonality (24 hours), a weekly seasonality (168 hours), and a monthly seasonality (672 hours) are all examples of these types of seasonality. The findings lend credence to the utilization of latest multiple seasonality time series models, such as the DSHW model, for the purpose of achieving credible data forecasting since they provide evidence. To improve the accuracy of future forecasts, it is necessary to identify these seasonal components before selecting a model. This will allow for more accurate predictions. Due to the fact that the data set is at its most abundant during the daily and weekly periods, I made the decision to incorporate these seasonalities into the DSHW model that is presented in this installment. These recurrences are consistent with previous research that has demonstrated how weather and human activities influence the amount of

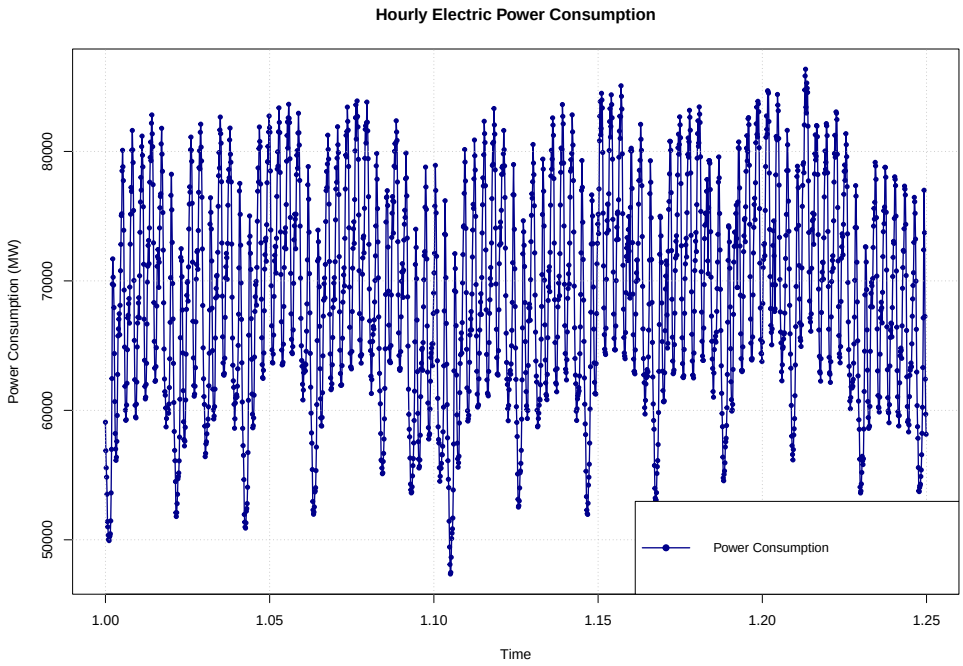

Figure 6: Power Usage in Brazil Per Hour from May 23, 2022 to January 01, 2023

power consumed, as stated by [78]. For the purpose of estimating consumption trends appropriately, these findings highlight the importance of developing intricate models that take into consideration all four seasons.

5.3.2 Forecasting Time Series with DSHW Model

Figure 7 shows that the DSHW time series model is well respected for its ability to make accurate forecasts. Reference [80] states that adding autoregressive (AR (1)) errors to the classic DSHW model improves its performance. Figure 7, "Forecasts from the DSHW model," show that, with AR(1) errors, the model projections have declined somewhat conspicuously from historical data. This implies that the current model might not be suitable for forecasting and demand for development.

We re-evaluated the model and eliminated the AR (1) error component to raise its predictive potential. Figure 7/2's predictions are in line with the pattern of prior data, even though Figure 7/1 contains AR(1) errors.

To improve the DSHW model's prediction accuracy, this better fit means that it needs to be tweaked to eliminate the AR (1) errors and then wait for another model (like the ARMA error) to be fitted for the error.
The predictions made by the first revised DSHW model free of AR (1) errors are more in line with the patterns seen in the historical data, as shown in the following figure. This first step toward change was required to improve the accuracy and reliability of the forecasting model [74].
The model is fitted and its performance evaluated, citing the R packages [81] and the 2003 work of James W. Taylor [80] as a reference. The emphasis is on executing the DSHW-AR(1) model to enhance time-series forecasting. Figure 7 shows the plot for seasonality for the hourly power consumption of Brazil from May 23, 2022 to January 01, 2023.
In order to evaluate the effectiveness compared to the DSHW-AR(1) version, it is designed to fit a DSHW model that does not contain AR(1) errors. The objective is to determine the effects of incorporating autoregressive error correction into the forecasting model as well as the consequences of not doing so. Refer to Figure 7/2 for illustration.

5.3.3 ARMA Errors

Figure 9 in this subtopic helps us understand the residuals of the DSHW-fitted models prior to the autoregressive moving average error consideration. As shown in the figures, the residuals deviate from a normal distribution with a mean of zero and constant variance. The fact that the errors deviate from a normal distribution implies that the model might lack some data patterns. The residuals' ACF shows many interesting lags that exceed the blue dashed line. The correlation between past and present mistakes is quite strong. In a well-fitting model, most delays should lie inside the blue dashed lines, implying no notable autocorrelation. Likewise, as the traditional Q-Q image shows, the red line indicating the expected average does not fit the residual distribution. Given their deviations from this line, the residuals are not usual. The residuals were also investigated using the Ljung-Box test. This test assumes that all au-

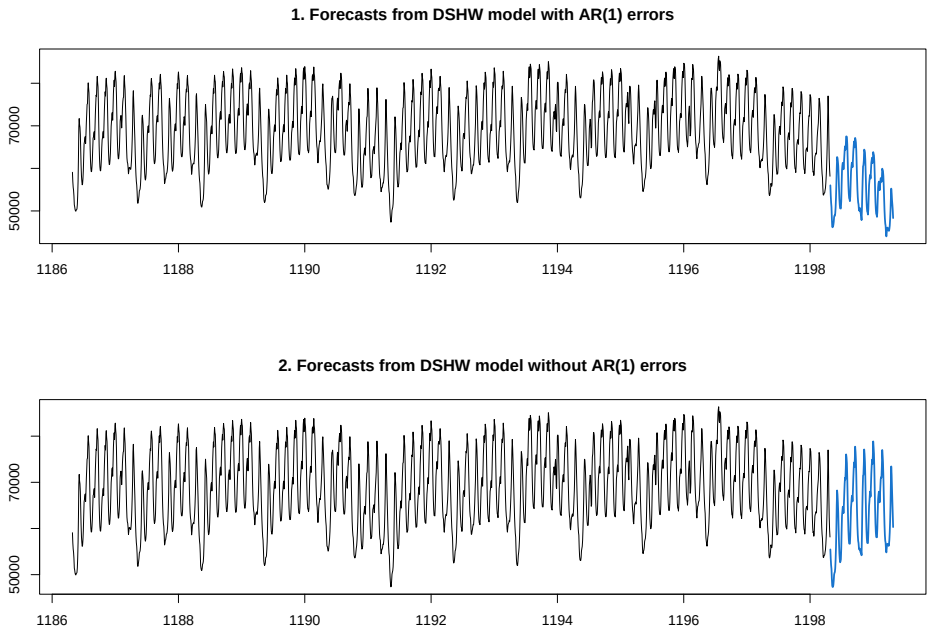

Figure 7: One week forecasts of DSHW model with AR (1) and without AR (1) residuals

tocorrelations for lags are zero. The results disprove the null hypothesis with a p-value less than 0.001. This suggests a substantial autocorrelation among the lags. Based on these results, the DSHW model needs to be changed to consider auto-correlated errors. Adding an ARMA (p, q) error term is a potential change that would help solve these problems.
I evaluated the predictive efficacy of a DSHW model devoid of AR(1) errors, augmented by the application of an ARMA(p,q) model to its residuals. The objective is to evaluate whether the integration of DSHW with the ARMA residual correction improves accuracy compared to the independent models DSHW or DSHW-AR(1) [80].

5.3.4 Models' Performance Evaluation Values

To evaluate the forecasting models, we derived the performance measures in Table 1. These metrics include ME, RMSE, MAE, MPE, MAPE,

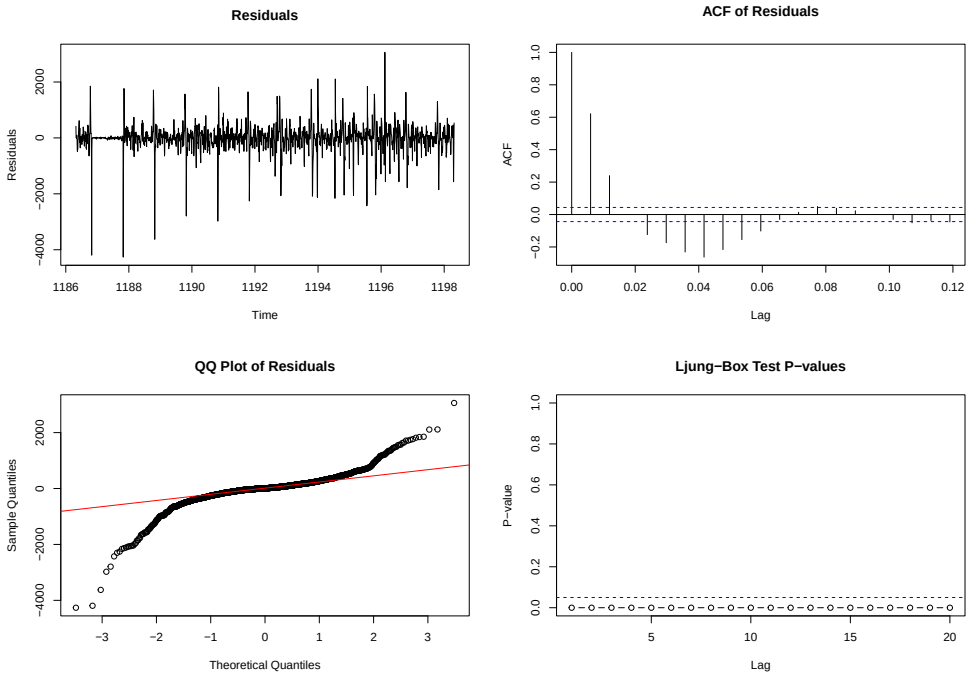

Figure 8: Plot for Residuals

"ACF1" and "Theil's U statistic" [48]. We want to compare the standard DSHW model with an AR(1) error component with my new combined model with ARMA errors. The combined or updated DSHW model with ARMA errors has the lowest values, as demonstrated by these performance measures as the most accurate. Consequently, this demonstrates that my revised model achieves a higher level of prediction accuracy than the earlier DSHW model, which had an AR (1) error. My modifications resulted in decreased values for ME, RMSE, MAE, MPE, MAPE, ACF1, and Theil's U, which indicates that the model's ability to predict outcomes was enhanced.

Table 1: Model Performance Metrics

Model	**Mean Err.**	**RMSE**	**MAE**	**MPE**	**MAPE**	**ACF1**	**Theil U**
DSHW	8440.580	9567.033	8486.932	12.873	12.969	0.965	4.395
Combined	584.189	3227.526	2532.749	0.865	4.030	0.951	1.561

Model Performance Plot

The newly created model's forecasting performance was evaluated using ME, RMSE, MAE, MPE, MAPE, ACF1, and Theil's statistic in Table 1. The new Combined Model outperforms the DSHW model. Figure 9 support this view. The black line in Figure 9 represents the entire dataset's test data. The blue line shows DSHW model projections with AR (1) error factors. Meanwhile, the red line shows the expected values from the newly developed Combined model, now called the Combined Model. Compared to the DSHW model, the Combined Model forecasts more accurately (Figure 9). An ARMA (p, q) model corrects residual autocorrelation, improving performance. Reference [80] used a more straightforward AR (1) model, undercutting the DSHW model's forecasting efficacy.

Given these results, we recommend the Combined Model for electric power consumption datasets and other forecasting purposes. This approach improves precision and reliability, benefiting energy policymakers and experts. The combined model combines ARMA error corrections and advanced state-space methods to set a new standard for time-series forecasting.

Recent studies have shown that residual analysis can improve the accuracy of models [40]. Reference [50] investigated the potential for seasonal decomposition and ARIMA models to mitigate residual autocorrelations. These ideas are expanded upon in this study's Combined Model, which incorporates ARMA (3,1) error corrections into the DSHW framework. Because they strike a mix between accuracy and complexity, we evaluated forecasting models using RMSE, MAPE, and AIC. The researcher [2] argues that assessing model fit requires the use of information criteria. Based on listing four, the combined model is shown to be more accurate and with residual testing than the DSHW. This validates past research on model corrections for overfit and underperformance in high-dimensional seasonal data.

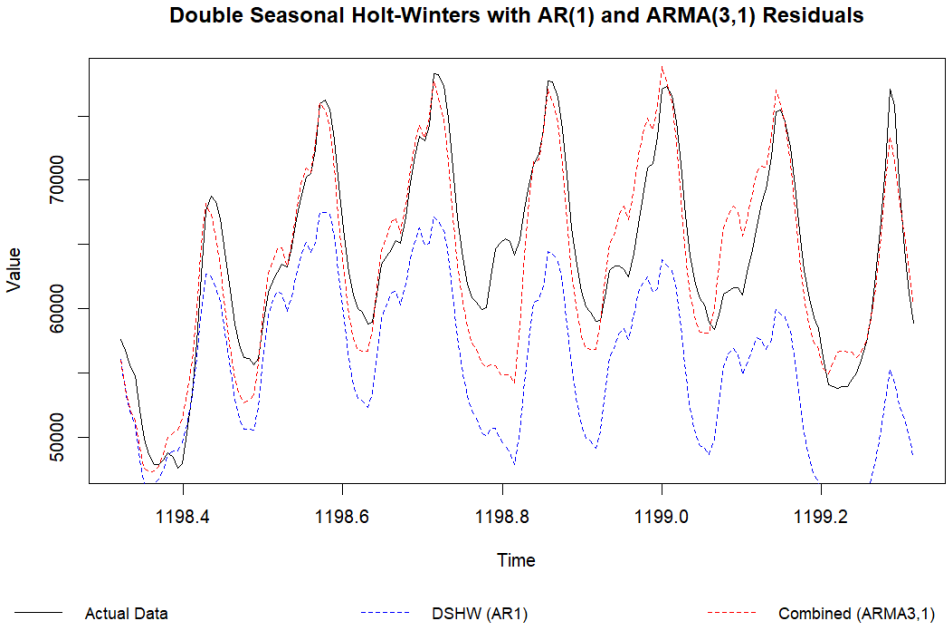

Figure 9: Comparison of DSHW model with AR (1) and ARMA (3,1)

5.4 Conclusions

Within the context of forecasting and modeling time-series data, this chapter demonstrates how the incorporation of ARMA (3,1) errors into the DSHW framework might be of use. Compared to the standard DSHW model, the Combined Model performed significantly better on each and every one of the metrics that were analyzed. For the sake of this performance analysis, we decided to use ME, RMSE, MAPE, and a few other metrics [51]. Through incorporation of ARMA-based errors into the model, we are able to rectify residual autocorrelation and enhance the accuracy of the forecast. The results illustrate that the model is capable of predicting the amount of energy that will be consumed. In addition to this, it can be utilized to deal with data that require careful management due to the fact that it contains a number of seasonalities and errors that are connected to among themselves.

5.5 Key Questions, and Contributions

Key Questions

1. How can ARMA (p, q) error corrections be incorporated into a state-of-the-art DSHW modeling framework?
2. Do time series forecasts become more accurate if ARMA error adjustments are incorporated into the DSHW model?

Finding/Contributions

Modified an advanced DSHW modeling framework enhanced with ARMA(p,q) error correction to significantly improve forecasting precision. This section introduces a hybrid forecasting model that enhances the Double Seasonal Holt-Winters (DSHW) framework by integrating ARMA(3,1) errors. Empirical results demonstrate that this combined model outperforms the standard DSHW across all evaluated metrics, including RMSE and MAPE. This contribution effectively corrects residual autocorrelation that mentioned in Taylor 2003, improving forecast accuracy for multiple time-series data characterized by multiple seasonalities and interdependent errors.

6 Utilizing Periodograms for Modeling and Forecasting Time Series with Multiple Seasonal Patterns

6.1 Introduction

We used the ARIMA and SARIMA models to look for basic seasonal patterns or nonseasonal patterns in time-series data collected on a daily, weekly, monthly, quarterly, and yearly basis [28]. Time series that fluctuate more frequently and show more pronounced seasonal trends tend to be more complicated.

Multiple time series exhibit complex seasonality. Multiple nested seasonality periods, various non nested and non integer seasonality periods, and non integer seasonality periods [21] are among the most commonly occurring complex seasonality types, according to the investigations conducted by [28]. Current exponential smoothing models have a number of drawbacks when it comes to simulating complicated seasonality [21], such as over parameterization, an inability to account for dual calendar effects, and non-integer period effects. A novel state-space modeling framework based on a trigonometric formulation has been proposed by them to address all of these seasonal problems.

References [28], and [48] indicate and refer to by [21] that advanced state-space modeling techniques, including the BATS and TBATS models, are employed to forecast intricate seasonal time series characterized by multiple seasonal periods, high-frequency seasonality, non-integer seasonality, and dual-calendar effects. The updated framework incorporates Fourier representations of the Box-Cox transformation, featuring time-varying coefficients and ARMA error correction. A clear and thorough approach for forecasting complex seasonal time series was developed on the basis of the assumption of Gaussian errors. This method encompassed mathematical formulations for point and interval predictions, along with likelihood evaluation.

The most popular seasonal models in the innovation state space frame-

work are those that support Holt-Winters additive and multiplicative approaches. Reference [80] added a second seasonal component to the Holt-Winters technique, as [28] and [48] indicated.

Many scholars have tried time-series forecasting with dual seasons. Reference [69] compares the TBATS model's predicting ability to the STL model with various seasonal periods. He found daily and weekly seasonality using PJM's website hourly power usage data in R. He concluded that STL outperforms TBATS. In addition to ETS models, STL robust time series decomposition can handle seasonal data. Loess predicts non-linear relationships.

Among the time-series filtering methods used by STL are trend, seasonal, and residual components. According to [22], the architecture consists of a series of loess smoother applications and enables fast computations, even for extremely large time series with multiple trends and seasonal smoothing. It also facilitates property testing.

Although the MLE of the parameters is not shown in the final fitted models for mathematical formulation, this is one method to handle model parameter overparameterization (References [28], [21] and [22]). They used their best prediction models for a broader set of data. The STL model outperforms TBATS in terms of forecasting, according to reference [69]. This study evaluates model forecasting with multiple seasonality and analyzes Brazil's hourly power consumption data from 2015 to 2022 [21] to determine the most dominant frequency, model, and forecast with various seasonal temporal series periods. It also aims to explain parameter estimations for the best-fit models.

The periodogram, as outlined by [75], is employed to analyze spectral density and identify significant seasonalities (sub-day, half day, daily). Eventually, a systematic approach was established for selecting and integrating these dominant seasonal periods into models. After that, we used commonly used accuracy metrics to train and assess BATS, TBATS, and STL models with the selected seasonalities [21]. By improving model configurations, the suggested spectral density-based technique successfully

identifies major seasonalities. This chapter highlights the importance of combining advanced forecasting approaches with spectral analysis in order to tackle the difficulties of complex time-series analysis at high frequencies. Practitioners looking for reliable forecasting approaches in dynamic environments will find this chapter's conclusions relevant.

6.2 Methodology

6.2.1 A State Space Model of Innovations for the MS Processes

The flexible ISSM models' time series data with MS processes allow the addition of explanatory factors and breaks down the observable series into trend, seasonality, and irregular variations. For MS processes with several seasonal patterns, the ISSM can be expanded to account for these variations. We can capture the complex dynamics and patterns in the data and include additional explanatory factors using the reference model [28], a State Space Model for Innovations aimed at various seasonal processes [21]. It has been established in reference [3] that under the context of exponential smoothing, the BATS model is capable of outperforming the basic SSM in terms of its ability to make accurate predictions. On the other hand, the BATS model behaves badly in situations where seasonality is complicated and high-frequency. This is the reason why the TBATS model was recommended in the reference [28]. In cases when seasonality occurs frequently, the model's parameters can be significantly reduced and its adaptability to complicated seasonality can be enhanced by using trigonometric representations of seasonality components.

6.2.2 BATS Model

As [28] said, 'exponential smoothing is based on non-linear adaptations of state-space models'.
The following is an extension of the DS model that incorporates T seasonal patterns, ARMA errors, and a Box-Cox transformation [28], [21],

and [48]:

$$y_t^{\omega} = \begin{cases} \frac{(y_t^{\omega})}{\omega} - \frac{1}{\omega}, & \text{if } \omega \neq 0 \\ \log(y_t), & \text{if } \omega = 0 \end{cases}$$

Here, ω refers Box Cox transformation.
The general formula for y_t^{ω}, l_t, and $s_t^{(j)}$ are given as:

$$\begin{aligned} y_t^{(\omega)} &= l_{t-1} + (b_{t-1})\phi + s_{t-m_1}^{(1)} + s_{t-m_2}^{(2)} + \cdots + s_{t-m_T}^{(T)} + w_t, \quad \text{as formulated by[28]} \\ &= l_{t-1} + (b_{t-1})\phi + \sum_{j=1}^{T} s_{t-m_j}^{(j)} + w_t, \quad \text{as formulated by[28]} \end{aligned}$$

Where: $\sum_{j=1}^{T} s_{t-m_j}^{(j)} = s_{t-m_1}^{(1)} + s_{t-m_2}^{(2)} + \cdots + s_{t-m_T}^{(T)}$ Here is the local time frame at $t-1$:

$$l_{t-1} = l_t - (b_{t-1})\phi - \alpha w_t$$

The short-term trend for period t is expressed as [21]:

$$b_{t-1} = \frac{b_t - b + \phi b - \beta w_t}{\phi}, \quad \text{where } \phi \neq 0$$

$$b_t - b + \phi b - \beta w_t = \phi b_{t-1}; \quad b \text{ is long trend}$$

At period t, the jth seasonal component is expressed as:

$s_t^{(j)} = s_{t-m_1}^{(1)} + s_{t-m_2}^{(2)} + \cdots + s_{t-m_T}^{(T)} + \gamma_j w_t$; m represents the jth seasonal periods

An ARMA (p, q) process at time t:

$$w_t = \phi_1 d_{t-1} + \phi_2 d_{t-2} + \cdots + \phi_p d_{t-p} + \theta_1 \varepsilon_{t-1} + \theta_2 \varepsilon_{t-2} + \cdots + \theta_q \varepsilon_{t-q} + \varepsilon_t$$

As [21] refers, a Gaussian white-noise process with zero mean (μ) and constant variance (σ^2) is represented by ε_t.

6.2.3 TBATS Model

As reference [28] cites, the trigonometric form of seasonal components, which is based on the Fourier series of references [43] stated as follows: A model:

$$y_t^{\omega} = \begin{cases} \frac{(y_t^{\omega})}{\omega} - \frac{1}{\omega}, & \text{if } \omega \neq 0 \\ \log(y_t), & \text{if } \omega = 0 \end{cases}$$

Here, ω refers to the value of Box Cox transformation, and y_t^{ω} is a series at time t. The general formula for y_t^{ω}, l_t, $s_t^{(j)}$ [21], and Seasonal parts are given as:

$$y_t^{(\omega)} = l_{t-1} + (b_{t-1})\phi + s_{t-m_1}^{(1)} + s_{t-m_2}^{(2)} + \cdots + s_{t-m_T}^{(T)} + w_t, \text{ as formulated by[28]}$$

$$= l_{t-1} + (b_{t-1})\phi + \sum_{j=1}^{T} s_{t-m_j}^{(j)} + w_t, \text{ as formulated by[28]}$$

Where: $\sum_{j=1}^{T} s_{t-m_j}^{(j)} = s_{t-m_1}^{(1)} + s_{t-m_2}^{(2)} + \cdots + s_{t-m_T}^{(T)}$ Here is the local time frame at $t-1$:

$$l_{t-1} = l_t - (b_{t-1})\phi - \alpha w_t$$

The short-term trend for period t is expressed as:

$$b_{t-1} = \frac{(b_t - b + \phi b - \beta w_t)}{\phi}, \text{ where } \phi \neq 0$$

$$\equiv b_t - b + \phi b - \beta w_t = (b_{t-1})\phi; \ b \text{ is long trend}$$

At period t, the jth seasonal component is expressed as:

$$s_t^{(j)} = s_{t-m_1}^{(1)} + s_{t-m_2}^{(2)} + \cdots + s_{t-m_T}^{(T)} + \gamma_j w_t; \ m \text{ represents the } j\text{th seasonal periods}$$

An ARMA (p, q) process at time t:

$$w_t = \phi_1 d_{t-1} + \phi_2 d_{t-2} + \cdots + \phi_p d_{t-p} + \theta_1 \varepsilon_{t-1} + \theta_2 \varepsilon_{t-2} + \cdots + \theta_q \varepsilon_{t-q} + \varepsilon_t$$

Seasonal part of the model:

$$s_t^j = s_{1,t}^1 + s_{2,t}^2 + \cdots + s_{i,t}^j = \sum_{i=1}^{k_j} s_{i,t}^j$$

$$s_{i,t}^j = s_{i,t-1}^j \sin\left(\frac{\pi}{2} - \lambda_j\right) + s_{j,t}^{*(i)} \cos\left(\frac{\pi}{2} - \lambda_j\right) + \gamma_1^j w_t$$

$$s_{i,t}^{*(j)} = -s_{i,t-1}^j \cos\left(\frac{\pi}{2} - \lambda_j\right) + s_{i,t}^{*(j)} \sin\left(\frac{\pi}{2} - \lambda_j\right) + \gamma_1^j w_t$$

Where: $\alpha, \beta, \gamma_1^j,$ and γ_2^j-smoothing parameters; k_j is the number of harmonics during the jth seasonality period [92]. In the jth seasonality period, there are k_j harmonics. The symbol ε_t represents a Gaussian white-noise process with a mean of zero (μ) and a variance of constant (σ^2) [21].

6.2.4 STL Model

According to [23], one common way to break down time series into its component parts [8] is using the STL model. Although the STL model was initially developed to cover only one season, it can be easily expanded to cover more than one. We can extract disassembled components that appropriately reflect our time series' trends and seasonal patterns by changing the STL model to operate with data from many seasons.
The MSTL+EST model extends the STL model with an exponential smoothing trend component and many seasonal periods. We combine exponential smoothing forecasting capabilities with the STL model's ability to accommodate many seasons.

MSTL+EST Model Equation

Here is a description of the MSTL + EST model equation:

$$y_t = l_t + b_t + s_t^{(1)} + s_t^{(2)} + \cdots + s_t^{(n)} + \varepsilon_t$$

$$y_t = l_t + b_t + \sum_{i=1}^{n} s_t^{(i)} + \varepsilon_t$$

Where:

- y_t is an observed value.
- As a measure of the entire average or the baseline, l_t denotes the local level.
- Here, b_t stands for the local trend element, which denotes the slope or the rate of change.
- With n being the total number of seasonal periods, $s_t^{(i)}$ represents the ith seasonal component.
- The error word ε_t, stands for the variable that is random or unexplained at time t.

6.3 Results and Discussion

6.3.1 Data

This chapter examined 201,318 observations over 23 years about hourly electric energy consumption in Brazil [79]. Any numbers were rounded to the following whole number and we exclusively utilized data from 2015 to 2022, the most current seven-year period, for our statistical analysis. If any hourly data points were missing, the gaps were filled by averaging the corresponding daily readings. Data are originally published by [85], and cited by [79].

6.3.2 Data Analysis and Discussion

We used the latest 7 years of data for our further analysis since the number of total data points is too large. So, we skipped the first 140,000 observations and started with 12/25/2015.
Figure 10 shows the hourly electricity consumption in Brazil from January 1, 2015, to January 1, 2023. The storyline exposes seasonality and trends.

Time-series models should incorporate seasonality and trend components if efficient analysis is dependent on them. Reference [20] observes that before analysis, the time series was modeled using seasonality correction. Seasonality-aware methods and models are advised in considering the non-stationary and seasonal data. This approach produces more accurate and valuable data insights.

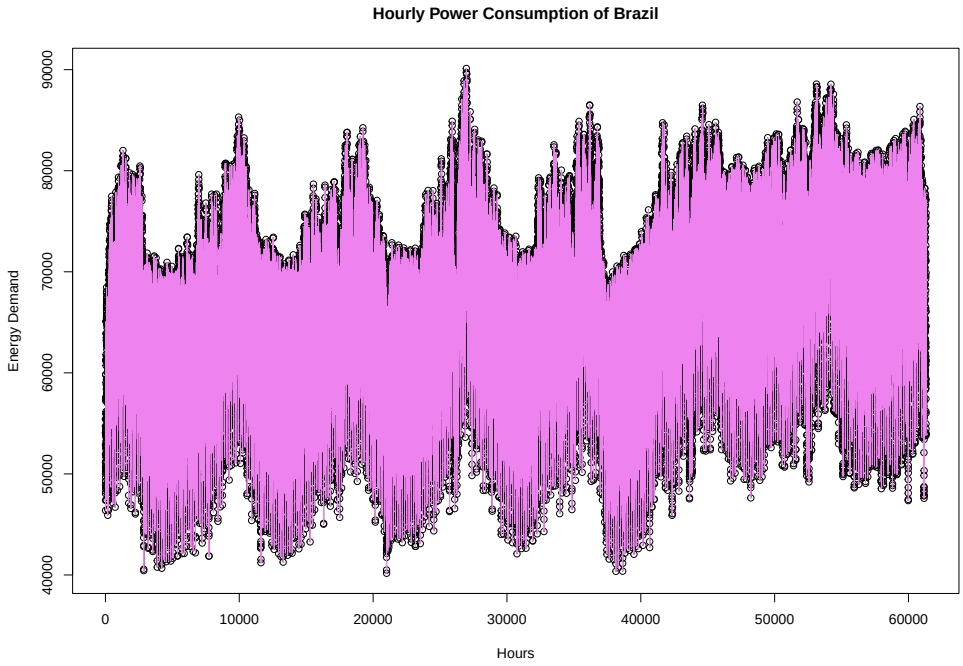

Figure 10: Plot for Brazil Energy Data

The summary statistics for the hourly power consumption are presented in Table 2.

Table 2: Summary Statistics

	Min	**1st Qu.**	**Median**	**Mean**	**3rd Qu.**	**Max**	**Variance**
Brazil Data	40,168	57,745	65,224	64,670	71,419	90,120	82,012,560

The variance is indeed quite big because of seasonal variation in Table 2. Electricity consumption tends to follow a seasonal pattern, with different

levels of consumption at different seasons of the year. For example, electricity consumption is higher in the summer months because people use more air conditioning.

It is essential to perform thorough data preprocessing and analysis before using advanced modeling techniques on time series data. The data may be transformed (e.g., using Box-Cox transformation) [46], must be checked for trends, and then differencing or de-trending must be performed before further analysis if it has a trend.

For further time series analysis, I should check the presence or absence of a trend, transform (Box-Cox transformation) if needed, and difference or de-trend if the trend exists in the data. We checked the lambda value of the original data. We use the Box-Cox transformation to stabilize variance, achieve normality, improve forecasting, handle outliers, and adjust for seasonality and trend effects. The output lambda value of 0.68 indicates the need for the Box-Cox transformation.

Figure 11 seeks to compare the distribution of the original data with that of its Box-Cox-transformed version to assess if the transformation improves the data's normality. Normality is often an essential attribute in statistical analysis, as many methods (e.g., linear regression, hypothesis testing) assume or demonstrate improved efficacy when data adhere to a normal distribution.

The analysis validates the effectiveness of the Box-Cox transformation in improving the normality of Brazil-data, as demonstrated by the histograms. This alteration can enhance the validity of ensuing statistical analyses that depend on the assumption of normality. Refer to Figure 11.

KPSS Test

We utilized the KPSS test to assess the stationarity of a time series [91], with particular emphasis on trend stationarity. The KPSS test is a commonly employed statistical instrument in time series analysis, utilized to ascertain whether a given series exhibits stationarity centered on an inevitable pattern or a constant mean. Unlike the ADF test, which assumes non-stationarity based on a unit root as its H_0, the KPSS test takes the

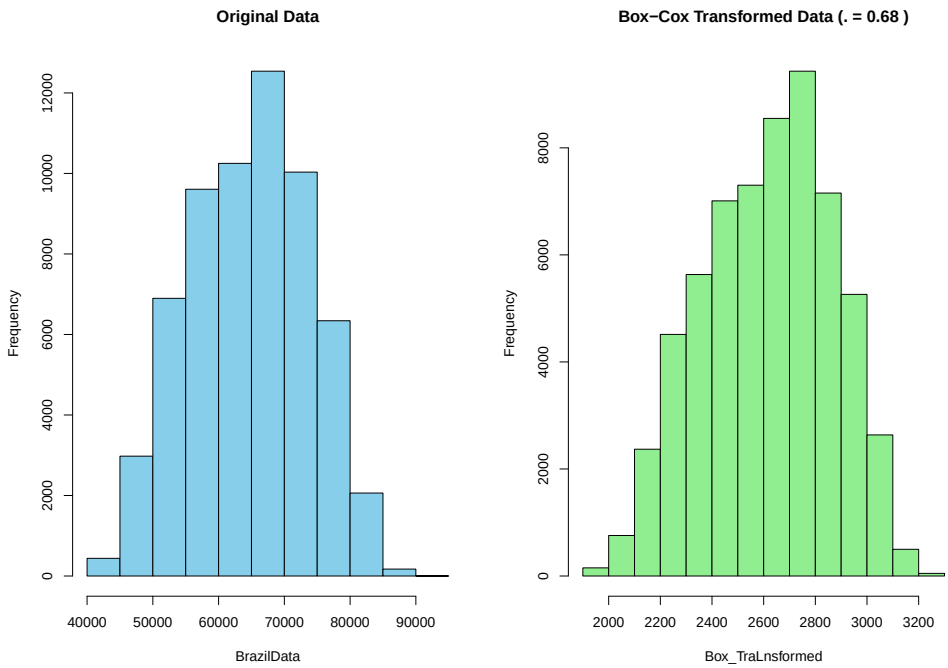

Figure 11: Histogram for Original and Transformed Data

opposite tack. A time series is considered stationary if and only if it follows a deterministic trend (trend stationarity) or if it demonstrates level stationarity (around a constant value; H_0). The H_1 states that the series does not have a stable distribution and, in fact, does have a unit root. The H_1 was set as "trend" and the KPSS test was run on the Box-Cox transformed time-series data (Box-TraLnsformed) to determine if the data are trend stationarity.

The test produced a p-value of 0.01, far less than the usual 0.05 cut for statistical relevance. We reject the H_0 since the p-value is tiny, and so the time-series is not trend stationarity. The series may thus have a unit root, in which case its patterns are steady and unaffected by time. This chapter on time-series modeling and forecasting have found that this aligns with many seasonal cycles. Trend stationarity is essential for complex seasonal changes and improved forecast accuracy of advanced time-series models. The non-stationary nature of the time-series emphasizes by the KPSS

test results, so applying differencing as a first preprocessing technique is essential.

In addition to that, a trend derived from preliminary tests and visual representations, indicating the need to detrend. This was accomplished through the process of differencing. The subsequent trend stationarity test results produced a p-value of 0.1, suggesting that H_0 cannot be rejected. Consequently, the data are determined to be trend stationary.

HEGY test

The statistical HEGY test finds unit roots in time series data with various seasonal frequencies [47]. For investigating time series with seasonal trends, this test can determine whether the data is seasonally stationary or has to be altered (e.g., by seasonal differencing). Based on Table 3 and Table 4, we can develop precise and reliable models, since our data do not have unit roots at seasonal frequencies.

Table 3: HEGY Test for Unit Roots

Component	**Statistic**	**p-value**
t_1	-118.88	< 0.001 ***
t_2	-87.81	< 0.001 ***
$F_{3:4}$	10336.70	< 0.001 ***
$F_{5:6}$	5354.27	< 0.001 ***
$F_{7:8}$	7124.02	< 0.001 ***
$F_{9:10}$	8042.02	< 0.001 ***
$F_{11:12}$	7238.35	< 0.001 ***
$F_{2:12}$	25985.00	< 0.001 ***
$F_{1:12}$	24463.71	< 0.001 ***

Note: Deterministic terms: constant + trend + seasonal dummies.
Significance codes: *** $p < 0.001$.

Table 4: Summary and Interpretation of the HEGY Test

Elements	**Details**
Test Used	HEGY test
Aim	Detect unit roots at seasonal frequencies in time series data
Null Hypothesis (H_0)	Unit root exists at least once per season (non-stationary)
Alternative Hypothesis (H_1)	No unit root at tested frequencies (seasonally stationary)
Results	p-value < 0.001; reject H_0; data is seasonally stationary
Implication	No seasonal differencing required (simplifies modeling)
Recommendation	Validate trend stationarity; select appropriate models

Periodogram: Top 10 Dominant Frequencies

The first step in choosing the top 10 most essential seasonality in a batch of time series data is identifying the most notable periodic trends in it. This stage is very important for reducing the underlying structure of the data in cases with many seasonal trends. Developed from spectral density analysis, the power spectrum - which gauges the intensity of every data frequency component - forms the basis of the selection. Let us examine the steps in Table 5.

Table 5: Top 10 Dominant Frequencies in the Power Spectrum

	Frequency	**Spectrum (dB)**	**Period**
1	0.041 666 67	76.214 37	24.000 000
2	0.083 333 33	73.704 71	12.000 000
3	0.083 349 61	66.175 03	11.997 657
4	0.166 666 67	65.026 88	6.000 000
5	0.083 365 89	62.786 32	11.995 314
6	0.166 682 94	62.630 88	5.999 414
7	0.130 957 03	61.727 52	7.636 092
8	0.083 219 40	61.546 94	12.016 429
9	0.047 623 70	61.465 05	20.997 949
10	0.208 333 33	61.156 01	4.800 000

Here is a detailed description of the procedure for achieving Table 5:

1. Spectral Density Analysis and Periodogram

The first step is to use a periodogram to perform spectral density analysis. Moreover, the periodogram breaks down the time series into its frequency components and determines the power (or strength) of each frequency. The spec.pgram function in the code calculates the periodogram, and the resulting spectrum is converted to decibels to make it easier to read. The frequencies are also transformed into periods (e.g., hours, days) in order to make the results easier to understand. This transformation enables us to determine not only the frequencies, but also the time intervals that correspond to the periodic patterns.

2. Ranking Frequencies by Power

Sort the frequencies by power after the periodogram computation. Each

frequency influences data variability according to the power spectrum. Higher power ratings imply more robust seasonal changes brought forth by dominating frequencies. The codes group frequencies, power levels (in dB), and durations into a data frame. To give the most crucial frequencies top priority, this data frame is then arranged in decreasing order by spectrum-dB.

3. Selecting the Top 10 Dominant Seasonalities

The initial 10 rows of the frequency power sorted data frame represent the predominant seasonalities. The frequencies indicate the dataset's principal periodic patterns. The identified seasonalities likely align with sub-daily, half-daily, daily, weekly, or monthly cycles in power consumption data. Concentrating on the top 10 emphasizes the most significant patterns and eliminates extraneous information. This selection method streamlines analysis and uncovers seasonal data factors.

4. Practical implications

Choosing the top 10 prevalent seasonalities affects modeling and forecasting practically, rather than only technically. In data on energy use, for example, finding half-daily or daily cycles can enable utilities schedule for periods of maximum demand. In retail or finance, too, knowledge of seasonal tendencies might enhance investment plans or inventory control. Separating the most important trends helps us to create more interpretable and accurate models that reflect the fundamental dynamics of the time series. This method also helps to uncover anomalies since variations from these dominating trends can indicate odd events or changes in the fundamental system. Choosing the top 10 prominent seasonalities is essentially a power spectrum analysis, frequency ranking based on strength, and pattern emphasis on the most important aspects. This procedure not only helps to reduce data complexity but also offers insightful analysis for predictive modeling and decision-making.

This analysis examines Brazilian power consumption data to identify and show the top 5 seasonality components. We use R's plotly package to construct an interactive periodogram that shows the spectrum and the top

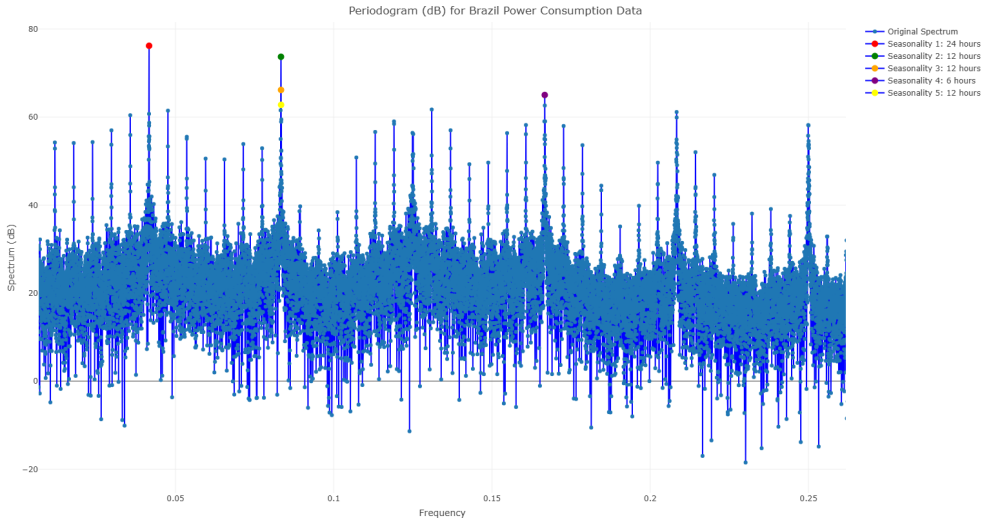

Figure 12: Top 5 dominant frequencies

5 dominating frequencies with markers and labels. This method helps us understand the data's structure by interpreting seasonal trends and their periods [29]. Table 6 shows the selected five dominant frequencies from the above general ideas [29].

Table 6: Top 5 Dominant Frequencies in the Power Spectrum

	Frequency	**Spectrum (dB)**	**Period**
1	0.041 666 67	76.214 37	24.000 00
2	0.083 333 33	73.704 71	12.000 00
3	0.083 349 61	66.175 03	11.997 66
4	0.166 666 67	65.026 88	6.000 00
5	0.083 365 89	62.786 32	11.995 31

For demonstration purposes, Table 6 is plotted as figure 12.

The periodogram and the top five seasonality components will assist us in understanding the periodic tendencies of Brazil's power consumption statistics. Data interpretation is made easier by the plotly constructed interactive labels and highlights each dominating frequency. Research and forecasting benefit much from the hourly lengths of the reported seasonal components. This approach helps to grasp periodograms better and is ready for advanced time series modeling and decomposition.

ACF to show the existence of multiple seasonality

The ACF revealed many seasonal trends in the Brazil dataset. The ACF statistically detects cycles by evaluating the time series' connection with its lagged values. We found sub-daily, half-day, daily, and weekly seasonality in the dataset using this method.

We can clearly see these seasonal patterns in Figure 13. It shows that the larger half-day seasonality is a subset of sub-daily seasonality, which is characterized by changes happening often during the day. This half-day seasonality shows the patterns that happen once every 24 hours; it is a subset of the daily seasonality. The daily patterns also have a regular structure that repeats every seven days because the daily seasonality is overlaid on top of the weekly seasonality. There is a hierarchy to seasonal patterns, with minor cycles within larger ones. This arrangement suggests that shorter-term patterns are not independent of longer-term seasonal cycles but are influenced by them.

The hourly electricity consumption data from Brazil exhibits multiple nested seasonal patterns (Figure 13). This indicates that energy consumption patterns are complex, influenced by a combination of sub-daily, daily, weekly, and other cycles that reflect both short-term fluctuations and long-term behavioral trends in power usage.

Data train and Data test

The training data set, referred to as Brazil-train0, was utilized to train the model, optimize its parameters, and mitigate the risk of overfitting by employing methods such as cross-validation. The Brazil-test data set offers a neutral assessment of model performance, confirming its ability to generalize to previously unobserved data. This split ensures reliable model development and validation [10].

Decomposition of time-series data

This section demonstrates the process of separating time series data with multiple seasonal components, such as those that fluctuate on a half-

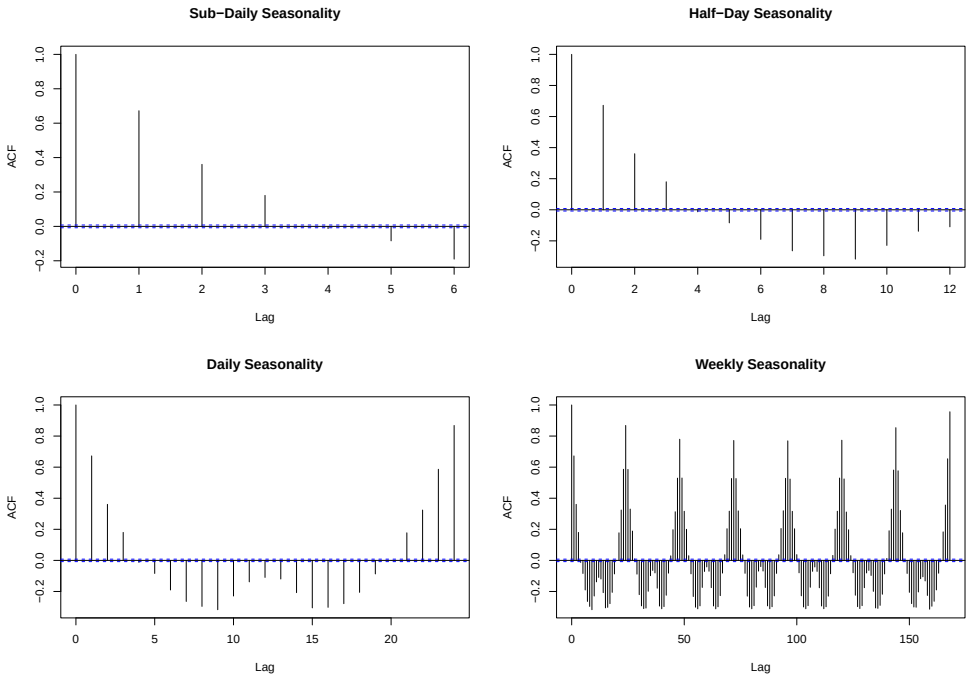

Figure 13: ACF to show the existing of multiple seasonality

day, daily, or sub-daily basis. The function takes care of several seasonal periods and shows the breakdown by turning the training data into a time series object with 1 as the base frequency. We create a multiple seasonal time series object with specified seasonal periods: 6hr (sub-daily), 12hr (half-daily), and 24hr (daily) [21]. Use the right symbols or methods (auto-plot) to show how the time series is broken into parts that show trends, seasonality, and remainders. Subsequently, the time series will be broken up and the results will be shown using MSTL as shown in Figure 14.

Forecasting time series with the TBATS model

A big step forward in time series analysis is the TBATS and BATS models, which can handle many seasons. A new method is introduced by the TBATS model, which is a version of the BATS model, by introducing several non-integer seasonality cycles into the time-series process. Reference [27] proposed this new model that merges BATS and trigonometric

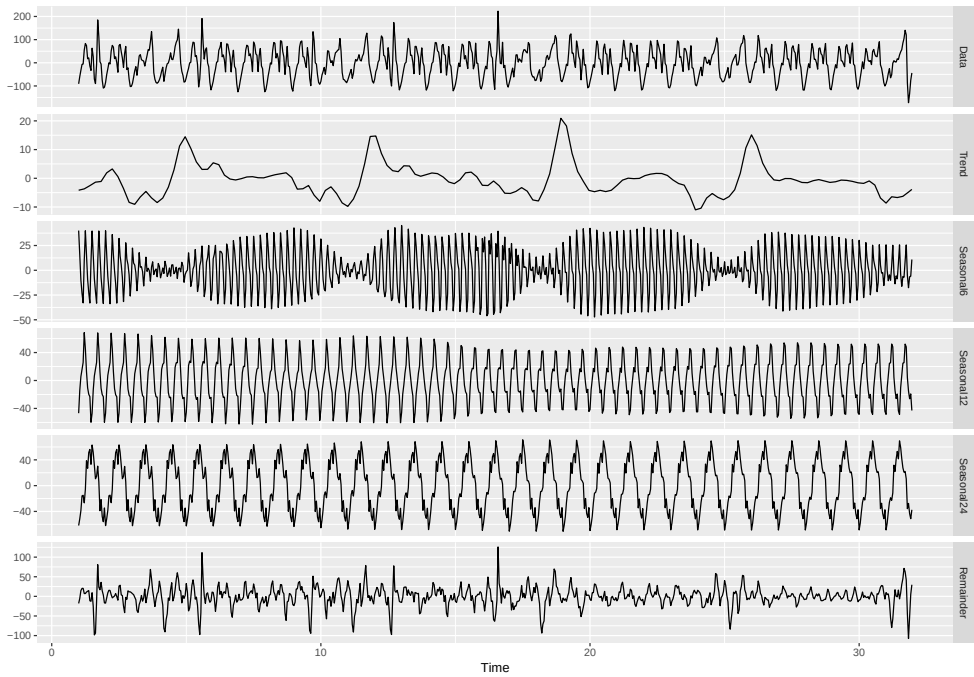

Figure 14: Plot for decomposition of time series data

seasonality. By expressing the seasonality terms trigonometrically, the model becomes better at handling complex seasonality. We use the residual ARMA adjustment to account for residual autocorrelation after we correct for non-linearity with the Box-Cox transformation.

Table 7 shows the TBATS model parameter estimations and their output using R.

Therefore, we could fit the following general TBATS Model for hourly energy power consumption by using [28] formula:

$$y_t = l_{t-1} + \phi b_{t-1} + \sum_{i=1}^{3} s_{t-1}^{(i)} + w_t$$

Since we took the Box-Cox transformation for y_t on $\omega = 0.68$, so

$$y_t = l_{t-1} + 0.829 b_{t-1} + s_{t-6}^{(1)} + s_{t-12}^{(2)} + s_{t-24}^{(3)} + w_t$$

Table 7: TBATS Model Estimated Parameters

Parameter	**Value**
Model Specification	TBATS(1, {3,4}, 0.829, {¡6,2¿, ¡12,1¿, ¡24,1¿})
Alpha	−0.11546
Beta	0.02284
Damping Parameter	0.82868
Gamma-1 Values	0.00083, 0.00034, 0.00014
Gamma-2 Values	−0.00136, 0.00035, 0.00063
AR coefficients	−0.22261, −0.30933, 0.37104
MA coefficients	0.90512, 0.64211, −0.15285, −0.31634
Sigma	28.6432
AIC	9977.474

Where:

$$
\begin{aligned}
l_t &= l_{t-1} + 0.829 b_{t-1} - 0.11546 w_t; \\
b_t &= 0.171 b + 0.829 b_{t-1} + 0.02284 w_t \\
s_t^{(1)} &= \sum_{j=1}^{2} s_{j,t}^{(1)}; \quad s_t^{(2)} = s_{j,t}^{(2)}, \quad s_t^{(3)} = s_{j,t}^{(3)} \\
s_{j,t}^{(1)} &= s_{j,t-1}^{(1)} \cos \lambda_j^{(1)} + s_{j,t-1}^{*(1)} \sin \lambda_j^{(1)} + 0.00083 w_t \\
s_{j,t}^{(2)} &= s_{j,t-1}^{(2)} \cos \lambda_j^{(2)} + s_{j,t-1}^{*(2)} \sin \lambda_j^{(2)} + 0.00034 w_t \\
s_{j,t}^{(3)} &= s_{j,t-1}^{(3)} \cos \lambda_j^{(3)} + s_{j,t-1}^{*(3)} \sin \lambda_j^{(3)} + 0.00014 w_t \\
s_{j,t}^{*(1)} &= -s_{j,t-1} \sin \lambda_j^{(1)} + s_{j,t-1}^{*(1)} \cos \lambda_j^{(1)} - 0.00136 w_t \\
s_{j,t}^{*(2)} &= -s_{j,t-1} \sin \lambda_j^{(2)} + s_{j,t-1}^{*(2)} \cos \lambda_j^{(2)} + 0.00035 w_t \\
s_{j,t}^{*(3)} &= -s_{j,t-1} \sin \lambda_j^{(3)} + s_{j,t-1}^{*(3)} \cos \lambda_j^{(3)} + 0.00063 w_t \\
\lambda_j^{(1)} &= \frac{2\pi j}{6} = \frac{\pi j}{3}, \quad j = 1, 2; \\
\lambda_j^{(2)} &= \frac{2\pi j}{12} = \frac{\pi}{6}, \quad j = 1; \\
\lambda_j^{(3)} &= \frac{2\pi j}{24} = \frac{\pi j}{12} = \frac{\pi}{12}, \quad j = 1
\end{aligned}
$$

and

$$
\begin{aligned}
w_t = -0.22261 w_{t-1} - 0.30933 w_{t-2} + 0.37104 w_{t-3} + 0.90512 \varepsilon_{t-1} + \\
0.64211 \varepsilon_{t-2} - 0.15285 \varepsilon_{t-3} - 0.31634 \varepsilon_{t-4} + \epsilon_t
\end{aligned}
$$

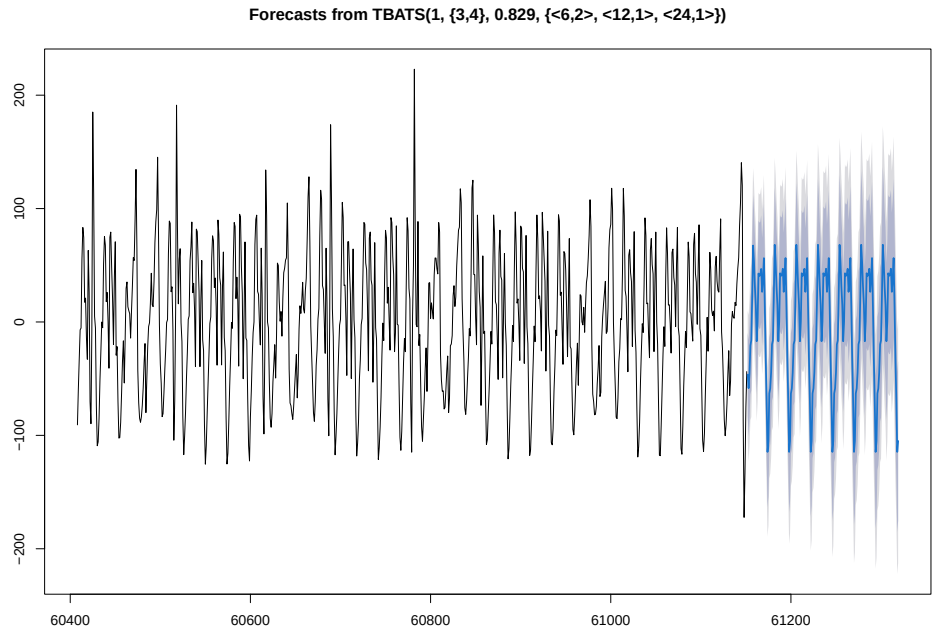

Figure 15: Hourly electricity power consumption forecasting by TBATS Model

The TBATS model has proven to be a valuable tool for Brazil's hourly energy power consumption. As we calculated, the fitted model, labeled TBATS [1, (3, 4), 0.829, (6, 2), (12, 1), (24, 1)] [21] in Table 7 and Figure 15, demonstrates its practical application. The model's suggestion is not made when Lambda equals one, as we had previously applied the Box-Cox transformation to the data. As a concrete example of the model's predictive power, the trend fell to 82.9 percent in each succeeding period as a result of the dampening value phi. An ARMA (3,4) process was used to mimic the ARMA error. After fitting the ARMA error model, the values of the AR(p) and MA(q) coefficients were 3 and 4, respectively. The model's seasonal periods are 6, 12, and 24 hours, and the numbers of seasonal harmonics of Fourier terms employed for each seasonality in the time series are 2, 1, and 1, respectively. The fitted forecast model, TBATS, has calculated parameters with a sigma of 28.643 and an AIC of 9977.474, providing practical insights into energy consumption forecast-

ing.

Forecasting time series with the BATS model

The BATS model is a comprehensive forecasting model that integrates several components. These include the 'ARMA model for residuals,' the 'Box-Cox Transformation,' and the 'Exponential Smoothing Method,' as stated in [27], [45], and [21]. Transformation for residuals are used to de-correlate time series data utilizing non-linear data. The author proved that the BATS model outperforms the simple state-space model with respect to forecast accuracy. However, one of the shortcomings of the model is that it doesn't work well with complex seasonality. Table 8 shows BATS models and its output using R.

Table 8: BATS Model Estimated Parameters

Parameter	**Value**
Model Specification	BATS(1, {5,0}, 0.998, {6,12,24})
Alpha	0.02925
Beta	0.00005
Damping Parameter	0.99835
Gamma Values	0.05369, 0.00622, −0.01774
AR coefficients	0.82257, −0.29863, 0.00289, −0.09035, 0.17738
Sigma	24.13716
AIC	9779.919

Figure 16 displays the predictions of the electricity usage data of BATS (1, (5,0), 0.998, (6, 12, 24)). Predicting the unknown parameters using a linear space model is the main strategy for this section. Such parameters include those for the transformation, the ARMA coefficients, the smoothing parameters, the damping parameters, and similar ones. This BATS-fitted forecast model is based on the generic formula proposed by [28] for exponential methods: "BATS (1, (5, 0), 0.998, (6, 12, 24))" [21] and the estimates, Sigma: 24.137 and AIC: 9779.919 calculated by [21].

Forecasting by STL + ETS model

We forecast time-series data using STL and different seasonal periods to prepare it for analysis. 6, 12, and 24. Two sets of data are used: the training set contains all observations except the last 168, and the testing

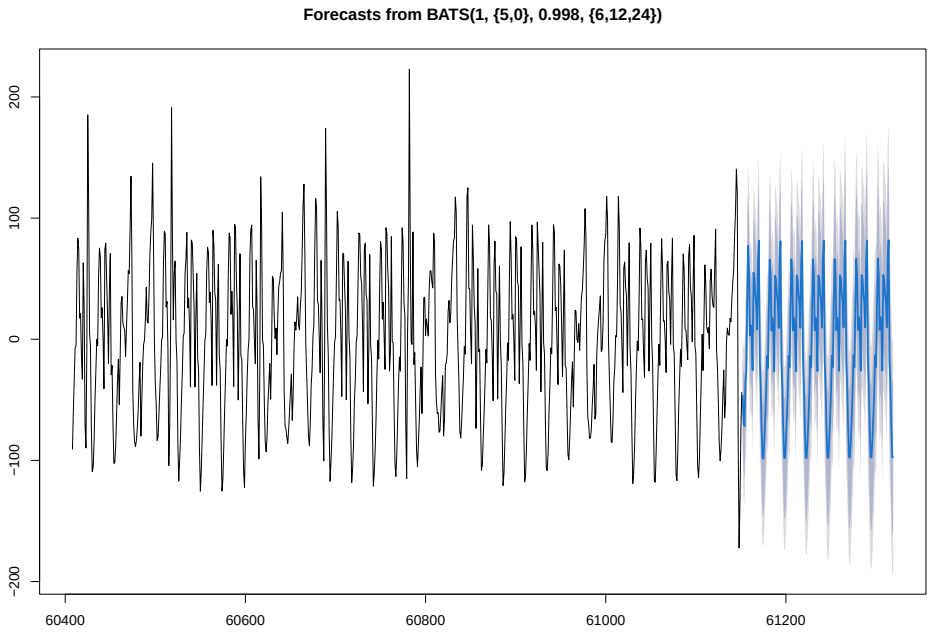

Figure 16: Hourly electricity power consumption forecasting by BATS Model

set contains the last 168. We limit the training data to only the most recent year (744 observations) to capture current trends and seasonality for reliable predictions.

Reference [23] developed robust and multifunctional STL decomposing time series models. The LOESS method calculates non-linear relationships. The STL model has been used to model seasonal dynamics in time-series. However, it also has significant flaws. Rather than automatically adjusting calendars, it merely offers additive decomposition. As shown, STL is Loess (LOcal regrESSion) smoothing. STL filters time series into residual components, seasonal, and trend. Reference [57] also noted that STL is useful for series of long-term, trending, and seasonal smoothing. The simplicity of the examination is made possible with a sequence of Loess applications in a basic architecture. The researchers found that algorithms with additive and multiplicative errors produce identical point forecasts but different prediction intervals. The model pa-

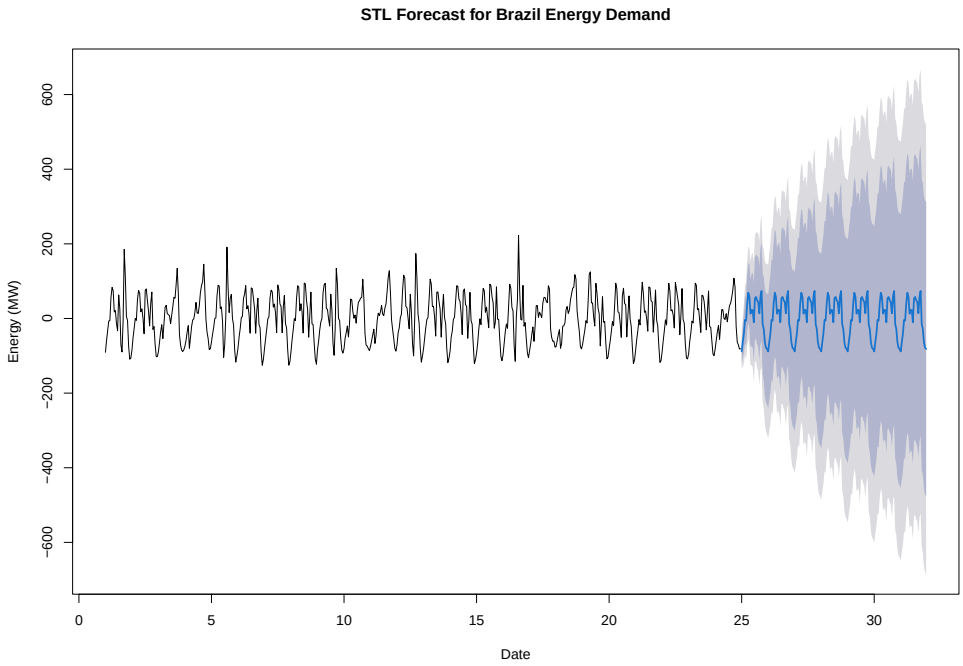

Figure 17: Hourly electricity power consumption forecasting by STL Model

rameters are ETS (A, N, N), alpha = 0.99, I0 = -24.3, sigma = 23.75, AIC = 7314.01, AICc = 7314.12, and BIC = 7327.15 [21]. Therefore, Figure 17 shows the projections of the hourly electrical power consumption for STL + ETS (A, N, N) in Brazil [21].

Table 9: Performance Metrics Comparison

Model	**MAE**	**MPE**	**MAPE**	**Theil's U**
TBATS_forecast	22.27283	163.60077	266.3995	0.62375
BATS_forecast	19.66056	-127.02622	280.3458	0.99675
STL_forecast	19.54752	-86.53971	248.1057	0.44585

Table 9 compares the STL, BATS, and TBATS models to the Brazilian electric power hourly consumption data. We evaluated these combination models by focusing on those with the lowest MAE and MAPE values. Since MAPE is straightforward, we use it to evaluate predicting strategies using available data. The least significant MAPE shows that STL models outperform the BATS and TBATS models. TBATS is the second best

model.

Using plots to compare various models' performance

In the previous sections, we demonstrated how the BATS, TBATS, and

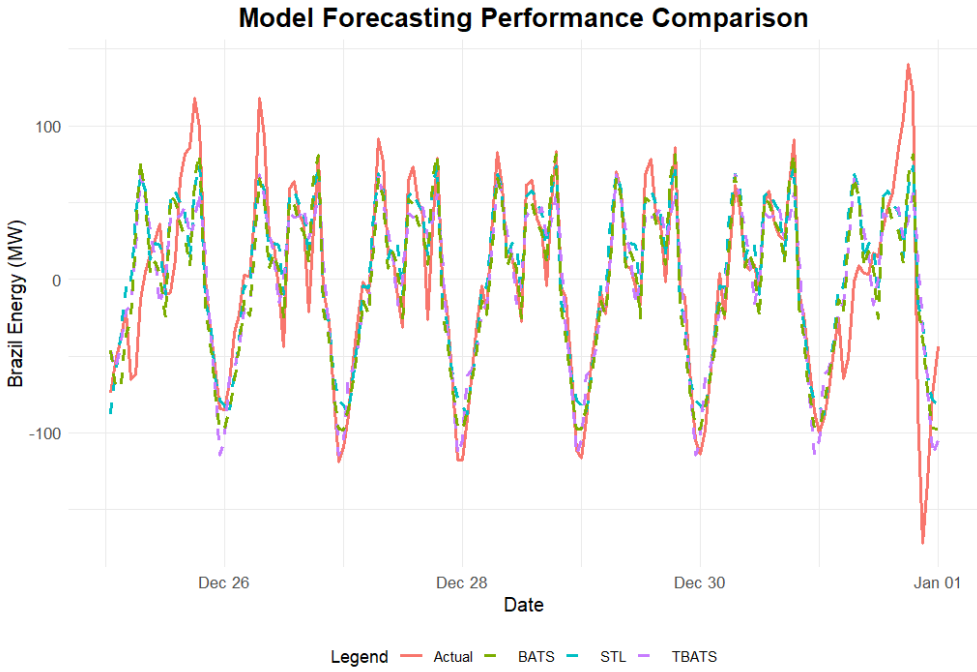

Figure 18: Comparing Forecasting Performance of BATS, TBATS, and STL Models

STL models' fitted models forecasted their individual results. Figure 18 illustrates the forecast performance and compares the models available for different seasonal data sets in Brazil. This study employs a number of STL models, as well as BATS and TBATS, to examine the multi-seasonal data sets. In projecting the different seasonal data, the STL (cyan color) models perform better than the BATS (olive color) and TBATS (purple color) models [21], as shown in Figure 18 and Table 9.

6.4 Conclusions

We introduced a new approach to the detection of various seasonalities using spectral density analysis. The most common frequency distributions that we considered were seasonalities daily, half-daily, and sub-daily.

Consequently, it appears that all three of these seasonality periods were present in the initial records. Using hourly kilowatt consumption data from a Brazilian database, We tested how well many seasonal time series models could make predictions. Then we used seasonality to fit the models with their newly estimated parameters. The results and discussions of the data output, as well as the early and additional analysis of the dataset, led us to draw conclusions. We used TBATS, BATS, and various STL models, which are all seasonal time series analysis tools. We also used these intricate seasonal time series models for comparisons and forecasts. We did not restrict the model to just one seasonality using seasonal differences; instead, we utilized the multiple-time series class, which handles a variety of seasonality series. This gave us the freedom to understand both integer and non-integer frequencies in the series, allowing me to detect any potentially significant frequency. In the discussion section, we detailed the mathematical formulations for each model and showed that they were well fitting multiple seasonal models with statistically significant parameter estimations. The intention is that they will serve as a starting point for others as they create field-specific fitting models. Data on energy power use were also used to compare models. We consider the autocorrelation function, models with the lowest mean error (MAPE, MPE, RME), and Theil's U statistic while evaluating these model combinations. Thus, the STL+ETS (A, N, N) models perform better than the TBATS and BATS models according to the specified least values. Since the STL models outperform the TBATS and BATS models when it comes to forecasting data from numerous seasons, they are the ones to choose. For companies, understanding the pros and cons of different time series models with dominant frequencies is crucial, especially since they rely on accurate forecasts for planning and operations. My main goal with the chapter's study is to find the most common frequency and compare how well different models work at different times, focusing on how well these models can find and predict different seasonal factors. Practitioners seeking dependable forecasting tools in ever-evolving scenarios can benefit

from this study's conclusions.

6.5 Key Questions, and Contributions

Key Questions

1. Are major seasonal phases in time series data efficiently identified by periodograms produced from spectral density analysis?
2. How accurate are seasonal models for predicting time series that exhibit different levels of seasonality?
3. How do seasonal models perform compared to other state-of-the-art methods for predicting time series?

Finding/Contributions

A methodology is presented in new approach for the identification of significant seasonal periods through the analysis of periodograms derived from spectral density. Subsequently, the forecasting efficacy of seasonal models constructed using these periods is evaluated against a suite of advanced time series forecasting methods. The primary contribution is the demonstration that STL+ETS models, guided by an initial spectral density analysis to detect dominant seasonalities, deliver superior forecasting performance for multi-seasonal time series compared to state-of-the-art alternatives like TBATS and BATS, as validated by key error metrics on real-world energy data.

7 Conclusion and Future Directions

7.1 Conclusion

Focusing on their ability to detect and anticipate various seasonal features, We employed an enhanced method to identify several seasonal patterns using spectral density analysis (Periodogram) to ascertain the prevailing frequency and assess the efficacy of various models over time. Consequently, it seems that all three seasonal phases were evident in the earliest recordings. We evaluated the predictive accuracy of various seasonal time series models utilizing hourly kilowatt consumption data from a Brazilian database to employ seasonality to calibrate the models with their newly estimated parameters. I employed TBATS, BATS, and STL models, all of which are tools for multiple seasonal time-series analysis. For the purposes of comparison and forecasting, we employed these various seasonal time series models. We utilized the multiple-time series class, which can accept various seasonal series, instead of limiting the model to a single seasonality through seasonal differences. This enabled us to comprehend both integer and non-integer frequencies within the series, facilitating the identification of any potentially significant frequency. In the discussion section, we elucidated the formulations for each model and demonstrated that they effectively matched several seasonal models with statistically meaningful parameter estimates. The aim of these studies is for them to serve as a foundation for others in developing field-specific fitting models. Data on energy consumption were utilized to compare models. —We evaluated these model combinations by considering the autocorrelation function, models with the lowest mean error (MAPE, MPE, RME), and Theil's U statistic. Consequently, the STL+ETS (A, N, N) models exhibit superior performance compared to the TBATS and BATS models based on the designated minimum values. The STL models are preferable for forecasting multi-seasonal data because of their high performance compared to the TBATS and BATS models. This study's outcomes provide valuable insights for practitioners in need of reliable

forecasting tools in dynamic environments.
Secondly, we explained how the incorporation of ARMA (3,1) errors into the DSHW framework could be useful in the context of predicting and modeling time-series data. Specifically, the implications of these inclusions are discussed. It was shown that the Combined Model performed much better on each and every one of the metrics that were studied when compared to the traditional DSHW model. By including errors based on ARMA into the model, we are able to improve the accuracy of the forecasting and correct for any residual autocorrelation that may have occurred. It is clear from the findings that the model is capable of accurately forecasting the amount of energy that will be utilized. Additionally, it can be utilized to deal with data that demands careful management owing to the fact that it contains a number of seasonalities and errors that are interrelated to each other.
In addition of that, we modeled and forecasted the modified coronavirus's multiplicative SARIMA model using Hungary COVID-19 data. The fairly fitted seasonal ARIMA model was utilized for forecasting. The time series plot displayed seasonality, trend patterns, and unstable variance patterns, indicating non-stationary data. The altered data approach's initial difference made the trend stationary. The ACF and PACF plots demonstrate seasonality in Hungarian COVID-19 daily deaths. Before data analysis, we modeled the time series and adjusted the weekly seasonality term for this seasonal trend. The suggested model is seasonal $ARIMA(1,1,2)(1,0,1)_{[7]}$. COVID-19 data from a recognized time series in Hungary is used to forecast daily fatalities. The fitted model $ARIMA(1,1,2)(1,0,1)_{[7]}$ is used for prediction. The date estimate suggests that daily deaths from COVID-19 are decreasing from day to day.

7.2 Future Directions

The computational efficiency of periodogram-based approaches is now being investigated, particularly with regard to the processing of enormous datasets [67]. Moreover, offering feasible alternatives for traditional pe-

riodograms is a key new advances in wavelet analysis and other spectral methods. Localized frequency analysis made possible by these approaches can help time series data showing non-stationarity or changing seasonal trends to benefit [3]. Periodograms, machine learning, and hybrid modeling—which combines several approaches—will probably continue to be useful tools for the study and forecasting of complex multiseasonal time series data as the field develops.

8 List of Publications

1. Chudo, S. B., and Terdik, G. (2025). Modeling and Forecasting Time-Series Data with Multiple Seasonal Periods Using Periodograms. (**Econometrics, 13(2), 14. https://doi.org/10.3390/econometrics13020014, Q2**)

2. S.B. Chudo, "Multiplicative Seasonal ARIMA Modeling and Forecasting of COVID-19 Daily Deaths in Hungary," 2022 10th International Conference on Bioinformatics and Computational Biology (ICBCB, ISBN: 978-1-6654-5135-2), Hangzhou, China, 2022, pp. 142-147, **IEEE, DOI: 10.1109/ICBCB55259.2022.9802498 (Best paper Award). Scopus Indexed**.

3. Chudo, S. B." State Space ARIMA Model Formulation and Its Application in Energy," In Proceedings of IEMTRONICS 2025 (978-981-95-0432-9, 646351-1-En, Chapter 7, 'Lecture Notes in Electrical Engineering, Vol. 1468), 2025, In Press, **Springer Nature, DOI: 10.1007/978-981-95-0433-6, Q4**.

4. Chudo, S. B. " Modeling and Forecasting Energy Consumption Using DSHW Model with ARMA Errors: The State Space Approach ," 2025, (**Submitted to Journal of Sustainable Energy, Grids and Networks, Q1**).

5. Chudo, S. B., and D. Gebeyehu, " Statistical Analysis of Determinants of Academic Outcomes of Public TVET Students: A Case Study at Dilla and Hawassa TVET Colleges, Ethiopia," 2025, (**Under the Review in the Journal of Technical Education and Training (JTET), Penerbit UTHM, Q3**).

Conference Contributions

6. Solomon Buke Chudo. (2022). Modeling and Forecasting Time Series with Multiple Seasonal Periods. The 2022 IEEE 2nd Conference

on Information Technology and Data Science (CITDS-2022), Debrecen, Hungary (Conference presentation).

7. Solomon Buke Chudo. (2022). Statistical Analysis of Determinants of Academic Outcomes of Public TVET Students: A Case Study at Dilla and Hawassa TVET Colleges, Ethiopia, 9th International Conference on Social Sciences and Humanities held on March 19-20, 2022, Burdur, Turkey (Conference presentation and Abstract publication,
   https://www.ispecongress.org/sosyal-bilimler, pg. 298).

8. Solomon Buke Chudo. (2024). " Time Series Models with Multiple Seasonal Periods: An Evaluation of Their Forecasting Performance", ICISDM2024 (The 8th International Conference on Information System and Data Mining), Los Angeles, USA, 2024,
   (https://www.icisdm.org/ICKMS Program - June 14. PDF, p.12).

Acknowledgments

Before anything else, I would like to thank my supervisor, Prof. Dr. György Terdik, for all of the help, encouragement, and direction he gave me while I was working on my Ph.D. This dissertation would not have been possible without his extensive knowledge, perceptive criticism, and unfailing support.
My dear parents, Bogalech Bejo and Buke Chudo, who taught me the importance of hard work and education, have my deepest gratitude. Their love, sacrifices, and aspirations for me continue to motivate me, even though they passed away while I was in my second year of PhD studies. I hope this work honors their memory.
Meskerem Elias, my lovely wife and my beloved sons (Tebibu Solomon and Leul Solomon), I am eternally grateful for your unending love, tolerance, and comprehension. You gave me the strength to continue even when things were tough because you believed in me no matter what happened. You and I both deserve credit for this success.

The wonderful financial support of the Stipendium Hungaricum Scholarship allowed me to pursue my Ph.D. studies, and for that I am really thankful. Dilla University (Ethiopia) and Debrecen University (Hungary) also deserve my deepest gratitude for providing me with the means to go on this educational adventure.
Finally, I extend my gratitude to all friends, colleagues, and mentors who supported me along the way. Your encouragement and companionship have been invaluable.

References

[1] Mostafa Abotaleb and Tatiana Makarovskikh. Advanced milk production modelling using high-order generalized least deviation method. *Modeling Earth Systems and Environment*, pages 1–29, 2024.

[2] Hirotugu Akaike. Stochastic theory of minimal realization. *IEEE Transactions on Automatic Control*, 19(6):667–674, 1974.

[3] John C Aldrin, Eric B Shell, Erin K Oneida, Harold A Sabbagh, Elias Sabbagh, R Kim Murphy, Siamack Mazdiyasni, and Eric A Lindgren. Model-based inverse methods for sizing surface-breaking discontinuities with eddy current probe variability. In *AIP Conference Proceedings*, volume 1706. AIP Publishing, 2016.

[4] Samuel Erasmus Alnaa and Ferdinand Ahiakpor. Arima (autoregressive integrated moving average) approach to predicting inflation in ghana. *Journal of economics and international finance*, 3(5):328–336, 2011.

[5] Nari Sivanandam Arunraj and Diane Ahrens. A hybrid seasonal autoregressive integrated moving average and quantile regression for daily food sales forecasting. *International Journal of Production Economics*, 170:321–335, 2015.

[6] John AD Aston and Siem Jan Koopman. A non-gaussian generalization of the airline model for robust seasonal adjustment. *Journal of Forecasting*, 25(5):325–349, 2006.

[7] Kasun Bandara, Christoph Bergmeir, and Slawek Smyl. Forecasting across time series databases using recurrent neural networks on groups of similar series: A clustering approach. *Expert systems with applications*, 140:112896, 2020.

[8] André Bauer, Marwin Züfle, Johannes Grohmann, Norbert Schmitt, Nikolas Herbst, and Samuel Kounev. An automated forecasting framework based on method recommendation for seasonal time series. In *Proceedings of the ACM/SPEC International Conference on Performance Engineering*, pages 48–55, 2020.

[9] P Bickel, P Diggle, S Fienberg, U Gather, I Olkin, and S Zeger. Springer series in statistics. *Principles and Theory for Data Mining and Machine Learning. Cham, Switzerland: Springer*, 2009.

[10] Christopher M Bishop and Nasser M Nasrabadi. *Pattern recognition and machine learning*, volume 4. Springer, 2006.

[11] George Box. Box and jenkins: time series analysis, forecasting and control. In *A Very British Affair: Six Britons and the Development of Time Series Analysis During the 20th Century*, pages 161–215. Springer, 2013.

[12] George Box and GM Jenkins. Analysis: Forecasting and control.". *San Francisco*, 1976.

[13] George EP Box and Gwilym M Jenkins. Some recent advances in forecasting and control. *Journal of the Royal Statistical Society. Series C (Applied Statistics)*, 17(2):91–109, 1968.

[14] George EP Box, Gwilym M Jenkins, Gregory C Reinsel, and Greta M Ljung. *Time series analysis: forecasting and control*. John Wiley & Sons, 2015.

[15] Peter J Brockwell. Representations of continuous-time arma processes. *Journal of Applied Probability*, 41(A):375–382, 2004.

[16] Peter J Brockwell, Richard A Davis, Peter J Brockwell, and Richard A Davis. Nonstationary and seasonal time series models. *Introduction to time series and forecasting*, pages 157–193, 2016.

[17] JAMES T CAIN, WILLIAM G VOGT, and MARLIN H MICKLE. Linear system canonical forms. *INTERNATIONAL JOURNAL OF GENERAL SYSTEM*, 1(3):197–202, 1974.

[18] Chris Chatfield. *Time-series forecasting*. Chapman and Hall/CRC, 2000.

[19] S. B. Chudo. State space ARIMA model formulation and its application in energy. In *Proceedings of the International IOT, Electronics and Mechatronics Conference (IEMTRONICS 2025)*, Lecture Notes in Electrical Engineering, Imperial College London, UK, 2025. Springer. In press, awarded. To be published in `https://www.springer.com/series/7818`.

[20] Solomon Buke Chudo. Multiplicative seasonal arima modeling and forecasting of covid_19 daily deaths in hungary. In *2022 10th International Conference on Bioinformatics and Computational Biology (ICBCB)*, pages 142–147. IEEE, 2022.

[21] Solomon Buke Chudo and Gyorgy Terdik. Modeling and forecasting time-series data with multiple seasonal periods using periodograms. *Econometrics*, 13(2):14, 2025.

[22] Robert B Cleveland and William S Cleveland. E mcrae, j., and terpenning, i.: Stl: A seasonal-trend decomposition procedure based on loess. *J. Offic. Stat*, 6:3–33, 1990.

[23] Robert B Cleveland, William S Cleveland, Jean E McRae, Irma Terpenning, et al. Stl: A seasonal-trend decomposition. *J. off. Stat*, 6(1):3–73, 1990.

[24] Jacques JF Commandeur and Siem Jan Koopman. *An introduction to state space time series analysis*. Oxford university press, 2007.

[25] Lars Dannecker. *Energy time series forecasting: efficient and accurate forecasting of evolving time series from the energy domain*. Springer, 2015.

[26] Sandra De Iaco, Sabrina Maggio, Monica Palma, and Donato Posa. Towards an automatic procedure for modeling multivariate space–time data. *Computers & Geosciences*, 41:1–11, 2012.

[27] Alysha M De Livera et al. Automatic forecasting with a modified exponential smoothing state space framework. *Monash Econometrics and Business Statistics Working Papers*, 10(10):6, 2010.

[28] Alysha M De Livera, Rob J Hyndman, and Ralph D Snyder. Forecasting time series with complex seasonal patterns using exponential smoothing. *Journal of the American statistical association*, 106(496):1513–1527, 2011.

[29] Ivo D Dinov. Data science and predictive analytics. *Cham, Switzerland*, 2018.

[30] James Durbin and Siem Jan Koopman. *Time series analysis by state space methods*. Oxford University Press (UK), 2012.

[31] Ligita Gaspareniene and Rita Remeikiene. Arima model for predicting the development of the price of gold: European approach. *Ekonomicko-manazerske spektrum*, 14(1):87–96, 2020.

[32] Andrew Gelman and Cosma Rohilla Shalizi. Philosophy and the practice of bayesian statistics. *British Journal of Mathematical and Statistical Psychology*, 66(1):8–38, 2013.

[33] Ramazan Gençay, Faruk Selçuk, and Brandon J Whitcher. *An introduction to wavelets and other filtering methods in finance and economics*. Elsevier, 2001.

[34] James Gentle. *Statistical analysis of financial data: With examples in R*. CRC Press, 2020.

[35] Osvaldo Gervasi, Beniamino Murgante, Ana Maria AC Rocha, Chiara Garau, Francesco Scorza, Yeliz Karaca, and Carmelo M Torre. Computational science and its applications–iccsa 2023 workshops. In *Proceedings of the 23rd International Conference on Computational Science and Its Applications, ICCSA*. Springer, 2023.

[36] Hans Gilgen. *Univariate time series in geosciences*. Springer, 2006.

[37] Elisa María Jorge González. *Analysis and development of a tourism demand forecast system at the canary islands*. PhD thesis, Universidad de La Laguna (Canary Islands, Spain), 2019.

[38] Phillip G Gould, Anne B Koehler, J Keith Ord, Ralph D Snyder, Rob J Hyndman, and Farshid Vahid-Araghi. Forecasting time series with multiple seasonal patterns. *European Journal of Operational Research*, 191(1):207–222, 2008.

[39] James D Hamilton. *Time series analysis*. Princeton university press, 2020.

[40] Frank E Harrell and FE Harrell. *Regression modeling strategies*, volume 54. Springer, 2001.

[41] P Jeffrey Harrison and Colin F Stevens. Bayesian forecasting. *Journal of the Royal Statistical Society Series B: Statistical Methodology*, 38(3):205–228, 1976.

[42] Andrew Harvey and Siem Jan Koopman. Forecasting hourly electricity demand using time-varying splines. *Journal of the American Statistical Association*, 88(424):1228–1236, 1993.

[43] Andrew Harvey, Siem Jan Koopman, and Marco Riani. The modeling and seasonal adjustment of weekly observations. *Journal of Business & Economic Statistics*, 15(3):354–368, 1997.

[44] Florian Heiss. Sequential numerical integration in nonlinear state space models for microeconometric panel data. *Journal of Applied Econometrics*, 23(3):373–389, 2008.

[45] Zachary C Herbert, Zeeshan Asghar, and Carlos A Oroza. Long-term reservoir inflow forecasts: enhanced water supply and inflow volume accuracy using deep learning. *Journal of Hydrology*, 601:126676, 2021.

[46] K Hipel. Geophysical model discrimination using the akaike information criterion. *IEEE Transactions on Automatic Control*, 26(2):358–378, 2003.

[47] Svend Hylleberg, Robert F. Engle, Clive W. J. Granger, and Bong S. Yoo. Seasonal integration and cointegration. *Journal of Econometrics*, 44(1-2):215–238, 1990.

[48] RJ Hyndman and G Athanasopoulos. Forecasting: Principles and practice, 3rd edn, otexts: Melbourne. *OTexts. com/fpp3. Accessed on July, 07th*, 2021.

[49] Rob J Hyndman and George Athanasopoulos. *Forecasting: principles and practice*. OTexts, 2018.

[50] Rob J Hyndman and Yeasmin Khandakar. Automatic time series forecasting: the forecast package for r. *Journal of statistical software*, 27:1–22, 2008.

[51] Rob J Hyndman and Anne B Koehler. Another look at measures of forecast accuracy. *International journal of forecasting*, 22(4):679–688, 2006.

[52] Rob J Hyndman, Anne B Koehler, Ralph D Snyder, and Simone Grose. A state space framework for automatic forecasting using exponential smoothing methods. *International Journal of forecasting*, 18(3):439–454, 2002.

[53] Mahdi Kalantari. Forecasting covid-19 pandemic using optimal singular spectrum analysis. *Chaos, Solitons & Fractals*, 142:110547, 2021.

[54] Rudolph Emil Kalman. A new approach to linear filtering and prediction problems. *Journal of Fluids Engineering*, 1960.

[55] Hellen W Kibunja, John M Kihoro, George O Orwa, and Walter O Yodah. Forecasting precipitation using sarima model: A case study of mt. kenya region. *Mathematical Theory and Modeling*, 2014.

[56] Siem Jan Koopman and Andrew Harvey. Computing observation weights for signal extraction and filtering. *Journal of Economic Dynamics and Control*, 27(7):1317–1333, 2003.

[57] Yakup Tarik Kranda and Ruya Samli. A novel clustering based algorithm to mitigate the demand of forecasting errors for newly deployed lte cells with insufficient historical data. *Computer Communications*, 190:190–200, 2022.

[58] Jian Liu, Junkang Guo, Lei Gao, Yuhang Wang, Aolei Liu, and Xin Zhang. Pptformer: A novel hybrid model for enhanced long-term time series forecasting with extreme value focus. *Knowledge-Based Systems*, 317:113456, 2025.

[59] Helmut Lütkepohl. Vector autoregressive models. In *Handbook of research methods and applications in empirical macroeconomics*, pages 139–164. Edward Elgar Publishing, 2013.

[60] Pauline Jin Wee Mah, FN Buhary, NH Abdullah, and SAM Saad. A comparative study of univariate time series modelling for natural rubber production in malaysia/pauline mah jin wee... [et al.]. *Malaysian Journal of Computing (MJoC)*, 3(2):108–118, 2018.

[61] Bashirahamad Momin and Gaurav Chavan. Univariate time series models for forecasting stationary and non-stationary data: A brief

review. In *International Conference on Information and Communication Technology for Intelligent Systems*, pages 219–226. Springer, 2017.

[62] HO Nasiru, RA Ipinyomi, HU Yahaya, and MA Zubair. Autoregressive integrated moving average (arima) model for the major airline disasters in the world from 1960 through 2013. *International Journal of Mathematics and Statistics Studies*, 4(6):25–37, 2016.

[63] Moyses Xavier Fontoura Neto. Nowcasting vat data in the retail trade sector using historical data and electronic payment data. Master's thesis, Universidade do Porto (Portugal), 2023.

[64] Kohei Ohtsu. *Model-based Monitoring and Statistical Control*. CRC Press, 2024.

[65] John Keith Ord, Anne B Koehler, and Ralph D Snyder. Estimation and prediction for a class of dynamic nonlinear statistical models. *Journal of the American Statistical Association*, 92(440):1621–1629, 1997.

[66] Our World in Data. Coronavirus pandemic (covid-19) – hungary, 2021.

[67] Donald B Percival and Andrew T Walden. *Wavelet methods for time series analysis*, volume 4. Cambridge university press, 2000.

[68] Dimitris N Politis and Tucker S McElroy. *Time series: A first course with bootstrap starter*. Chapman and Hall/CRC, 2019.

[69] Ajeng Prastiwi. Forecasting time series with multiple seasonal. `https://rpubs.com/AlgoritmaAcademy/multiseasonality`, 2019. Accessed: [Insert Date].

[70] Tommaso Proietti and Diego J Pedregal. Seasonality in high frequency time series. *Econometrics and Statistics*, 27:62–82, 2023.

[71] Dinda Ayu Safira, Heri Kuswanto, and Muhammad Ahsan. Improving the forecast accuracy of pm2. 5 using setar-tree method: Case study in jakarta, indonesia. *Atmosphere*, 16(1):23, 2024.

[72] Jeffrey D Scargle. Studies in astronomical time series analysis. ii-statistical aspects of spectral analysis of unevenly spaced data. *Astrophysical Journal, Part 1, vol. 263, Dec. 15, 1982, p. 835-853.*, 263:835–853, 1982.

[73] Jürgen Schmidhuber, Sepp Hochreiter, et al. Long short-term memory. *Neural Comput*, 9(8):1735–1780, 1997.

[74] V Sharmila, S Kannadhasan, A Rajiv Kannan, P Sivakumar, and V Vennila. *Challenges in Information, Communication and Computing Technology: Proceedings of the 2nd International Conference on Challenges in Information, Communication, and Computing Technology (ICCICCT 2024), April 26th & 27th, 2024, Namakkal, Tamil Nadu, India*. CRC Press, 2024.

[75] Robert H Shumway and David S Stoffer. Time series analysis and applications, 2016.

[76] Robert H Shumway and David S Stoffer. State space models. In *Time series analysis and its applications: with R examples*, pages 289–384. Springer, 2017.

[77] Robert H Shumway, David S Stoffer, and David S Stoffer. *Time series analysis and its applications*, volume 3. Springer, 2000.

[78] Michael Stanley Smith. Copula modelling of dependence in multivariate time series. *International Journal of Forecasting*, 31(3):815–833, 2015.

[79] Aruã Souza. 23 years of hourly electric energy demand (brazil). Retrieved from Kaggle, 2022. Accessed: [Insert Date].

[80] James W Taylor. Short-term electricity demand forecasting using double seasonal exponential smoothing. *Journal of the Operational Research Society*, 54(8):799–805, 2003.

[81] R Developement Core Team. R: A language and environment for statistical computing. *(No Title)*, 2010.

[82] Howell Tong. *Non-linear time series: a dynamical system approach*. Oxford university press, 1990.

[83] Wim J Van der Linden and Wim van der Linden. *Handbook of item response theory*, volume 1. CRC press New York, 2016.

[84] Alestair Varghese, Harpreet Tarhen, Aquib Shaikh, Prasenjit Banik, and Ashish Ramadasi. Stock market prediction using time series. *International Journal on Recent and Innovation Trends in Computing and Communication*, 4(5):427–430, 2016.

[85] Carlos E Velasquez, Matheus Zocatelli, Fidellis BGL Estanislau, and Victor F Castro. Analysis of time series models for brazilian electricity demand forecasting. *Energy*, 247:123483, 2022.

[86] VVilliam VV S VVei. *Time Series Analysis*. Greg Tobin, 2006.

[87] Shengwei Wang, Juan Feng, and Gang Liu. Application of seasonal time series model in the precipitation forecast. *Mathematical and Computer modelling*, 58(3-4):677–683, 2013.

[88] Teng Wang, Guoliang Lu, and Peng Yan. A novel statistical time-frequency analysis for rotating machine condition monitoring. *IEEE Transactions on Industrial Electronics*, 67(1):531–541, 2019.

[89] William Wei. *Time Series Analysis: Univariate and Multivariate Methods, 2nd edition, 2006*. Greg Tobin, 01 2006.

[90] Hexuan Weng. Cellular traffic forecasting and analysis with efficiency transformer. *PQDT-Global*, 2023.

[91] Wikipedia contributors. Kpss test. `https://en.wikipedia.org/wiki/KPSS_test`, 2023. [Online; accessed ¡February 23, 2025¿].

[92] Ashton T Williams, Ryan E Sperl, and Soon M Chung. Anomaly detection in multi-seasonal time series data. *IEEE Access*, 11:106456–106464, 2023.

[93] Peter R Winters. Forecasting sales by exponentially weighted moving averages. *Management science*, 6(3):324–342, 1960.

[94] Guotian Xie, Jingdong Wang, Ting Zhang, Jianhuang Lai, Richang Hong, and Guo-Jun Qi. Interleaved structured sparse convolutional neural networks. In *Proceedings of the IEEE Conference on Computer Vision and Pattern Recognition*, pages 8847–8856, 2018.

[95] G Peter Zhang. Time series forecasting using a hybrid arima and neural network model. *Neurocomputing*, 50:159–175, 2003.

[96] Mingda Zhang. Time series: Autoregressive models ar, ma, arma, arima. *University of Pittsburgh*, 2018.

[97] Zhiyong Zhang, Ellen L Hamaker, and John R Nesselroade. Comparisons of four methods for estimating a dynamic factor model. *Structural Equation Modeling: A Multidisciplinary Journal*, 15(3):377–402, 2008.